# IMPROVING THE ACCURACY OF CHEMICAL MEASUREMENTS IN THE BRAIN: NEW INSIGHTS INTO DOPAMINERGIC MECHANISMS BY FAST-SCAN CYCLIC VOLTAMMETRY AND MICRODIALYSIS

by

Laura M. Borland

B.S. Chemistry, Drake University, 2000

Submitted to the Graduate Faculty of

Arts and Science in partial fulfillment

of the requirements for the degree of

Doctor of Philosophy

University of Pittsburgh

2005

UNIVERSITY OF PITTSBURGH

FACULTY OF ARTS AND SCIENCES

This dissertation was presented

by

Laura M. Borland

It was defended on

November 8, 2005

and approved by

Shigeru Amemiya, Ph.D., Assistant Professor

Martyn G. Boutelle, Ph.D., Professor

Stephen G. Weber, Ph.D., Professor

Adrian C. Michael, Ph.D., Associate Professor
Dissertation Director

IMPROVING THE ACCURACY OF CHEMICAL MEASUREMENTS IN THE BRAIN: NEW INSIGHTS INTO DOPAMINERGIC MECHANISMS BY FAST-SCAN CYCLIC VOLTAMMETRY AND MICRODIALYSIS

Laura M. Borland, Ph.D.

University of Pittsburgh, 2005

The neurotransmitter dopamine is implicated in cognitive function, emotion, and movement, as well as multiple disease states, like Parkinson's disease, schizophrenia, and drug abuse. Two commonly used techniques used for in the *in vivo* measurement of dopamine are microdialysis and voltammetry with carbon fiber microelectrodes. Unfortunately, these techniques yield conflicting results, complicating our understanding of the dopaminergic mechanisms at work in the brain. Microscopy studies reveal significant disruption to the tissue surrounding microdialysis probes, suggesting that alterations in functionality of the damaged tissue might contribute to the discrepancy between microdialysis and voltammetry. In this dissertation, microelectrodes were implanted near microdialysis probes to examine the effect of probe implantation on stimulated dopamine release and uptake in the tissue surrounding microdialysis probes. Voltammetric studies revealed a gradient in the activity of stimulated dopamine release and dopamine uptake near the probe. Additional pharmacological studies revealed a disrupted blood-brain barrier near the probe, suggesting another level of tissue disruption caused by microdialysis probe implantation.

Glutamate is implicated alongside dopamine in a number of the same diseases, including schizophrenia and drug abuse. Although dopaminergic and glutamatergic projections into the striatum fail to form direct synaptic contact, an earlier voltammetric study found that local antagonism of ionotropic glutamate receptors caused a decrease in striatal dopamine levels,

suggesting that glutamate acts locally within the striatum to regulate extracellular dopamine levels. This dissertation expanded on that study to reveal that ionotropic glutamate receptors control a non-vesicular release process that contributes to the resting level of extracellular dopamine in the brain.

Microdialysis and voltammetry results show large discrepancies between levels of dopamine after uptake inhibition. Recent voltammetric studies suggest that $D_2$ receptors participate in a homeostatic feedback mechanism that regulates extracellular dopamine levels after uptake inhibition. In this study, the mechanism of dopamine release after uptake inhibition in rats pretreated with a $D_2$ receptor antagonist was identified. Dopamine released after systemic nomifensine administration in sulpiride-pretreated rats originates from an impulse-dependent (vesicular) pool of dopamine, suggesting that $D_2$ receptors may modulate release by controlling vesicular stores and/or vesicular transport.

## TABLE OF CONTENTS

## LIST OF EQUATIONS

## LIST OF FIGURES

## PREFACE

I'd like to take this chance to thank all those who have helped me through this wonderful journey in becoming a real and true scientist. First, I would like to thank Dr. Adrian C. Michael, mostly for his patience, but also for his support, passion, and instruction; he has truly inspired me to become a great scientist and has taught me more about being a leader and teacher than anyone I have ever met.

I would like to thank the members of my proposal and doctoral committees, Dr. Stephen Weber, Dr. Shigeru Amemiya, Dr. Dave Waldeck and Dr. Martyn Boutelle. Thanks for all of your guidance and advice and for traveling great distances (Dr. Boutelle) to be a part of my "big day". I would also like to thank the wonderful support staff of the chemistry department, including, but not limited to, the Electronic Shop staff, the Machine Shop staff, and the Secretarial staff. You folks really run this place and can teach a Ph.D. a thing or two about paperwork! Finally, I would like to thank the 30+ folks I was so privileged to work beside in the Michael lab. Contrary to popular belief, research is a group effort and I would not be the scientist I am today without the support and criticism of my fellow group members.

I would also like to thank my parents for all their never-ending support (money, food, van, etc.). I may be Mrs. Habay now, but I'll always be Dr. Borland, just for you. Now you finally have a doctor in the family, Mom!

And last, but certainly not least, I would like to thank my partner-in-crime, my husband, Stephen Habay. Thanks so much for your never-ending support and love; I really could not have made it without you.

# 1. AN INTRODUCTION TO ELECTROCHEMICAL METHODS IN NEUROSCIENCE

Neuroscientists employ numerous tools to examine the workings of the brain and central nervous system. Electrochemical methods are versatile techniques for the study of numerous neurochemical environments and molecules, specifically, but not exclusively, catecholaminergic neurotransmitters. These electrochemical methods, which include the use of microelectrodes with various voltammetric techniques, are used to monitor and measure a variety of neurochemicals in diverse environments, including synaptic vesicles, single cells, tissues, the anesthetized brain, and the awake, unanesthetized brain. The versatility of microelectrodes and electrochemical methods extends to their use with other techniques, like patch clamp and electrophysiology, to obtain additional insight into these investigations. This chapter will serve as an introduction into the history of electrochemistry in the neurosciences, including its rough beginnings and triumphs; the applications of electrochemistry in the neurosciences, where electrochemistry can be used, what it can be used to detect, measure and study; and finally, an introduction to the fundamentals of electrochemistry, including oxidation and reduction, diffusion, electrochemical methods, and electrode properties.

## 1.1. ELECTROCHEMISTRY IN THE BEGINNING: EARLY LESSONS IN SELECTIVITY

The foundations of the electrochemical research and methods employed in neuroscience today originated from the Nobel Prize-winning work of Jaroslav Heyrovsky. Heyrovsky and his contemporaries were interested in measuring and studying analytes at metal surfaces by electrolysis, or the adding or subtracting electrons through the application of a voltage difference, or potential. Heyrovsky correctly predicted and measured the deposition of sodium ions by measuring the current produced at a dropping mercury electrode, establishing the first electro-analytical measurement. His novel technique for identifying and quantifying analytes became known as "polarography", named after the automated device (the "polargraph") developed to record the current-voltage plot. Today, polarography is known as voltammetry, but the principles are still the same; monitoring and measuring the current produced by different analytes at different applied potentials. Heyrovsky won the Nobel Prize in 1959 for his discovery of polarography, which started the field of analytical electrochemistry, enabling scientists to examine electrode processes, chemical reactions and to measure numerous analytes, both in solution and in more adventurous media, like the brain.

Fifty years after Heyrovsky's initial discovery, electrochemist Ralph Adams would boldly go where no electrochemist had gone before - into the brain. Adams' interest in monitoring neurochemicals *in vivo* began with his study of the electrooxidation of phenols, catechols and catecholamines. He hypothesized that small electrodes could be implanted into the brain and used to oxidize the electroactive catecholaminergic neurotransmitters, namely dopamine and norepinephrine, and their equally active metabolites, such as homovanillic acid and DOPAC (Kissinger et al., 1973; Wightman et al., 1976; Adams, 1976). *In vivo* voltammetry

with micro-sized graphite paste electrodes were used to monitor and measure these neurotransmitters, as well as the electroactive neurotransmitter serotonin (5-hydroxytryptamine) and its metabolites (Schenk et al., 1983). While Adams worked with carbon paste microelectrodes, Francois Gonon and his colleges in France were implanting microelectrodes composed of carbon fibers into rodent brains to detect and monitor neurotransmitters (Ponchon et al., 1979; Gonon et al., 1980).

The early *in vivo* electrochemical studies by Adams and Gonon were not without complications. The limited selectivity of electrodes *in vivo* was a major issue. Interfering species in the brain, such as ascorbic acid (AA) and neurotransmitter metabolites, often masked the species of interest and led to a number of misinterpretations of early data (Gonon et al., 1980). Selectivity improved with the introduction of different electrode pre-treatments and electrochemical techniques. Gonon improved selectivity by electrochemically pretreating carbon fiber microcylinder electrodes, which altered the surface properties of the electrode so that ascorbic acid and catechols were oxidized at different potentials (Gonon et al., 1981). Unfortunately, electrical pretreatment of microelectrodes was not the definitive answer to the selectivity problem, in fact, it created some bigger problems. Overzealous electrochemical pretreatment increased selectivity and sensitivity; however, the response time of the electrode decreased significantly, diminishing the valued temporal resolution of the technique and distorting subsequent interpretation of electrochemical measurements (Gonon et al., 1984). As an alternative to electrochemical pretreatment, electrodes were coated with polyanionic polymers, such as the perfluorinated polymer Nafion. This coating electrostatically rejects the anionic AA, while allowing the passage of cationic catechols with minimal temporal deficits (Gerhardt et al., 1984; Leszczyszyn et al., 1991). While numerous novel electrode treatments are

investigated for use in creating the "perfect" electrode, which is both highly sensitive and selective, electrochemists continue to explore new environments and discover new neurochemical features with "less than perfect" electrodes.

In the absence of a "perfect" electrode, the electrochemistry community has established criteria for chemical identification and verification of electrochemical signals from this inherently "less" sensitive technique. These critical guidelines are actually supplemental experiments used to verify *in vivo* signals as originating from a particular analyte. These critical experiments include electrochemical verification, such as *in vivo* voltammogram identification; anatomical and physiological verification, such as post-mortem analysis or electrochemical measurement from an area of excess analyte or an area with an absence of analyte; pharmacological verification, such as the use of drugs to induce changes in analyte synthesis, metabolism, release or uptake; and independent chemical verification, as in comparing the electrochemical response to another comparable technique (Phillips and Wightman, 2003). These criteria have helped to clarify the origins of the electrochemical signals generated *in vivo* without concentrating solely on maximizing the performance of the electrode.

## 1.2. IN VIVO ELECTROCHEMISTRY: THE BENEFITS OF SIZE AND SPEED

Electrochemical methods are best suited for measuring transient changes in concentration. Electrochemical techniques provide superior temporal resolution over sampling techniques, such as microdialysis, by allowing subsecond measurements of neurochemical changes in the brain and central nervous system. Neurochemical events can be observed in real-time with electrochemical methods, which have resulted in the development of kinetic models for

neurotransmitter synthesis, release, uptake, and metabolism (Wightman and Zimmerman, 1990; Wu et al., 2002; Michael et al., 2005). The kinetic parameters for dopamine, $K_m$ (the Michaelis-Menton constant for uptake) and $V_{max}$ (maximal uptake rate), were previously unattainable due to the time constraints of microdialysis measurements. Monitoring changes in these parameters under different circumstances, such as after cocaine administration (inhibiting uptake) or after receptor blockade, leads to a better understanding of how dopamine neurotransmission functions in the brain (Wu et al., 2001; Garris et al., 2003). Naturally occurring transient increases in dopamine concentration have recently been detected on a subsecond time scale by voltammetric methods (Robinson et al., 2003; Cheer et al., 2004; Robinson and Wightman, 2004; Roitman et al., 2004). These transients are virtually invisible to even the fastest microdialysis measurements, which occur in the minute time scale, nearly 100 times slower than the voltammetric measurements. Real-time dopamine diffusion *in vivo*, volume transmission (Venton et al., 2003), the kinetics of drugs of abuse (cocaine and amphetamine) (Jones et al., 1995; Greco and Garris, 2003), and transient dopamine release (Robinson et al., 2003; Cheer et al., 2004; Robinson and Wightman, 2004; Roitman et al., 2004) are all issues that can only be resolved with the superior temporal resolution afforded by electrochemical methods.

In addition to the superior temporal resolution, electrochemical methods can be used to investigate environments off-limits to larger measuring devices. Microelectrodes, some with dimensions in the single micron range, can measure cellular and subcellular events with ease. Microelectrodes and microsensors have been used in conjunction with numerous electrochemical techniques to monitor the release of different neurochemicals from single cells (Boudko et al., 2001; Kumar et al., 2001; Smith and Trimarchi, 2001). Quantal size and vesicular volume have also been investigated using microelectrodes (Kozminski et al., 1998; Pothos et al., 1998;

Colliver et al., 2000; Pothos et al., 2000), an impossible task for the much larger microdialysis probe. While microdialysis probes may have the excellent selectivity and sensitivity, these devices are much too large to accurately and quickly sample the contents of a neurotransmitter-containing vesicle. Most sampling devices would have to sample the entire cell, diminishing the spatial resolution obtained by using microelectrodes. In addition, selectivity at the cellular level is often not necessary, as cells like the norepinephrine-releasing chromaffin cell only release one neuroactive species (Leszczyszyn et al., 1991; Mosharov et al., 2003). The enhanced spatial resolution of localized neurochemical events is only possible through the use of microelectrodes in conjunction with electrochemical methods.

The small size of the electrodes used for *in vivo* electrochemical measurements makes this device particularly useful as an exploratory probe for use in delicate systems, like the brain and CNS. Evidence of damage to the brain tissue surrounding implanted microdialysis probes suggests that theses devices are too large to use *in vivo* without disrupting the normal anatomy and physiology of the area. Microscopy studies show a hole surrounded by dead cells and broken blood vessels extending at least 1 mm from the site of an implanted microdialysis probe (Clapp-Lilly et al., 1999; Zhou et al., 2001). Recent evidence of disrupted flow through capillaries in the vicinity of implanted microdialysis probes suggests that blood flow and the integrity of the blood-brain barrier may also be compromised near microdialysis probes (Motzko and Michael, unpublished data). On the other hand, ultrastructure of the brain tissue surrounding implanted microelectrodes revealed tracts too small to be followed by light microscopy, with no visible damage except for an occasional neuron with darkened cytoplasm (Peters et al., 2004), suggesting that microelectrodes have little negative impact on the structure of the surrounding tissue. Recently, microelectrodes and cyclic voltammetry were used to monitor dopamine

activity in the vicinity of the microdialysis probe, revealing a gradient of disrupted dopamine release and uptake in the tissue extending at least 220 μm from the microdialysis probe (Borland et al., 2005), supporting the idea that larger microdialysis probes negatively affect both the structure and function of the surrounding tissue. Obviously, the small size of the microelectrode is an advantage not only for studying small environments (cells, vesicles), but for studying intact, functional tissue and systems.

New electrochemical methods and designs continue to develop, producing better, smaller, and faster electrodes, improving this already versatile technique, while simultaneously discovering new features and functions of the brain and other neurochemical environments. Nearly 30 years after Adams and Gonon first began their *in vivo* experiments, thousands of papers demonstrate the versatility and functionality of electrochemistry for *in vivo* detection, with the field continuing to grow, expand and explore new neurochemical arenas.

## 1.3. APPLICATION OF ELECTROCHEMISTRY IN THE NEUROSCIENCES

Electrochemical methods and devices provide superior spatial and temporal resolution in the detection of numerous species *in vivo*, making it a useful tool in the neurosciences. Electrochemical methods have explored the release of neurotransmitters from vesicles (Kozminski et al., 1998; Pothos et al., 1998; Colliver et al., 2000; Pothos et al., 2000), monitored chemical secretion from single cells (Boudko et al., 2001; Kumar et al., 2001; Smith and Trimarchi, 2001), examined the effect of pharmacological manipulation on dopamine release in brain tissue slices (Avshalumov et al., 2003; Avshalumov and Rice, 2003), monitored glutamate activity in the anesthetized brain (Kulagina et al., 1999), and correlated locomotor activity to

changes in dopamine levels in the awake brain (Stuber et al., 2005). The versatility of electrochemical methods extends to its use with other techniques, such as patch clamp and electrophysiology. The scope of electrochemistry in the neurosciences extends as far as the imagination wishes to take it, with many new discoveries lying ahead.

Many neurochemical species have been studied using electrochemistry. The electrochemically active catecholamines, including dopamine, norepinephrine, and their metabolites, are perhaps the most studied neurochemicals. In physiological media (pH 7.4) or *in vivo*, the catechol moiety of the catecholamines is oxidized to an ortho-quinone, as shown in Figure 1.1. Serotonin and its tryptamine-derived metabolites are also electro-active and have been studied *in vivo* with voltammetry and microelectrodes (Daws et al., 1998). The phenollic portion of serotonin and its metabolites is also oxidized, to form a ketone, as shown in Figure 1.1. While not considered "traditional" neurotransmitters, numerous electro-active species play significant roles in the brain and are frequently monitored using electrochemistry. Ascorbic acid, nitric oxide, oxygen, and hydrogen peroxide are easily measured with microelectrodes, with their electrochemical schemes represented in Figure 1.2.

Ascorbic acid is a particularly interesting neurochemical. Levels of ascorbic acid in the brain range from 200-400 μM, making it one of the most prevalent molecules in the brain. Unfortunately, ascorbic acid is oxidized at potentials close to that of dopamine and norepinephrine, often times masking the voltammetric response of these neurotransmitters. The "interferant" effects of ascorbic acid on the electrochemical detection of dopamine can be controlled by increasing the scan rate of the applied potential. Interferent signals from the oxidation of ascorbic acid are decreased by increasing the scan rate because of the slow rate of charge transfer of ascorbic acid at the electrode surface. Ascorbic acid can also interfere with the

reduction of dopamine-o-quinone back to dopamine, resulting in an increase in the dopamine signal at the electrode, but this effect can also be diminished by using a fast scan rate. Despite its reputation as an *in vivo* electrochemical interferant, ascorbic acid is considered by some to be a neuromodulator of catecholamine function in the brain (Christensen et al., 2000; Rebec and Wang, 2001).

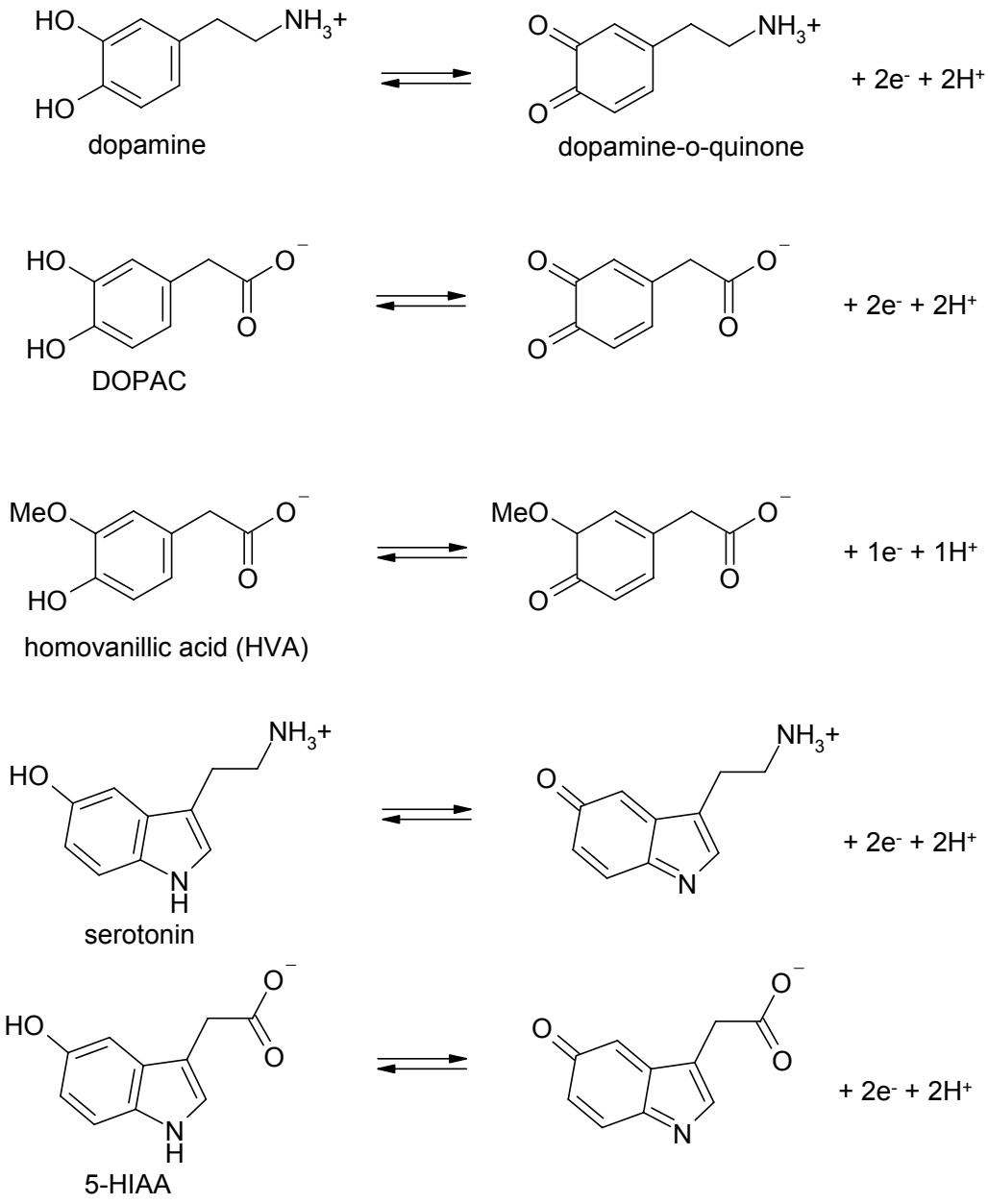


**Figure 1.1. Electroactive neurotransmitters and their metabolites.**

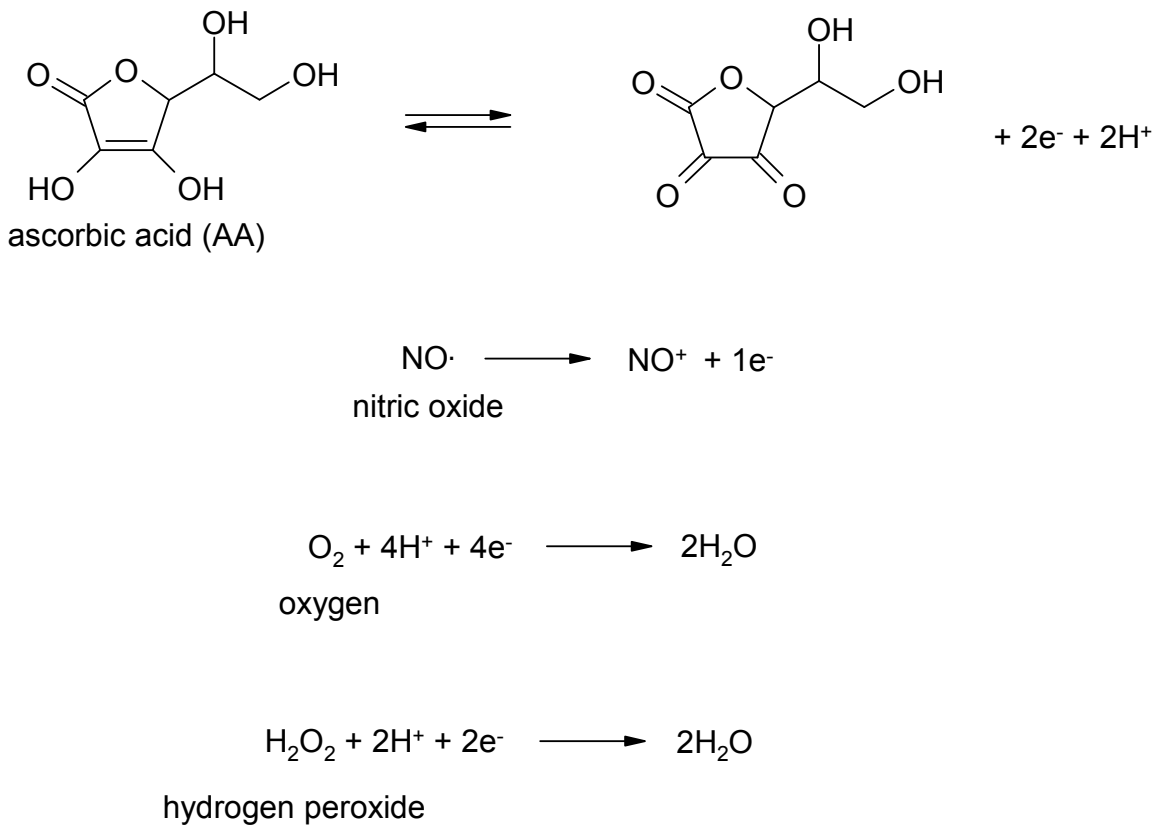


**Figure 1.2. Additional electroactive species found in the brain – ascorbic acid, nitric oxide, oxygen, and hydrogen peroxide.**

The electrochemical methods used in the neurosciences are not exclusive to the detection of neurotransmitters and their metabolites, but includes the detection and measurement of small molecules and biologically significant ions, as well. Ion selective electrodes, such as pH electrodes, are often used *in vitro*, but can be miniaturized for use in various *in vivo* neurochemical applications (Boudko et al., 2001). The Clark oxygen sensor is a small-molecule, rather than ion-selective, electrode that has applicability *in vivo*. Oxygen ($O_2$) is reduced to produce a measurable current at the electrode surface. The oxygen sensor is constructed simply of a membrane-coated platinum wire electrode; however carbon fiber cylinder electrodes have also been used, in place of platinum, to detect oxygen (Kennedy et al., 1992). Nitric oxide (NO) is another small molecule with relevance *in vivo*. Nitric oxide sensors, which strongly resemble

oxygen sensors, have been constructed to study and measure NO in a number of different environments (Zhang et al., 2000; Kumar et al., 2001; Zhang et al., 2002). Another small molecule of interest to neuroscientists is hydrogen peroxide ($H_2O_2$). This molecule is easily detected at carbon fiber or platinum electrodes; however it is often oxidized at the electrode in the same potential window as many other electroactive species. Consequently, a more selective electrode or sensor is required to detect and measure $H_2O_2$ *in vivo*. Luckily, naturally occurring enzymes selective for peroxide are available and can be coupled with electrodes to make a $H_2O_2$ sensor (Kulagina and Michael, 2003).

Electrode selectivity for electroactive compounds like peroxide and ascorbic acid can also be improved with the addition of electrode coatings and additives. Electrode coatings include electrodeposited polymers (1,2 diaminobenzene), electronically conducting polymers (polypyrrole) and polyelectrolytes (Nafion). Coating electrodes with a thin film composed of polyelectrolytes, like Nafion, is a simple method for increasing electrode selectivity to particular analytes *in vivo*. Nafion-coated electrodes are ion-selective, as the anionic composition of the thin Nafion films promotes preferential permeability to cations (Gerhardt et al., 1984; Leszczyszyn et al., 1991). Polyelectrolyte films, along with a number of different conducting and non-conducting electropolymerizable coatings, can also be used to capture or immobilize enzymes on an electrode surface, creating a species-selective sensor (review: Bartlett and Cooper, 1993). Enzyme-based electrochemical microsensors are also used to increase selectivity for electro-active analytes, like peroxide and AA, and to create novel detection schemes for non-electroactive compounds, like glucose, glutamate, choline, and lactate (Kulagina et al., 1999; Cui et al., 2001; Kulagina and Michael, 2003).

Many non-electroactive species, such as glucose, glutamate, lactate and choline, are studied using electrochemistry. In order to measure non-electroactive species, electrodes are constructed with specialized coatings and additives, which selectively generate electrochemical signals in response to a particular analyte. Oxidase enzymes are the most commonly encapsulated or immobilized enzymes for use in electrochemical sensors, particularly in the detection of glucose, glutamate, choline, and lactate. These enzymes catalyse the conversion of a particular substrate between the reduced or oxidized state, which can be then be detected at the electrode surface (Bartlett and Cooper, 1993). These "redox" enzymes typically undergo the following reaction scheme to generate an electrochemically sensitive species, which is monitored at the electrode surface:

substrate(RED) + enzyme(OX) → product(OX) + enzyme(RED)

enzyme(RED) + co-substrate(OX) → enzyme(OX) + co-product(RED)

Oxidase enzymes use oxygen ($O_2$) as the primary co-substrate, generating hydrogen peroxide ($H_2O_2$) as the final co-product, which can be electrochemically oxidized at the electrode surface. Ideally, the rate of $H_2O_2$ production is directly related to the concentration of the analyte detected by the enzymes at the electrode. For example, the oxidation of glutamate and subsequent oxidation of $H_2O_2$ is as follows:

glutamate + GluOx(OX) → α-ketoglutarate + $NH_3$ + GluOx(RED)

GluOx(RED) + $O_2$ → GluOx(OX) + $H_2O_2$

At electrode surface: $H_2O_2 \rightarrow 2H^+ + O_2 + 2e^-$

In this type of electrochemical sensor, the redox enzymes are immobilized in thin films so as to decrease the distance $H_2O_2$ has to travel to electrode surface to be oxidized. Thin films assist in limiting peroxide diffusion or superfluous reaction of $H_2O_2$, which would result in low sensor

sensitivity. The response time of the electrode also decreases with decreasing film thickness, as the diffusion distance of the substrate into the film to react with the enzyme decreases (review: Heller, 1992). Thin films of encapsulated or immobilized redox enzymes are often used electrochemical methods of detection that could be easily and readily extended for use in the neurosciences.

There is another type of electrochemical sensor that utilizes enzymes for detection of different species, but does not require immobilization of the enzyme on the electrode surface. This type of sensor, instead, "wires" enzymes to the electrode using a cross-linked polymeric redox macromolecule composed of a poly(vinylpyridine) complexed to $Os(bpy)_2Cl$ (Gregg and Heller, 1990; Heller, 1992; Kulagina et al., 1999; Kulagina and Michael, 2003). The redox polymer forms a three-dimensional gel that incorporates, but does not immobilize, enzymes, while at the same time allowing for rapid in and out diffusion of substrates and products. Electrons transferred during the reduction of the enzyme are rapidly "wired" through the redox centers of the polymer to the electrode surface and are detected as changes in the current response. Electrochemical sensors of this nature can be constructed to detect and measure different non-electroactive species simply by changing the functional enzyme, from glutamate oxidase to choline oxidase. One type of enzyme-wired electrode for the detection of glutamate utilizes a cascade consisting of a glutamate oxidase and horseradish peroxidase (HRP). HRP is used in this sensor to reduce the $H_2O_2$ produced by the glutamate oxidase reaction with glutamate. The HRP subsequently oxidizes the osmium redox polymer, generating a current change in response to glutamate detection (Kulagina et al., 1999)

It should be mentioned that electrochemistry is used in the neurosciences in many capacities, most commonly as an end-line detector for sampling and separation devices, like

microdialysis and HPLC; however, this introduction will focus on the utility of this technique as an *in vivo* analytical device. The benefits of using microelectrodes coupled to voltammetry *in vivo* include real-time, microsecond recording and improved spatial resolution. The small size of microelectrodes also limits implantation-induced damage to the brain tissue, while still allowing for extremely fast recording of analytes in the nanomolar concentration range. The numerous features that make microelectrodes excellent tools for *in vivo* electrochemical applications in neuroscience will be described in more detail later in this introduction. This introduction will concentrate on the applications of electrochemical methods *in vivo*, but with the awareness that microelectrodes and electrochemical detection is also widely used in other capacities in the neurosciences.

## 1.4. ELECTROCHEMISTRY FUNDAMENTALS

In the most basic sense, chemical reactions that produce or consume electrons are deemed electrochemical reactions. Corrosion of a metal car bumper is an electrochemical process (oxidation). The batteries that power virtually every gadget we use, from laptop computers, to cell phones, to portable CD players, rely on electrochemical reactions to function. A flow of electrons is required for the cells in our body to generate ATP *via* oxidative phosphorylation. This section will briefly describe the fundamentals behind some of the commonly used electrochemical methods for *in vivo* neurochemical detection.

Electrochemical processes occur at electrode surfaces. These processes are oxidation, the transfer of an electron away from an analyte, and reduction, the addition of an electron to an analyte. Oxidation or reduction can occur at an electrode surface when an applied potential

approaches the potential where the analyte is oxidized or reduced, known as the formal potential. Rapid electron transfer at the electrode surface is necessary for analytical electrochemical measurements; otherwise the electrochemical information used for identification of the analytes, such as the oxidation or reduction potentials, will be obscured and indecipherable. Current, i, is the rate at which electrons are moved from the analyte to the electrode,

$$\mathrm{i} = \frac{\partial \mathrm{Q}}{\partial t} = \frac{nF\partial \mathrm{N}}{\partial t} \qquad \textbf{Equation 1}$$

where Q is charge, n is number of electrons, F is Faraday's constant, and N is moles of analyte. From this relationship, we can see that current is dependent upon the concentration of analyte at the electrode surface. The movement of the analyte of interest from its local environment to the electrode surface is dictated largely by diffusion, or random molecular motion. The rate of electrolysis of the analyte, or flux (J), is dependent upon the diffusion coefficient (D) for the analyte and the concentration gradient (dC/dx) that develops at the electrode surface. This relationship is stated in Fick's first law (Equation 2):

$$\mathrm{J} = \frac{-\mathrm{D}\partial C}{\partial x} \qquad \textbf{Equation 2}$$

The magnitude of the current response can now be defined as the flux of the analyte to the electrode surface. Current produced at the electrode surface can come from the solution itself, known as the charging current, or from the oxidation or reduction of an analyte, known as the faradaic current. Charging current arises from additional electrochemical processes at the electrode surface, particularly the build up of potential differences between the solution and the electrode. The electrode is said to behave like a capacitor in this instance, with the charging current, sometimes referred to as capacitive current, being proportional to the area of the electrode. All current, faradaic or charging, is dependent upon the applied potential of the

electrode, which plays a large role in dictating the rate of the electron transfer and subsequent electrolysis of the analyte.

The simplest method for monitoring the current produced by an analyte at an electrode surface is chronoamperometry, which is the monitoring of current with respect to time. In chronoamperometry, the applied potential of the electrode is stepped up from a "resting" potential, where little to no electrolysis of the analyte occurs, to an applied potential higher than the formal potential of the analyte, which causes oxidation of the analyte. The stepped potential is diagrammed in Figure 1.3A. The current monitored during the potential step ($E_2$) is directly proportional to the concentration of the analyte. Chronoamperometry under diffusion controlled conditions, such as those present in most neuroscience applications, produces a specific current-time response as stated in the Cottrell equation (Equation 3):

$$i(t) = \frac{nFA\sqrt{D_o}C_o}{\sqrt{\pi \cdot t}} \qquad \textbf{Equation 3}$$

where A is the electrode surface area, $D_o$ is the diffusion coefficient for the analyte, $C_o$ is the concentration of the analyte and t is time. The concentration profile for an analyte being oxidized in a chronoamperometric experiment is diagrammed in Figure 1.3C. The current versus time response for a chronoamperometric experiment is shown in Figure 1.3B.

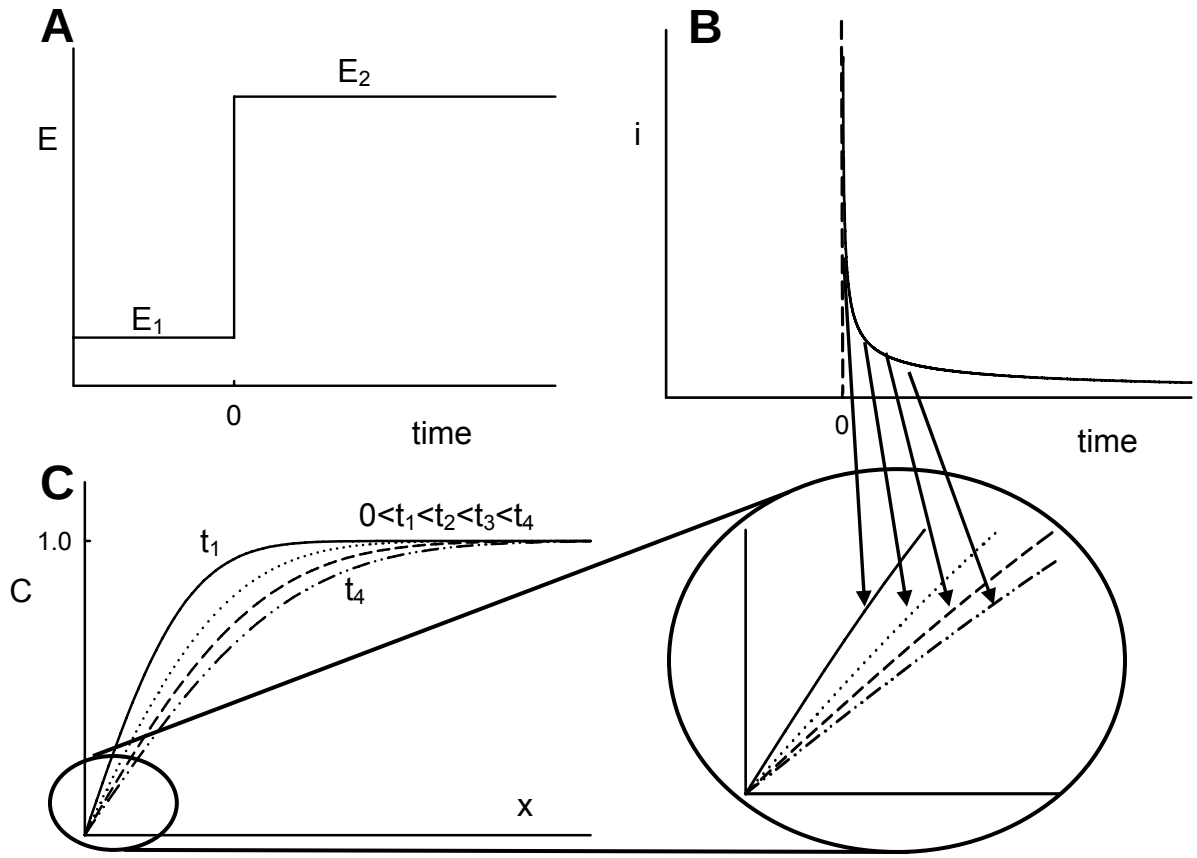


**Figure 1.3. A. Diagram of the step potential used in chronoamperometry. B. Current vs. time response generated in a chronoamperometric experiment. C. Concentration profile for times after the start of the chronoamperometric experiment. Circled Inset: The decrease in the current response during the experiment corresponds to a decrease in the slope of the concentration, as described by the Cottrell equation (Equation 3).**

An alternative of chronoamperometry, normal pulse voltammetry (NPV), uses a multi-step, or multi-pulse, potential profile to oxidize or reduce analytes. Just as in chronoamperometry, the electrode is held at a resting potential ($E_1$) and stepped up to a higher, oxidizing potential ($E_2$). After a designated length of time, the step is ended and the potential is dropped back down to the resting potential. After an interval at the resting potential, the potential is stepped back up to a potential ($E_3$) higher than the first step ($E_2$), where it is held for the same time interval as the previous step before dropping back to the resting potential again.

This potential profile, or waveform, is diagrammed in Figure 1.4. The current produced during each step is proportional to the analyte concentration, as in chronoamperometry. Normal pulse voltammetry has the added benefit of limited electrode fouling or filming and prevents accumulation of excess oxidized analyte, which can be neurotoxic. This is due to the stepping down of the potential at each step, which reduces the newly produced oxidized analyte species. Also, NPV can be used to help identify the electrolyzed species through examination of the ratio of oxidation to reduction current for the species.

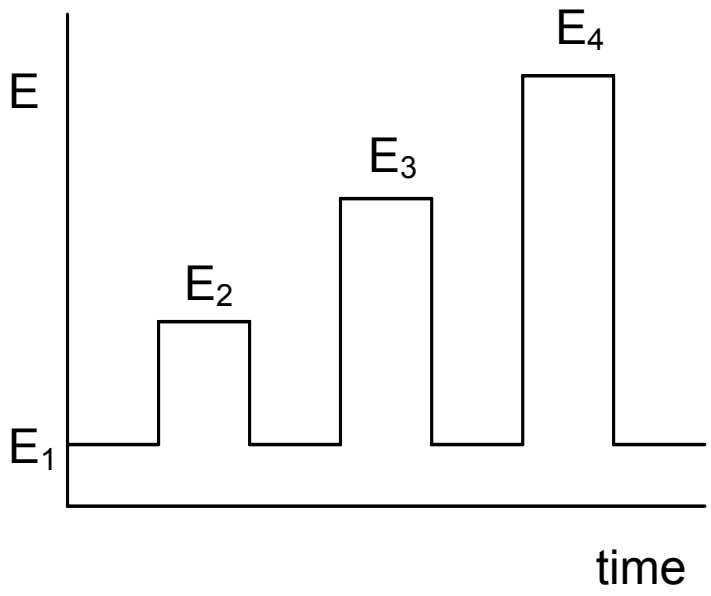


**Figure 1.4. Diagram of the potential waveform used in normal pulse voltammetry.**

Differential pulse voltammetry (DPV) is another electrochemical technique that can provide increased sensitivity and more efficient differentiation and resolution of different species. This technique resembles normal pulse voltammetry, but with a few modifications. The potential waveform for DPV is diagrammed in Figure 1.5A. DVP differs from NPV in that the resting potential does not return to the initial potential, but changes with each step. This new

resting potential is often referred to as the "base" potential. The step rises in DVP are also kept relatively small in comparison to NPV, ranging from 10 – 100 mV per step, and are kept constant in respect to the base potential. Unlike NPV, the current is sampled immediately before the potential is stepped up ($i_a$) and immediately before the potential is stepped down ($i_b$). The difference between these current responses, ($i_b$-$i_a$), is plotted against base potential to produce a DPV voltammogram. The DPV produces a peaked current-potential plot, or voltammogram, which provides a more qualitative description of the electrolyzed species, leading to increased selectivity and easier identification. An example of the DPV voltammogram is shown in Figure 1.5B.

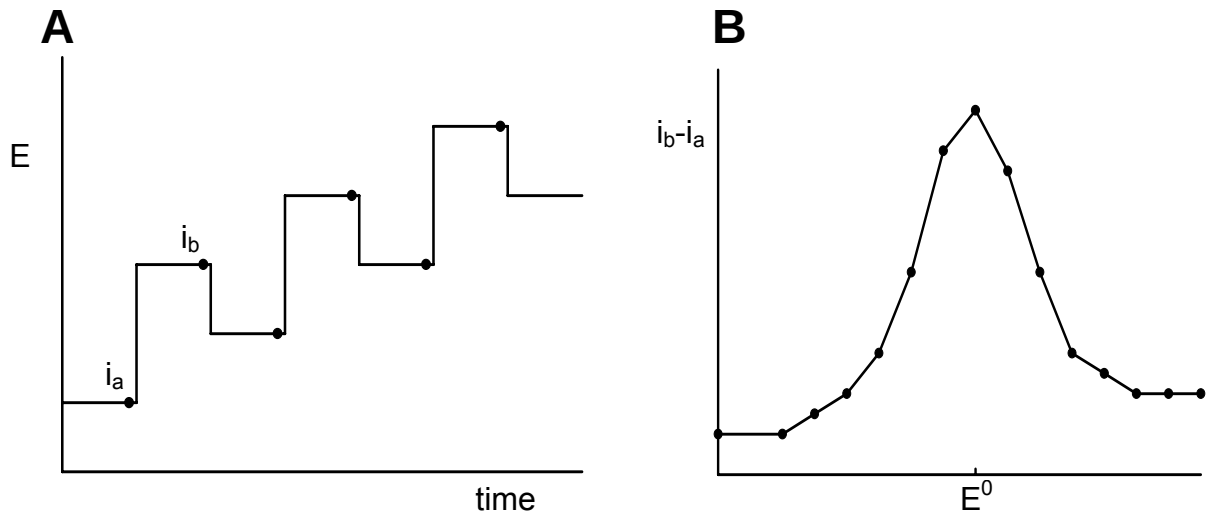


**Figure 1.5. A. Diagram of the potential waveform used in differential pulse voltammetry. B. Differential pulse voltammogram.**

Chronoamperometry, NPV, and DPV measure current with respect to time; however, increased sensitivity and selectivity can be achieved with yet another electrochemical method, linear sweep voltammetry (LSV). In this method, the potential applied to the electrode is increased progressively over a designated time interval. The current is monitored as a function of the applied potential, producing a voltammogram. The waveform and resultant voltammogram for an analyte electrolyzed by LSV is displayed in Figure 1.6A and B. The voltammogram contains much information about the electrolyzed species. The height of the oxidation peak of the voltammogram is proportional to the analyte concentration, while the potential at the point of maximum slope of the voltammogram is the formal potential of the analyte, which is used in identifying the electrolyzed species. Linear sweep voltammetry can be used in reverse, to regenerate the original analyte be reducing the oxidized form of the analyte. The method of sweeping the potential forward to oxidize and then sweeping the potential back to reduce the newly produced oxidant is called cyclic voltammetry. A waveform and voltammogram generated from a cyclic voltammetry experiment are shown in Figure 1.6A and B. Careful examination of cyclic voltammograms produced *in vivo* can provide qualitative information for distinguishing a mixture of analytes without additional separation. For example, increasing the potential scan rate eliminates the current response of ascorbic acid, which would normally overlap with that of the catecholamines, like dopamine. This method is used frequently in the neurosciences and can be used to obtain much information, including reaction kinetics, electrode properties and quantitative measurement of numerous species.

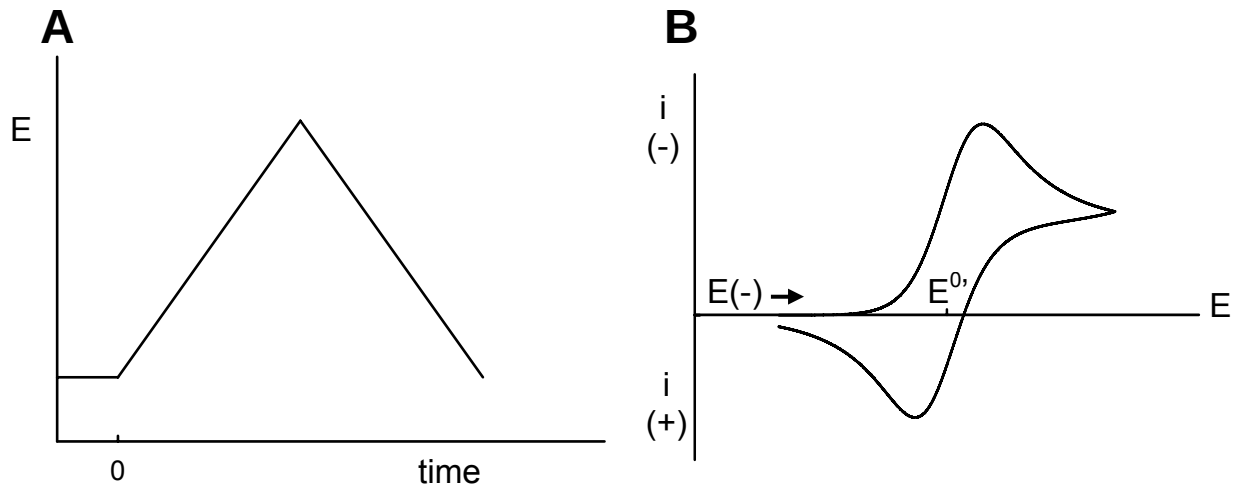


**Figure 1.6. A. Diagram of a potential waveform used in linear sweep (cyclic) voltammetry. B. A cyclic voltammogram.**

## 1.5. THE BENEFICIAL PROPERTIES OF MICROELECTRODES

The device that makes *in vivo* electrochemistry possible is the ultramicroelectrode (review: Wightman, 1981). Small electrodes produce small currents, which enables microelectrodes be used in solutions of high resistance, like those found in physiological media or the brain. The time scale of an experiment utilizing microelectrodes is also quite small, due to the reduced size of the diffusion layer the analyte must penetrate to reach the electrode surface. The charging, or capacitive, current of an electrode decreases exponentially with a decrease in the surface area, while the time-dependent faradaic current decreases linearly with surface area, thus resulting in an increase in the faradaic to charging current ratio, which translates to rapid measurements. Catalytic reactions, where O → R → O, such as that which occurs when dopamine is oxidized in the presence of ascorbic acid, produce less interference at microelectrodes. This occurs because the average distance the reduced species can diffuse is larger than the radius of the

microelectrode, so only a minimal amount of regenerated oxidant is formed at the electrode surface, contributing only minimally to the measured current. Electrochemical measurements *in vivo* are certainly dependent on microelectrode size, in which smaller is better.

Besides the electrochemical benefits of smaller electrodes, single-digit-micron sized electrodes do much less damage to nervous system tissue than larger, hundred-micron sized devices (as described in detail in a previous section). The small size also allows greater spatial resolution, allowing investigators to get closer to sites of relevance, like vesicles, synapses, and single cells. Over the years, microelectrodes have been constructed from different materials and in many shapes of electrodes for *in vivo* electrochemical experiments. Adams' original electrodes were disk-shaped, constructed from graphite paste pressed and sealed into a plastic or glass mold (Adams, 1976). Disk-shaped electrodes are still used; however the graphite paste has been replaced by cut and polished carbon fibers encased in glass capillaries. Perhaps the most common and popular electrode, today, is the carbon fiber cylinder electrode (Kovach et al., 1984). This microelectrode is easily constructed from commercially available carbon fibers pulled and sealed into glass capillaries. They are available commercially, but are regularly fabricated in the laboratory with little labor or cost. The next generation of electrodes for neuroscience application may involve the use of carbon nanotubes, platinum nanowires constructed using nanolithography, or even composites of nanoparticles. Recent advances point to trends involving increased miniaturization of these already micro-sized electrodes.

## 1.6. CONCLUSION

Electrochemical methods are versatile tools for detecting, monitoring and measuring various neurochemical species. Microelectrodes, in conjunction with the electrochemical techniques presented within this chapter, have been used to explore environments too small or too fragile to be examined by many other devices. Electrochemical techniques have also been used to examine chemical phenomena on a subsecond time scale, providing new kinetic information and real-time measurements of neurochemical events. Overall, the ease of use and flexibility in application make electrochemical methods ideal for studies requiring superior temporal and spatial resolution of neurochemicals in physiological environments.

# 2. VOLTAMMETRIC STUDY OF EXTRACELLULAR DOPAMINE NEAR MICRODIALYSIS PROBES ACUTELY IMPLANTED IN THE STRIATUM OF THE ANESTHETIZED RAT

## 2.1. ABSTRACT

Establishing in vivo microdialysis methods for the quantitative determination of dopamine concentrations in the extracellular space of the brain is an important yet challenging objective. The source of the challenge is the difficulty in directly measuring the microdialysis recovery of dopamine during an in vivo experiment. The recovery value is needed for quantitative microdialysis, regardless of whether conventional or no-net-flux methods are used. Numerical models of microdialysis that incorporate both diffusion and active transport processes suggest that dopamine recovery is strongly affected by processes occurring in the tissue closest to the probe. Some evidence suggests that the tissue adjacent to the probe becomes disrupted during probe implantation. Hence, the objective of the present study was to further identify whether the tissue adjacent to the probe is disrupted and, if so, whether that disruption might affect dopamine recovery. The experiments were conducted with microdialysis probes implanted acutely in the striatum of rats anesthetized with chloral hydrate. Carbon fiber voltammetric microelectrodes were used to monitor extracellular dopamine at three sites near the probes; immediately adjacent to the probe, 220-250 μm from the probe, and 1 mm from the probe. Probes were lowered slowly over a 30-min period, so that dialysate dopamine levels were stable, in the low nanomolar range, and partially TTX-sensitive by the time experiments began. Starting 2 hr after probe

implantation, dopamine was monitored by fast-scan cyclic voltammetry during electrical stimulation of the medial forebrain bundle and during administration of the dopamine uptake inhibitor, nomifensine. The findings of this study show that a gradient of dopamine release and uptake activity extends at least 220 μm from microdialysis probes implanted acutely in the striatum of the anesthetized rat.

## 2.2. INTRODUCTION

Microdialysis has been employed over the past several years to sample dopamine from the extracellular space of the brain (Parsons and Justice, 1992; DiChiara et al., 1996; Camp et al, 1997; Bradberry, 2002). Nevertheless, quantitative determination of the extracellular dopamine concentration is challenging because existing methods for in vivo calibration of the probes are not so simple (Tang et al., 2003). Without in vivo calibration of the probe, it is not possible to know the relative recovery of dopamine, which is necessary for quantification by both conventional and no-net-flux microdialysis. Conventional microdialysis involves the determination of concentrations in dialysate collected with unmodified perfusion fluid. No-net-flux microdialysis involves reverse dialysis to find the point at which the concentration at the probe outlet, $C_d^{out}$, is the same as the concentration at the probe inlet, $C_d^{in}$. Originally, it was thought that the no-net-flux concentration, $C_{nnf}$, should provide a quantitative measure of the concentration in the external medium, $C_e^{\infty}$, where the infinity symbol denotes concentrations far from the probe (Lonnroth et al., 1987; Bungay et al., 1990; Morrison et al., 1991).

However, where the in vivo microdialysis of dopamine is concerned, some recent studies have raised the question of whether $C_{nnf}$ does in fact equal $C_e^{\infty}$ (Peters and Michael, 1998; Yang et al.,

1998; Lu et al., 1998; Yang et al., 2000; Bungay et al., 2003; Chen, 2005). These studies suggest instead that the relationship between $C_{nnf}$ and $C_e^{\infty}$ is:

$$C_e^{\infty} = \frac{E \cdot C_{nnf}}{R} \qquad \textbf{Equation 4}$$

where E and R are the extraction fraction and relative recovery, respectively. According to Equation 4, $C_{nnf}$ is a quantitative measure of $C_e^{\infty}$ only when the extraction fraction and relative recovery are equal to one another. In many examples of microdialysis (e.g. Zhao et al., 1995; Song and Lunte, 1999) the extraction fraction and relative recovery are equal to each other and it is appropriate to use the no-net-flux method for quantitative analysis. In cases where the relative recovery has not been measured, however, caution is necessary when assuming that E equals R (Peters and Michael, 1998; Yang et al., 1998; Lu et al., 1998; Yang et al., 2000; Bungay et al., 2003; Chen, 2005a).

In general, there are two contributions to the concentration at the outlet of a microdialysis probe; the concentration recovered from the medium external to the probe and the concentration in the perfusion fluid that is not lost due to extraction:

$$C_d^{out} = (1 - E) \cdot C_d^{in} + R \cdot C_e^{\infty}$$

Data collected during reverse dialysis procedures are usually represented on a concentration difference plot (Figure 2.1), the form of which is obtained by rearranging the previous expression:

$$C_d^{in} - C_d^{out} = E \cdot C_d^{in} - R \cdot C_e^{\infty} \qquad \textbf{Equation 5}$$

Equation 4 is obtained by rearranging Equation 5 after setting the left-hand side to zero. Equation 5 also shows that the slope of the concentration difference plot gives the extraction fraction:

$$E = \frac{\Delta y}{\Delta x} = \frac{\Delta(C_d^{in} - C_d^{out})}{\Delta C_d^{in}}$$

which is evaluated by dividing the vertical distance by the horizontal distance (the 'rise-over-run') between two reference points on the line (Figure 2.1):

$$E = \frac{\left(C_d^{in} - C_d^{out}\right)_2 - \left(C_d^{in} - C_d^{out}\right)_1}{\left(C_{d\,2}^{in} - C_{d\,1}^{in}\right)}$$

where the subscripts 1 and 2 identify the reference points. Usually, but quite arbitrarily, the point of no-net-flux is chosen as one of the reference points, so:

$$(C_d^{in} - C_d^{out})_1 = 0 \quad \text{and} \quad C_{d\,1}^{in} = C_{nnf}$$

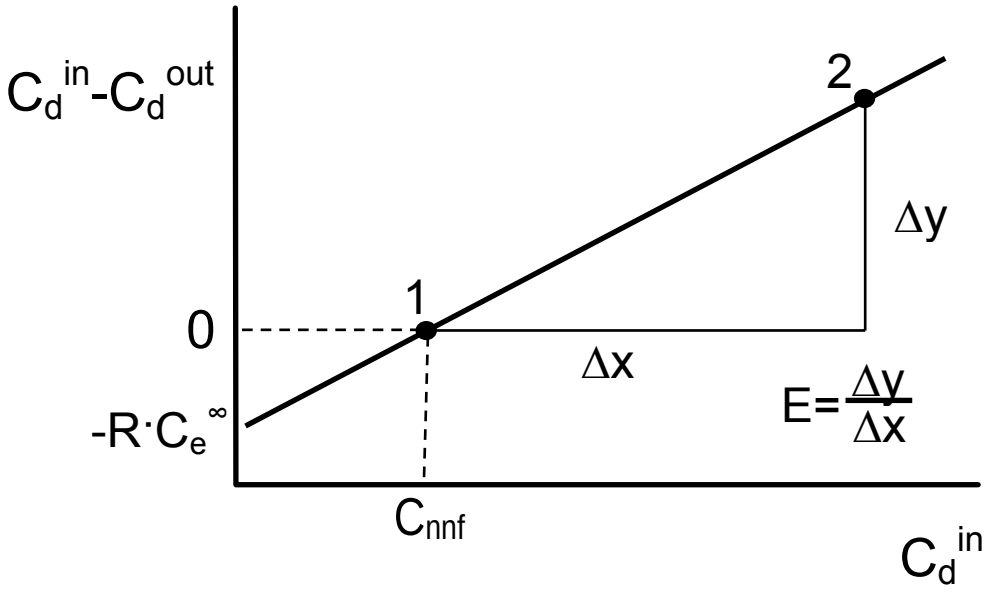


**Figure 2.1. Schematic to illustrate how the extraction fraction is obtained from the slope of the concentration differences plot. When the point of no-net-flux, labeled 1 on the plot, is used as a point of reference, Equation 5 of the text is obtained. Note that the relative recovery, R, is contained only in the y-intercept of the plot. Terms are defined in the text.**

and E becomes:

$$E = \frac{\left(C_d^{in} - C_d^{out}\right)_2}{\left(C_{d\ 2}^{out} - C_{nnf}\right)}$$

which is normally written without the subscript 2:

$$E = \frac{C_d^{in} - C_d^{out}}{C_d^{out} - C_{nnf}} \qquad \textbf{Equation 6}$$

While E is can be determined explicitly from the slope of the concentration difference plot, the situation is not so straightforward for the recovery. The recovery is contained within the intercept of the concentration difference plot, i.e. where $C_d^{in} = 0$ and $C_d^{out}$ is the value from conventional microdialysis:

$$R = \frac{C_{d\ \ conventional}^{out}}{C_e^{\infty}} \qquad \textbf{Equation 7}$$

Equation 7 shows that the relative recovery cannot be found unless $C_e^{\infty}$ is independently known, and vice versa. Equations 4 and 7 are expressions that contain two unknown quantities and so cannot be further solved, which explains why in vivo calibration is necessary for quantitative analysis by both conventional and no-net-flux microdialysis.

In the case of dopamine, it has been suggested that the extraction fraction and relative recovery may not be equal during in vivo microdialysis (Peters and Michael, 1998; Yang et al., 1998; Lu et al., 1998; Yang et al., 2000; Bungay et al., 2003; Chen 2005a). Briefly, we hypothesize that this is a consequence of the ability of dopamine uptake to promote dopamine extraction but inhibit dopamine recovery. Exactly how and why this occurs, however, remains to be fully and quantitatively explained (Chen 2005b). For example, some evidence suggests that a layer of traumatized tissue adjacent to the microdialysis probe (Clapp-Lilly et al., 1999; Zhou et

al., 2001) also contributes to the difference between E and R (Yang et al., 2000; Tang et al., 2003; Bungay et al., 2003). Mathematical models of microdialysis that incorporate diffusion, active transport, and a trauma layer adjacent to the probe support the idea that the extraction and recovery values may not be the same (Yang et al., 2000; Bungay et al., 2003; Chen 2005a). In contrast, Chen (2005b) suggests that a minor trauma layer (a 40% loss of dopamine release in a 20-μm thick trauma layer) will not cause dopamine recovery to be suppressed by dopamine uptake. Hence, it remains to be determined if the trauma layer that exists during in vivo microdialysis experiments is sufficient to compromise quantitative measurements of extracellular dopamine levels.

The objective of the present study was to obtain more information about the situation that exists during acute in vivo microdialysis experiments in the striatum of anesthetized rats. Previously, (Lu et al., 1998; Yang et al., 1998) we placed carbon fiber microelectrodes immediately adjacent to and 1 mm from the microdialysis probes. In the present study, we also positioned microelectrodes at a distance of 220-250 μm from the probes. We monitored evoked dopamine release during electrical stimulation of the medial forebrain bundle (MFB) prior to probe implantation, after implantation, and after administration of a dopamine uptake inhibitor (nomifensine, 20 mg/kg i.p.). In addition, voltammetry and microdialysis were used to monitor dopamine simultaneously, without electrical stimulation, after nomifensine administration.

## 2.3. MATERIALS AND METHODS

### 2.3.1. Analytical techniques

Voltammetric microelectrodes (7 μm in diameter, 400 μm in length) were prepared and used exactly as described before (Yang et al, 1998). Individual carbon fibers (Thornell T300, Amoco Performance Products, Inc., Greenville, SC, USA) were sealed with epoxy into pulled glass tubes and trimmed to a length of 400 μm. Electrodes were calibrated before and after in vivo experiments in an artificial cerebrospinal fluid (aCSF; 145 mM $Na^+$, 1.2 mM $Ca^{2+}$, 2.7 mM $K^+$, 1.0 $Mg^{2+}$, 152 mM $Cl^-$ and 2.0 mM phosphate adjusted to pH 7.4) containing known concentrations of dopamine. Dopamine was detected by fast-scan cyclic voltammetry (Yang et al., 1998). Voltammetric currents recorded *in vivo* were converted to units of dopamine concentration by postcalibration of the microelectrodes if the background subtracted voltammograms were consistent with the in vivo detection of dopamine (Baur et al., 1988; Borland and Michael, 2004).

Vertical concentric microdialysis probes (220 μm o.d., 4 mm long) with an integrated carbon fiber microelectrode mounted on the outer surface (Figure 2.2) were constructed with hollow fiber dialysis membrane (Spectra-Por RC Hollow Fiber, MWCO: 13,000, 160 μm i.d., Spectrum Laboratories Inc., Rancho Dominguez, CA, USA) and fused silica outlet lines (150 μm o.d., 75 μm i.d., Polymicro Technologies, Phoenix, AZ, USA). The integrated carbon fiber microelectrode (800 μm long) was mounted immediately adjacent to the outer surface of the microdialysis membrane, exactly as described before (Yang et al., 1998). For simplicity of notation, we call the combined microdialysis-voltammetry probe a 'dialytrode.'

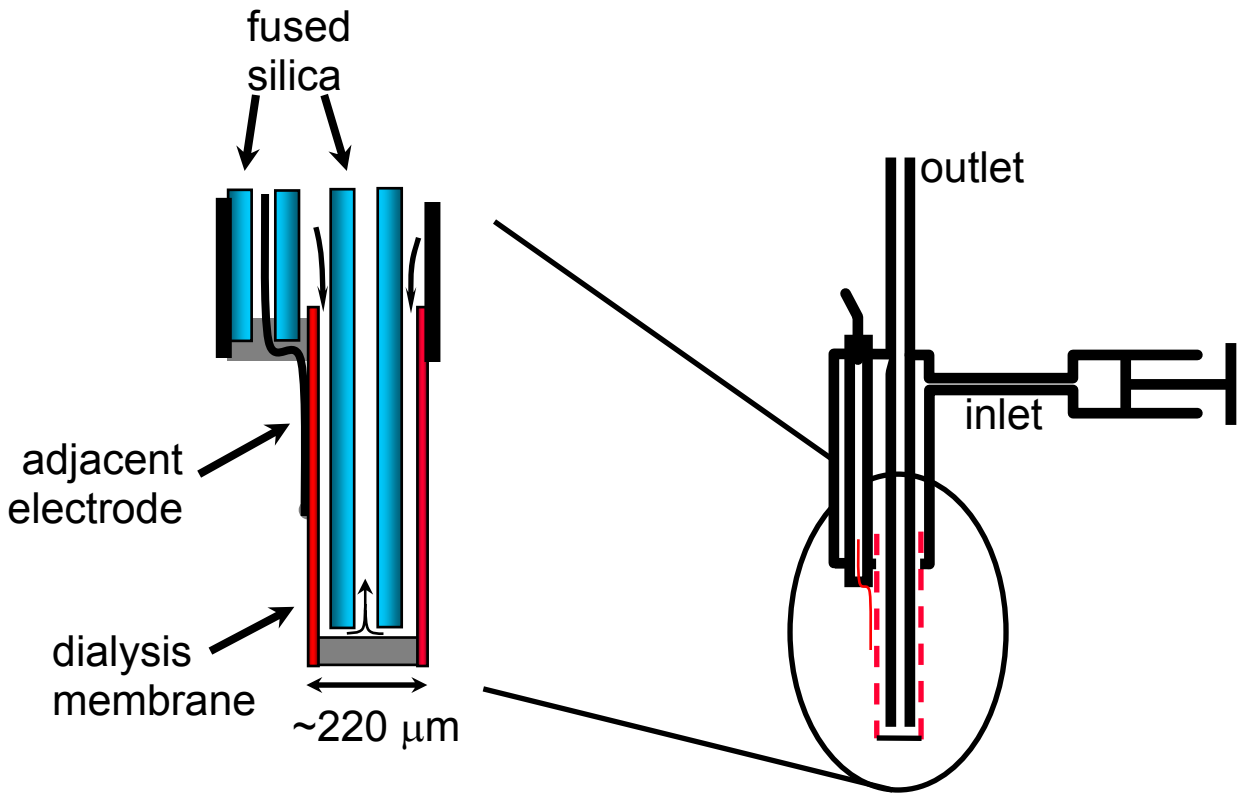


**Figure 2.2. Schematic to illustrate how the carbon fiber microelectrode is incorporated into the design of the microdialysis probes used during this work. The microelectrode is placed immediately adjacent to the outer surface of the probe and held in place with a minimal amount of epoxy applied to the tip of the electrode. The combined device is called a dialytrode in the text.**

### 2.3.2. Animals and surgical procedures

All procedures involving animals were conducted with approval of the Institutional Animal Care and Use Committee of the University of Pittsburgh. Male Sprague-Dawley rats (250-375 g, Hilltop, Scottdale, PA, USA) were anesthetized with chloral hydrate (initial dose of 300 mg/kg i.p. with additional doses of 50 mg/kg i.p. as needed to maintain anesthesia) and wrapped in a homeothermic blanket (EKEG Electronics, Vancouver, BC, Canada). The rats were placed in a stereotaxic frame (David Kopf Instruments, Tujunga, CA, USA) with the incisor bar set at 5 mm

above the interaural line (Pellegrino et al., 1979) and appropriately placed holes were drilled through the skull. Electrical contact between brain tissue and a Ag/AgCl reference electrode was established with a salt bridge (a plastic pipet tip plugged with tissue paper and filled with PBS).

### 2.3.3. Evoked dopamine release immediately adjacent to and 1 mm from microdialysis probes

Carbon fiber microelectrodes were implanted at two sites in the striatum, separated by a distance of 1 mm in the sagital plane. The posterior site was 1.8 mm anterior to bregma, 2.5 mm lateral from midline, and 4.5 mm below dura. The anterior site was 1 mm anterior to the first location. A stainless steel bipolar stimulating electrode (MS303/1; Plastics One, Roanoke, VA, USA) was lowered towards the ipsilateral MFB until evoked dopamine release produced a response of at least 30 nA in amplitude at both voltammetric electrodes. The optically isolated stimulus waveform was a biphasic, constant-current square wave with a pulse duration of 2 ms, a pulse height of 280 μA, a frequency of 45 Hz, and a train length of 25 s. Stimuli were delivered at 20-min intervals.

Once stable stimulus responses were established at both electrodes, the microelectrode was removed from the anterior site and replaced with a dialytrode. The dialytrode was lowered over a period of 30 minutes until its tip was 7.0 mm below dura. By this procedure, the tip of the integrated carbon fiber was lowered to approximately the same depth as the original stand-alone microelectrode. The dialytrodes were perfused with aCSF at a rate of 0.109 μL/min. Electrical stimulation of the MFB recommenced 2 hrs after placement of the dialytrode and continued at 20-min intervals. Nomifensine (20 mg/kg i.p.) was administered 5 min after the third stimulus, and a post-drug response was recorded 20 min later.

### 2.3.4. Evoked dopamine release 220-250 μm from microdialysis probes

In a separate series of experiments, evoked dopamine release was monitored with a microelectrode positioned 220-250 μm from a microdialysis probe. For these experiments, it was necessary to implant the microelectrode at an angle of $5^{o}$ from the vertical to prevent the barrel of the electrode from colliding with the body of the microdialysis probe. Due to this angle, the bottom of the carbon fiber was approximately 220 μm from the outer surface of the microdialysis probe while the top of the fiber was approximately 250 μm from the probe. The microelectrode was positioned in the striatum and a stimulating electrode was lowered into the MFB until a response of at least 30 nA was established using the same stimulus parameters as described above. The microdialysis probe was implanted over a period of 30 min to the following coordinates: 2.5 mm anterior to bregma, 2.5 mm lateral to from midline and 7.0 mm below dura. The probe was perfused at 0.109 μL/min. Electrical stimulation of the MFB recommenced 2 hrs after placement of the probe and continued at 20-min intervals. Nomifensine (20 mg/kg i.p.) was administered 5 min after the third stimulus was delivered, and a post-drug response was recorded 20 min later.

### 2.3.5. Effect of uptake inhibition on nonevoked dopamine levels near microdialysis probes

Microelectrodes and dialytrodes were implanted in the striatum by the procedures explained above. The dialytrodes were perfused with aCSF at 0.586 μL/min for two hours, after which the

collection of 20-min microdialysate samples began. Nomifensine (20 mg/kg i.p.) was administered just after the collection of the third 20-min microdialysate sample, with adjustment for the time needed for the dialysate sample to pass through the probe's outlet line. FSCV recording continued *in vivo* throughout. In a separate group of animals, tetrodotoxin (TTX) was added to the perfusion fluid.

The dopamine concentration in microdialysate samples was determined by means of HPLC and electrochemical detection (BAS, West Lafayette, IN). The small-bore column (1.0 mm in inner diameter and 100 mm in length) was packed with $C_{18}$ stationary phase on 3-μm particles. The mobile phase (50 mM sodium phosphate, 0.1 mM sodium EDTA, 2.6 mM sodium octylsulfate, 5.0 mM triethylamine and 15% methanol (v/v), pH 5.6) was delivered at a flow rate of 70 μL/min. Dopamine was detected at an applied potential of 650 mV vs Ag/AgCl.

### 2.3.6. Drugs and solutions

Chloral hydrate, nomifensine, and dopamine were used as received from Sigma (St. Louis, MO, USA). Chloral hydrate and nomifensine were dissolved in phosphate buffered saline (PBS; 155 mM NaCl, 100 mM phosphate, pH 7.4). All solutions were prepared with ultrapure water (NANOPure; Barnstead, Dubuque, IA, USA).

## 2.4. RESULTS

### 2.4.1. Impact of probe implantation on evoked dopamine release

Voltammetric responses to electrical stimulation of the MFB were noticeably different at the three recording sites (see Figure 2.3 for individual representative responses). Prior to implantation of a microdialysis probe, electrical stimulation of the MFB evoked voltammetric responses of similar amplitude at pairs of carbon fiber microelectrodes placed 1 mm apart in the ipsilateral striatum (solid lines in Figure 2.3, A and C). There was no significant difference between the response amplitudes observed at the posterior and anterior sites, 17.9 ± 8.8 μM and 15.9 ± 7.4 μM (mean ± standard deviation, n = 12 rats), respectively.

After the preliminary stimulus responses had been recorded, the microelectrode was removed from the anterior site and replaced with a dialytrode. The microelectrode at the posterior site was not disturbed during this operation. The stimulus response amplitude recorded at the posterior site 2 hr after probe implantation (12.5 ± 7.5 μM; mean ± s.d., n=12), was noticeably but not significantly smaller than the response amplitude recorded before probe implantation (Fig. 2.3A). Probe implantation caused nearly a 10-fold decrease of, but did not completely abolish, the evoked response at microelectrodes positioned 220-250 μm from the probe (Fig. 2.3B). The response amplitudes observed after probe implantation were 12.6 ± 8.3 % (mean ± s.d., n=5) of those recorded before probe implantation. The decrease was significant (t-test, $p<.001$). No evoked responses were observed at the microelectrodes mounted on dialytrodes (Fig. 2.3C), suggesting that evoked dopamine release is completely abolished near the probes.

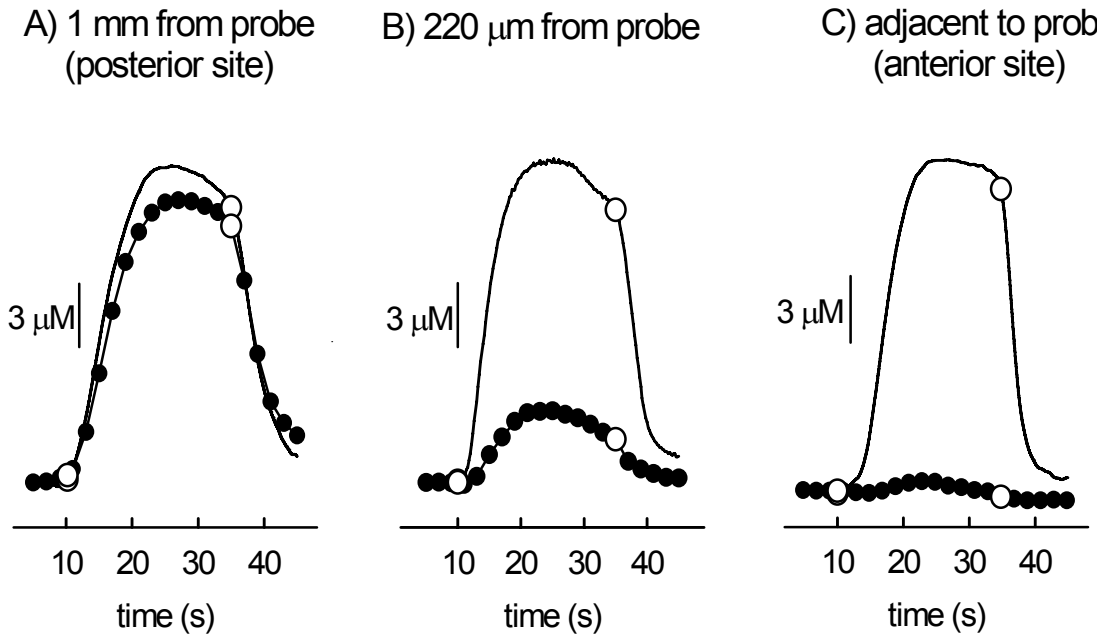


**Figure 2.3. Individual representative stimulus responses recorded with a voltammetric microelectrode at the posterior site 1 mm away from the probe (A), the site 220-250 μm away from the probe (B), and the anterior site adjacent to the probe (C). The results in panel (A) and (C) were recorded at two electrodes in the same rat. The results in (B) are from a different rat. At each site, the solid line is the voltammetric response observed before probe implantation and the line with round symbols is the response observed 2 hrs after probe implantation. The open circles signify the start and end of the electrical stimulation. The concentration scale bars were determined by postcalibration of the microelectrodes.**

### 2.4.2. Evoked dopamine release after nomifensine administration

The magnitude of the effect of systemic nomifensine administration (20 mg/kg i.p.) on the voltammetric stimulus responses was also different at the three recording sites (see Figure 2.4 for individual representative responses). Nomifensine increased the response amplitude 1.5- to 2-fold at the microelectrodes placed 1 mm from the probes (Fig 2.4A). Nomifensine increased the response amplitude 3- to 4-fold at the microelectrodes placed 220-250 μm from the probes (Fig 2.4B). A stimulus response was detectable after nomifensine administration at the

microelectrodes mounted on dialytrodes (Fig 2.4C), whereas no response was observed prior to uptake inhibition.

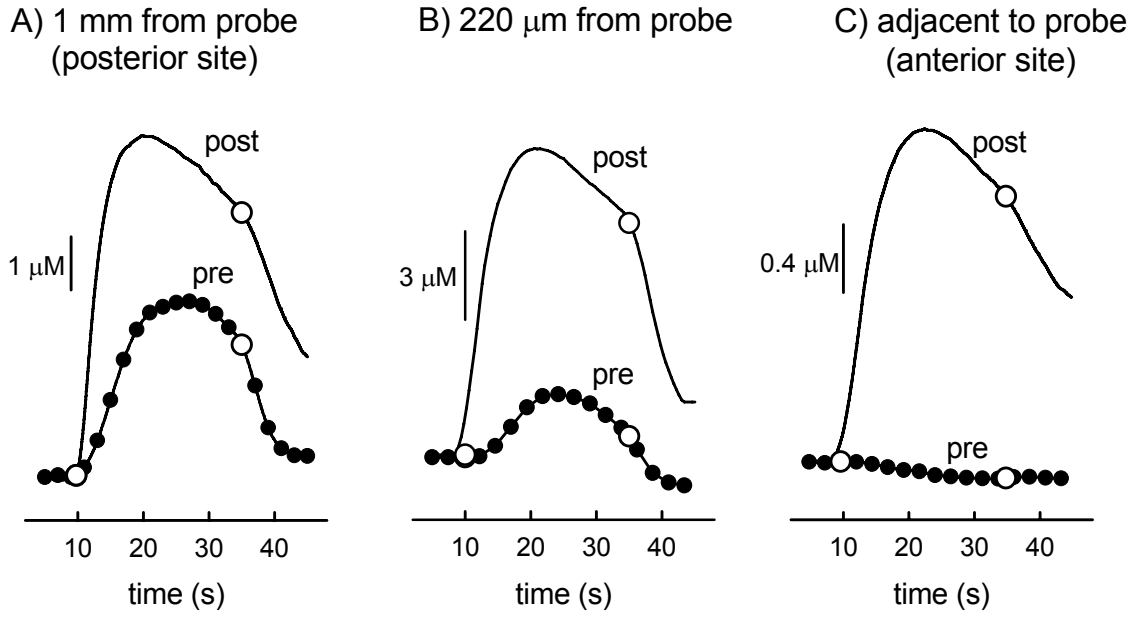


**Figure 2.4. Individual representative stimulus responses recorded with a voltammetric microelectrode before and 20 min after systemic administration of nomifensine (20 mg/kg i.p.). Responses were recorded at sites 1 mm from the probe (A), 220-250 μm from the probe (B), and adjacent to the probe (C). The results in panels (A) and (C) were recorded from two electrodes implanted in the same rat. The results in (B) are from a different rat. The responses were recorded before (pre, dotted line) and 20-25 min after (post, solid line) systemic nomifensine (20 mg/kg i.p.). The results in (B) are from a different rat. At each site, the solid line with round symbols is the response recorded before nomifensine and the solid line is the response observed after nomifensine. The open circles signify the start and end of the electrical stimulation. The concentration scale bars were determined by postcalibration of the microelectrodes.**

### 2.4.3. Summary of the stimulus responses

A summary of the results from a group of rats (Fig 2.5) shows that the stimulus response amplitude was affected by the distance between the microelectrodes and the microdialysis probes. Probe implantation did not significantly alter the stimulus response amplitude at the site 1 mm from the probes, decreased the response amplitude by nearly 10-fold at the site

220-250 μm from the probes, and completely abolished the response at the microelectrodes mounted on dialytrodes. A trend is also evident in the responses observed after nomifensine administration, which were largest at the site 1 mm from the probes, smaller at the site 220-250 μm from the probes, and smaller still at the dialytrode. On the other hand, the proportional effect of nomifensine on the stimulus response amplitude was modest at the site 1 mm from the probe (169 ± 31% of the predrug amplitude, mean ± stnd. err.), larger at the 220-250 μm from the probe (415 ± 170% of the predrug amplitude, mean ± stnd. err.), and larger still at the site of the dialytrode. Because of the absence of a detectable response prior to uptake inhibition at the microelectrodes mounted on the dialytrodes, it is not possible to quantify a percentage increase at this recording site.

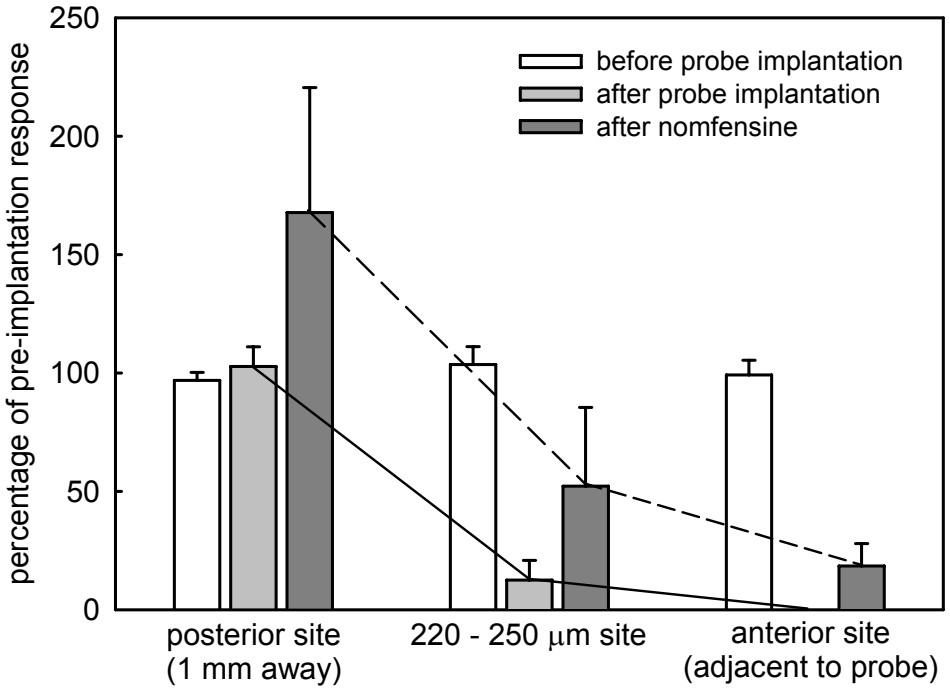


**Figure 2.5. Summary of the effect of probe implantation and uptake inhibition after probe implantation on the amplitude of evoked dopamine responses recorded at voltammetric microelectrodes placed 1 mm from, 220-250 μm from, and adjacent to microdialysis probes. The bars represent the mean ± s.d. (n=3 observations at the posterior and anterior sites; n=5 observations ate the site 220-250 μm from the probes). The solid trend line connects the responses obtained after probe implantation. The dashed trend line connects the responses obtained after nomifensine administration.**

The increase in response amplitude after nomifensine administration at the site 1 mm from the probes (169 ± 31%, mean ± stnd. err, n = 3) which was not significantly different from the increase at stand-alone microelectrodes (168 ± 32% mean ± stnd. err., n=3).

### 2.4.4. Simultaneous microdialysis and voltammetry without electrical stimulation

Basal levels of dopamine in dialysate samples collected beginning two hours after the completion of probe implantation were stable, in the low nanomolar range, and decreased by 60 ± 14% (mean ± stnd. dev., n=3) 1 hr after addition of TTX (10 μM) was added to the perfusion fluid (data not shown). Systemic administration of nomifensine (20 mg/kg i.p.) caused a significant increase in dialystate dopamine levels (Fig 2.6A). Dialysate dopamine levels reached a maximum of 144.1 ± 18.9 nM (mean ± s.d., n=5), a 10-fold increase over the predrug level. The effect of nomifensine was significant (one-way ANOVA, $f=76.7$, $df=6,28$, $p<0.001$). According to Duncan's multiple range test, the dopamine concentrations in all four samples collected after nomifensine administration were significantly increased compared to the predrug basal level ($p<0.05$).

In the absence of electrical stimulation, systemic administration of nomifensine (20 mg/kg i.p.) caused no dopamine response at microelectrodes implanted alone in the striatum or at microelectrodes placed 1 mm from microdialysis probes. On the other hand, systemic administration of nomifensine caused a noticeable voltammetric response (non-evoked) at microelectrodes placed 220-250 μm from the probes (Fig. 2.6B). At this recording site, the voltammetric signal began to increase within 5 min of drug administration, peaked 15-20 min after administration, and then returned steadily towards the predrug signal level. Background

subtracted voltammograms obtained near the maximum of the response confirmed that the increase in the voltammetric signal was due to an increase in extracellular dopamine (inset, Fig. 2.6B). The voltammograms exhibit the expected peaks for the oxidation of dopamine and the reduction of dopamine-*o*-quinone. In shape, position, and relative size, these peaks match those observed during postcalibration of the microelectrodes in dopamine standard solutions. The voltammetric currents were therefore converted by postcalibration of the microelectrodes to units of dopamine concentration. The solid line in Fig. 2.6B is the average change in dopamine concentration as measured by FSCV, which reached a maximum of $2.0 \pm 1.2$ μM (mean ± stnd. dev., n=6) above the predrug baseline. The symbols in Fig. 2.6B show the average and standard deviation of the response at 10 min intervals. The effect of nomifensine on the data symbols was significant (one-way ANOVA: $f=3.76$, $df=4,25$, $p<0.05$). Duncan's test showed that the results obtained 15 and 25 min after drug administration were significantly different from those obtained 5 min before drug administration ($p<0.05$).

Fig. 2.6C directly compares the amplitude and time course of the change in dopamine concentration after nomifensine administration as measured by voltammetry (solid line) and microdialysis (solid line with round symbols). The absolute amplitude and the time to reach the maximum response are clearly different between the two methods. Some of this difference may be caused by the fact that the microdialysis reports the average dopamine recovered over the 20 min prior to the collection of the sample. To account for this, 20-min averages of the voltammetric responses were also calculated (solid line with triangular symbols). Indeed, whereas the raw voltammetric trace peaked 15-20 min after nomifensine administration, the 20-min averaged results peaked at 40 min. However, the peak in the microdialysis response was

at 40-60 min, suggesting additional temporal delay in the response from sources other than averaging.

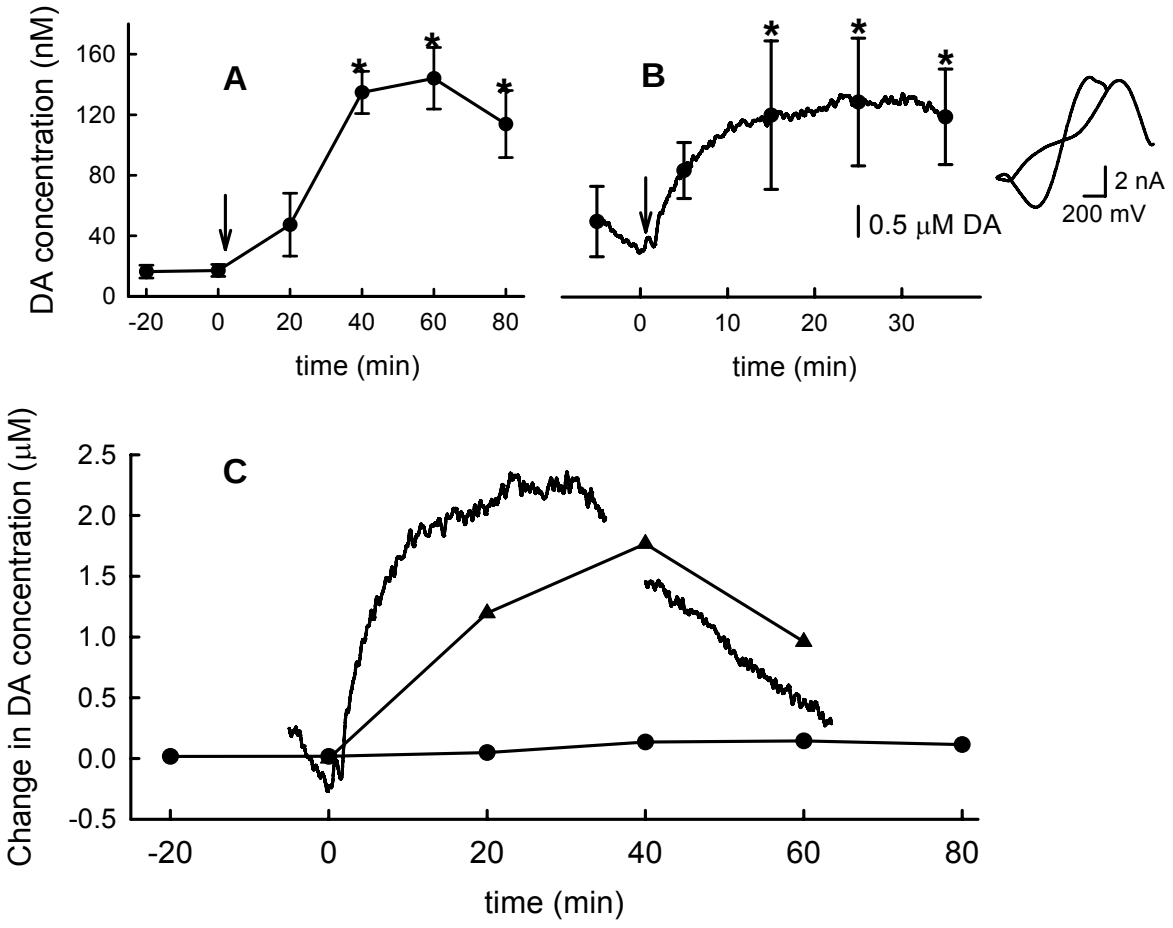


**Figure 2.6. (A) The effect of nomifensine (20 mg/kg i.p.) on the dopamine concentration in striatal microdialysate (mean ± standard deviation, n=5). The asterisks indicate a significant difference compared to the concentration at 0 min (ANOVA followed by Duncan's test, $p<0.05$). (B) The effect of nomifensine on dopamine as measured by FSCV with microelectrodes placed 220-250 μm from dialytrodes. The solid line is the average of the response recorded in 6 animals. The symbols indicate the mean ± the standard deviation of the signal at 10-min intervals. The asterisks indicate a significant difference compared to the response observed 5 min prior to nomifensine administration (ANOVA followed by Duncan's test, $p<0.05$). Inset: A representative background subtracted cyclic voltammogram obtained in one rat displaying the features expected for dopamine. (C) Dialysate and voltammetric responses for dopamine after uptake inhibition are plotted together to show the contrast in the responses observed by these two techniques. The solid line is the averaged voltammetric response from panel (B). The triangular symbols were obtained by time-averaging the voltammetric signals over the 20-min intervals just prior to the time at which the symbols are plotted. The round symbols are the microdialysis results from panel (A).**

No nonevoked voltammetric response was observed at the microelectrodes placed adjacent to the microdialysis probes. Since no nonevoked response was evident at microelectrodes 1-mm from the probes and adjacent to the probes, it appears that the tissue 220-250 μm from the probe responds in a unique fashion to the systemic administration of nomifensine.

## 2.5. DISCUSSION

During this study, voltammetric microelectrodes were placed at three recording sites near microdialysis probes acutely implanted in the striatum of rats anesthetized with chloral hydrate. Voltammetric recordings of evoked dopamine release produced different responses at each recording site, both before and after the administration of the dopamine uptake inhibitor, nomifensine (20 mg/kg i.p.). One of these sites also yielded a voltammetrically-detectable increase in nonevoked dopamine after nomifensine. The observation that no two recording sites produced equivalent results reveals the presence of a gradient in dopaminergic activity in the tissue surrounding acutely implanted probes. These findings suggest that disruption of the dopaminergic system associated with probe implantation extends at least 220-250 μm from the probes, although slight disruption was noticed 1 mm from the probe where stimulus response amplitudes were noticeably but not significantly decreased after probe implantation.

### 2.5.1. Methodological considerations

The objective of this study was to further examine if implantation of microdialysis probes disrupts dopaminergic activity in the adjacent tissue. We reasoned that this can be accomplished by placing carbon fiber microelectrodes near the probes. The diameter of the carbon fiber microelectrodes is less than 15 times that of the microdialysis probes and the electrodes are also shorter. The volume of the probes is ~10,000 times that of the microelectrodes. Given that the extent of trauma associated with implantation is related to the size of the implanted device (Szarowski et al., 2003), we reason that the additional trauma caused by the microelectrodes would be negligible compared to the trauma caused by the probes. This reasoning is consistent with our recent ultastructural study of carbon fiber implantation sites, which showed that physical tissue damage is mainly limited to a region about 3 μm larger than the fiber (Peters et al., 2004). Other studies suggest that microdialysis probes lead to disruptions extending for hundreds to thousands of micrometers (Clapp-Lilly et al., 1999; Zhou et al., 2001). It must be noted; however, that ultrastructural studies have not yet been performed after acute microdialysis, such as was performed during the present study.

The majority of microdialysis studies use a wait time of 16-24 hrs between implantation of the microdialysis probe and the collection of dialysate samples for analysis. In the present study, however, the wait time was only 2 hrs because the experiments were performed in anesthetized animals to allow close placement of the microdialysis probes and the microelectrodes using stereotaxic carriers. Nevertheless, this acute study is relevant in that it provides an indication of the volume of tissue impacted by disruption associated with probe implantation. Our findings clearly show that the tissue 220-250 μm from the probes is disrupted

at the time of probe implantation, which is important to know. It remains to be determined if this same tissue recovers 16-24 hrs after implantation. Histological results suggest that it might not. Szarowski et al. (2003) have demonstrated that glial activation is detectable on the day after the implantation of a micro-machined device of dimensions similar to those of microdialysis probes. Retterer et al., (2004) show that increased MAPK immunoreactivity, an accepted marker of cell stress, is present one hour after implantation and extensive on the day after implantation. The inclusion of an extended wait period is an accepted practice in dopamine microdialysis because dialysate dopamine levels are stable and TTX-sensitive 16-24 hr after probe implantation. Yet, it remains unclear if these are characteristics of tissue in a new 'perturbed steady-state' or tissue that has returned to normal after the probe-induced disruption.

In the present study, microdialysis probes were lowered slowly through brain tissue. We spent 30 min lowering the probe tip to a depth of 7 mm below the surface of the brain. This was primarily to assure the survival of the integrated carbon fiber microelectrodes, which can be torn away from the probe if care is not used. With this slow-lowering procedure, we found that dialysate dopamine levels were stable and in the low-nanomolar range essentially immediately after implantation. Moreover, 2 hrs after implantation, dopamine output was largely, but not completely, TTX-sensitive. Together, these observations may indicate that the slow lowering procedure allows the tissue to reach a new stable state rapidly after probe implantation. Other laboratories have also noticed the benefit of slowly lowering the microdialysis probe (DeBoer and Abercrombie, 1996; West and Grace, 2002).

### 2.5.2. A gradient in evoked release near microdialysis probes

The amplitude of the voltammetric response to MFB stimulation became steadily smaller as the distance between the microelectrode and the probe became smaller (Figs. 2.3 and 2.5). This same trend was also evident in the absolute amplitude of the stimulus responses observed after nomifensine administration (Figs. 2.4 and 2.5). On the other hand, the proportional effect of nomifensine on the amplitude of stimulus response tended to increase as the separation between the electrode and the microdialysis probe decreased. These results reveal the presence of a gradient in the activity of evoked dopamine release and dopamine uptake that extends at least 220-250 μm from the probe. The stimulus responses support the idea that the recovery of evoked dopamine is inherently low because evoked dopamine release is negligible near the probes compared to evoked release in the normal surrounding tissue. In addition, the responses support the idea that the relative recovery of evoked dopamine is increased after uptake inhibition. We attribute the latter observation to the increased ability of dopamine to diffuse to the probe after uptake inhibition.

### 2.5.3. A gradient in nonevoked dopamine levels near microdialysis probes after nomifensine

Nomifensine administration did not elicit a voltammetrically detectable increase in extracellular dopamine at stand-alone microelectrodes or at microelectrodes placed 1 mm from the microdialysis probes. In contrast, an increase in extracellular dopamine (nonevoked) was observed at the microelectrodes placed 220-250 μm from the probes (Fig. 2.6). Similar to the

case with evoked dopamine release, this result can be attributed to the enhanced ability of dopamine to diffuse into the disrupted tissue after uptake inhibition. Consistent with this idea, we recently found that the blockade of ionotropic glutamate receptors in the striatum leads to a ca. 2-μM drop in extracellular dopamine levels from their resting values, suggesting that the resting dopamine concentrations in striatal tissue may normally be in the micromolar range (Kulagina et al, 2001, Borland and Michael, 2004). The normally high concentration of dopamine in the surrounding normal tissue creates a concentration gradient towards the probe. Prior to uptake inhibition, however, the dopamine penetration distance, $\sqrt{D/k}$, might be too small to permit extensive diffusion to the probe. After uptake inhibition, however, the penetration distance should increase, allowing greater absolute and relative dopamine recovery. This explanation is consistent with the idea that dopamine uptake continues to operate in the tissue adjacent to the probe despite the disruption to that tissue (Bungay et al., 2003).

Apparently, however, the increased penetration of dopamine into the disrupted tissue is sufficient only to cause a voltammetrically detectable increase of the dopamine concentration at the microelectrode placed 220-250 μm from the probe but not at the microelectrode placed adjacent to the probe. This is likely due to the fact that the dopamine concentrations in the immediate vicinity of the probe remain below the detection limits of FSCV, even after uptake inhibition. The nanomolar concentrations found in the microdialysate samples (Fig. 2.6A) are consistent with this idea. This reinforces our previous suggestion that the microdialysate concentration of dopamine tracks the concentration of dopamine in the tissue immediately adjacent to the probe while the concentrations in the surrounding tissue may exhibit different behaviors.

Although increased diffusion of dopamine from the normal surrounding tissue into the disrupted tissue adjacent to the probe provides a simple explanation for the contrast between the dopamine responses at each recording site, other processes might also be involved. For example, several factors regulate the kinetics of the dopamine transporter (see review by Gulley and Zahnizer, 2003). Dopamine transporter levels can change rapidly due to transporter trafficking (Saunders et al., 2000), transporter kinetics are regulated by D2 receptors (Meiegerd et al., 1993; Cass and Gerhardt, 1994; Garris et al., 2003), and transporter kinetics are voltage dependent (Hoffman et al., 1999). It is possible that any one or a combination of these regulatory factors could alter uptake kinetics differently in the disrupted tissue adjacent to the probe compared to the normal tissue. However, the present study was not appropriately designed to address these possibilities in detail. For one, the study involved an acute preparation and it remains to be seen how the results would be different had the usual 16- to 24-hr recovery period been used. In addition, the present study was performed under chloral hydrate anesthesia, which itself affects dopamine clearance (Sabeti et al., 2003). Thus, further conclusions regarding the involvement of the various mechanisms that regulate dopamine uptake kinetics at the different recording locations should not be drawn from the results of the present study.

The numerous factors that regulate the kinetics of the dopamine transporter may also be involved in the absence of an obvious FSCV response at stand alone microelectrodes and microelectrodes placed 1 mm from the probes. Preliminary reports from this laboratory (Khan and Michael, 2003; Mitala and Michael, 2003;) show that dopamine levels increase substantially when dopamine uptake inhibitors are given to rats pretreated with dopamine D2 receptor antagonists. These observations suggest that dopamine levels as measured by fast scan

voltammetry are subject to a homeostatic mechanism mediated by D2 receptors after uptake inhibition.

### 2.5.4. Implications for quantitative microdialysis

The results of this study provide further support for the idea that uptake inhibition causes an increase in dopamine recovery (Peters and Michael, 1998; Yang et al., 1998; Lu et al., 1998; Yang et al., 2000). Nomifensine caused a 10-fold increase in the dialysate concentration of dopamine, even though no such 10-fold increase was evident at the voltammetric site 1 mm from the probe. A recent study from this laboratory suggested that dopamine levels in the striatum of the anesthetized rat, as measured by FSCV, rest near 2 μM (Kulagina et al, 2001, Borland and Michael, 2004). A 10-fold increase from this resting level would undoubtedly be detectable, even by FSCV. Prior to this study, our conclusion that uptake inhibition causes an increase in dopamine relative recovery was based only on studies of evoked release (Yang et al., 1998; Lu et al, 1998), a strategy that has been criticized (Chen, 2005b). But, the present study supports the same conclusion on the basis of measurements performed without electrical stimulation. However, it also appears from our results (Fig. 2.6) that the somewhat unique response of the tissue 220-250 μm from the probe may contribute substantially to the increase in relative recovery. It is import to emphasize, therefore, that the definition of relative recovery is based on concentrations in the external medium sufficiently far from the probe so that the external medium is no longer perturbed by the probe, i.e., $C_e^{\infty}$ in Equations 4 and 7, above.

Quantitative microdialysis requires that the extraction fraction and relative recovery be equal to each other (Equation 4). However, there is now evidence to suggest that this is unlikely

to be the case for dopamine. Smith and Justice (1994) demonstrated that uptake inhibition decreases the slope of the dopamine concentration difference plot and, therefore, the extraction fraction of dopamine (Equation 6). The present study supports the idea that the relative recovery increases under the same conditions. Two parameters that change in the opposite direction at the same time cannot be equal to each other.

Several research groups have developed numerical models of microdialysis that incorporate descriptions of diffusion, active transport, and tissue disruption (Yang et al., 2000; Bungay et al., 2003; Chen 2005a). In each of these models, however, the traumatized tissue was described as a thin layer possessing a sharp, well defined boundary with the surrounding normal tissue. Chen (2005a), for example, used a 20-μm thick layer of tissue in which dopamine release is decreased by 40% to describe the traumatize tissue. At least under the acute conditions of the present study, the dimensions of the disrupted layer is 10-fold larger at least. The loss of evoked release is complete immediately adjacent to the probe and 90% at 220-250 μm. So, existing microdialysis models probably have not yet fully accounted for the magnitude of probe-induced tissue disruption or the fact that there is a gradient of disruption rather than a sharp boundary between the disrupted and surrounding normal tissues.

# 3. VOLTAMMETRIC STUDY OF BLOOD BRAIN BARRIER PERMEABILITY IN THE AREA SURROUNDING MICRODIALYSIS PROBES

## 3.1. ABSTRACT

Microdialysis and fast-scan cyclic voltammetry with carbon fiber microelectrodes are two techniques for measuring dopamine in the extracellular space of the brain. Unfortunately, these two techniques give differing results for the concentration of dopamine in the brain. The discrepancy in results may be attributable to differences in the tissue structure surrounding these two different devices. We recently reported that microdialysis implantation creates a gradient of dopamine activity in the tissue surrounding microdialysis probes, as measured by FSCV with microelectrodes (Borland et al., 2005). In the present study, we expand on this theme to examine the effects of microdialysis probe implantation on the permeability of the blood-brain barrier (BBB). HPLC was used to assess the movement of the BBB-impermeable drug, carbidopa, across the BBB after probe implantation. Carbon fiber microelectrodes and FSCV were used to examine the effect of carbidopa on stimulated dopamine release in the tissue 220-250 μm from microdialysis probes. Carbidopa was detected in microdialysate by HPLC; however, systemic carbidopa had no effect on stimulated dopamine after probe implantation. These findings suggest that microdialysis probe implantation increases BBB permeability, but that the tissue surrounding microdialysis probes may suffer from additional functional deficiencies.

## 3.2. INTRODUCTION

Microdialysis is a commonly used technique to sample extracellular brain fluid (ECF) and is used extensively in the study of neurotransmitters in the brain. This universally simple technique operates on the principle of diffusion, where small molecules move across a concentration gradient from the extracellular space and into the dialysis fluid inside the microdialysis probe. The sampled dialysate is collected and analyzed *via* high performance liquid chromatography (HPLC) or capillary electrophoresis (CE).

Another technique used to monitor neurotransmitters *in vivo* is fast-scan cyclic voltammetry (FSCV). In FSCV, a triangular waveform potential is applied to a carbon fiber microelectrode to oxidize or reduce electroactive species, which generates a current response. Electroactive species can be identified through their characteristic cyclic voltammograms, which are based on the formal potential of the species. This allows for a high degree of temporal and chemical resolution (Robinson, et al., 2003).

The neurotransmitter dopamine is implicated in a number of disease states, including Parkinson's disease, schizophrenia and drug abuse. Investigations into this ubiquitous neurotransmitter have employed both microdialysis and FSCV with microelectrodes. However, voltammetric and microdialysis studies report differences in the concentration of resting, or basal, dopamine in extracellular brain fluid (Borland and Michael, 2004). The discrepancy in results may be attributable to differences in tissue structure surrounding these two different devices, the microdialysis probe vs. the carbon fiber microelectrode.

Ultrastructural analysis of the brain tissue surrounding microdialysis probes reveals a zone of damaged tissue extending a least 1 mm from the site of implantation (Zhou et al, 2001; Clapp-Lily, et al., 1999); however, light microscopy revealed virtually no tissue damage from an

implanted microelectrode (Peters et al., 2004). Subsequent voltammetric studies of extracellular dopamine in the vicinity of acutely implanted microdialysis probes reveal a gradient of dopamine release and uptake (Borland et al, 2005), suggesting that probe-induced tissue damage affects dopamine activity, as well. The connection between microdialysis probe-induced tissue damage and decreased dopaminergic function in the vicinity of the probes is the subject of intense investigation in this laboratory.

Damage due to probe insertion inevitably causes damage to the surrounding blood vessels, as the size of a typical microdialysis probe (220 μm diameter x 4 mm length) is significantly larger than the intercapillary distance in the brain (Morgan et al., 1996). Disrupted blood flow, particularly the disruption of oxygen delivery to the surrounding tissue, may contribute to the impairment of dopamine activity in the region. During hypoxia, oxygen levels decrease and levels of reactive intermediates, including reactive oxygen species and excitotoxic glutamate, also increase. These factors could contribute to the decreased function of dopamine near microdialysis probes by interfering with the normal functioning of the dopamine-releasing terminals or by contributing to the death of said terminals. Damage to brain capillaries could also adversely affect the functions of the blood brain barrier (BBB). The BBB carefully regulates the passage of nutrients and other water-soluble compounds from the bloodstream to the brain. Evidence of changes in BBB permeability after insertion of microdialysis probes suggests that the BBB is disrupted during microdialysis (Groothuis et al., 1998). We speculate that damage to blood vessels and subsequent changes in BBB permeability affect the activity of neurotransmitters and other species in the tissue surrounding microdialysis probes.

Evidence of increased BBB permeability after insertion of a microdialysis probe suggests that species have uninhibited access to cross over from the blood stream and into the brain tissue

to interact with the surrounding environment. The amino acid decarboxylase (AADC) inhibitor, carbidopa, is normally restricted from entering brain tissue by the BBB, regulating its function to the periphery. However, probe implantation increases its permeability into the brain, increasing its ability to affect dopamine levels (Kaakkola et al., 1992). Similarly, other drugs or treatments administered through the bloodstream could artificially affect dopamine processes in the brain, due to increased permeability of the BBB, affecting the perceived outcome of microdialysis experiments.

In this study, we extend our examination of the tissue surrounding microdialysis probes, focusing the permeability of the BBB near microdialysis probes. Systemic carbidopa was administered to anesthetized rats and microdialysate samples analyzed by HPLC-PFET to access the permeability of the BBB after microdialysis probe implantation. Carbon fiber microcylinder electrodes (3.5 μm radius) in conjunction with fast scan cyclic voltammetry were used to assess the effect of systemic carbidopa on stimulated dopamine release and probe implantation on stimulated dopamine release in the tissue adjacent to (220-250 μm) acutely implanted microdialysis probes.

## 3.3. MATERIALS AND METHODS

### 3.3.1. Microdialysis probes

Vertical concentric microdialysis probes (220 μm o.d., 4 mm in length) were constructed with hollow fiber dialysis membrane (Spectra-Por RC Hollow Fiber, MWCO: 13,000, 160 μm i.d., Spectrum Laboratories, Inc., Rancho Dominguez, CA, USA) and fused silica outlet lines (150

μm o.d., 75 μm i.d., Polymicro Technologies, Phoenix, AZ, USA) as described elsewhere (Abercrombie et al., 1989). Probes were perfused with aCSF at a rate of 0.586 μL/min for all experiments.

### 3.3.2. Voltammetric microelectrodes and techniques

Carbon fiber microcylinder electrodes were constructed as described previously (Borland and Michael, 2004). Briefly, a single 7 μm diameter carbon fiber (Thornell Carbon Fiber, T300, Amoco Performance Products, Inc. Greenville, SC, USA) was sealed with epoxy into a borosilicate glass capillary and trimmed to a length of 400 μm. The electrodes were pre-treated with 100 cycles of 0-2 V vs. Ag/AgCl triangular waveform delivered at 200 V/s. Dopamine was detected by fast-scan cyclic voltammetry. The applied potential was held at 0 V vs. Ag/AgCl between scans. Dopamine was detected by linearly sweeping the potential to +1.0 V, then to -0.5 V, and back to the resting potential at a rate of 300 V/s, with the scans repeated every 100 ms. The dopamine oxidation signal was obtained by calculating the average current value between 0.6 and 0.8 V on the first sweep of each scan. Electrodes were calibrated before and after use in artificial cerebral spinal fluid (aCSF: 145 mM $Na^+$, 1.2 mM $Ca^{2+}$, 2.7 mM $K^+$, 1.0 $Mg^{2+}$, 152 mM $Cl^-$ and 2.0 mM phosphate adjusted to pH 7.4) containing known concentrations of dopamine.

### 3.3.3. Animals and surgical procedures

All procedures involving animals were carried out with the approval of the Institutional Animal Care and Use Committee of the University of Pittsburgh. Male Sprague-Dawley rats (Hilltop,

Scottsdale, PA, USA) (250-375g) were anesthetized with chloral hydrate (400 mg/kg i.p.) and wrapped in a homoeothermic blanket (EKEG Electronics, Vancouver, BC, Canada) to maintain a body temperature of 37$^{o}$C. The rats were placed in a stereotaxic frame (David Kopf Instruments, Tujunga, CA, USA) with the incisor bar 5 mm above the interaural line (Pellegrino et al., 1979). Holes were drilled through the skull in the appropriate positions to expose the underlying dura and brain tissue. In the experiments requiring a reference electrode, the reference electrode made contact with the brain tissue via a modified salt bridge. The dura was removed with a scalpel to allow for placement of the microelectrode and/or microdialysis probe into the brain tissue with minimal disruption to the surrounding blood vessels.

### 3.3.4. HPLC analysis of carbidopa and dopamine in microdialysate

In a separate set of animals, a microdialysis probe was lowered over 30 min into the striatum (2.5 mm anterior to bregma, 2.5 mm lateral from midline and 7.0 mm below dura). Microdialysate was sampled every 10 minutes beginning 2 hours after probe implantation. Carbidopa (150 mg/kg i.p.) or vehicle (PBS) was administered 3 hours after probe implantation. Sampling continued at 10 minute intervals after drug administration. All samples were collected in 0.65 μL of 1M acetic acid to aid in dopamine and carbidopa detection.

Carbidopa and dopamine concentration in the microdialysate samples were determined by means of high performance liquid chromatography with photoluminescence following electron transfer (HPLC-PFET). Two HPLC pumps (models 590 and 600/626S, Waters, Milford, MA) or a syringe pump (model 100DM, ISCO, Lincon, NE) with simple tees as flow splits delivered solutions at ~1 μL/min. One pump was used to deliver the mobile phase and

another to deliver the PFET reagent. The mobile phase consisted of an aqueous buffer containing a mixture of monochloroacetic acid and sodium acetate (total concentration of 100 mM), 0.15 mM disodium EDTA, SOS (pH adjusted with concentrated NaOH solution) and acetonitrile. The mobile phase was passed through a Nylon filter with 0.45 μm pores (Osmonics, Minnetonka, MN). The PFET reagent, $Os(bpy)_3(PF_6)_2$ **(1)** was prepared and recrystallized in our laboratory according to previously reported procedures (Gaudiello et al., 1984). Crystals of osmium complex were dissolved in acetonitrile, to make a 1.0 mM stock solution. Aliquots of the stock solution were diluted in an acidic electrolyte solution (0.2% TFA and 0.1 M $NaClO_4$ in acetonitrile) to prepare the PFET reagent solution. The resulting solution was used after filtering through a disposable 0.45 μm PTFE/PP syringe filter (Chrom Tech, Apple Valley, MN).

Homemade capillary columns were packed by previously described techniques (Beisler et al., 2004) using 100 μm i.d., 360 μm o.d. fused-silica capillaries as the column blank. The capillary column was slurry packed to 7.6 cm with 2.6 μm XTerra MS-$C_{18}$ (Waters, Milford, MA) reversed phase particles and connected directly to an Upchurch loop microinjector (Oak Harbor, WA), which introduced 500 nL of each sample into the column. A Capillary Taylor Reactor (CTR) was used to mix the chromatographic eluents and the postcolumn PFET solution. They were prepared according to the previously reported procedure (Beisler et al., 2004; Jung and Weber, 2005; Sahlin et al., 2002)

A laser beam from a 30-mW variable-power blue-line argon ion laser (model 2201-30BL, Cyonics/Uniphase, San Jose, CA) passed through a 488-nm band-pass filter and was focused onto an optically transparent capillary. Photoluminescence from $\mathbf{1}^{2+}$ was measured using an epifluorescence optical setup: a microscopic objective lens (Plan Neofluar 20x, NA 0.5, Carl Zeiss, Thornwood, NY) focused the optical emission from the capillary and a combination of a

dichroic mirror (cutoff at 500 nm) and optical filters (a 600-nm long-pass filter and a 750-nm band-pass filter, angle tuned) allowed the photoluminescence into an IR-sensitive photomultiplier tube (R374, Hamamatsu, Bridgewater, NJ). A Keithley 6485 picoammeter (Cleveland,OH) converted photocurrent from the photomultiplier tube to a dc voltage signal. An IBM-compatible computer with a PeakSimple Chromatographic Data System (SRI Instruments, Torrance, CA) collected the dc signal after a 0.4-Hz eight-pole low-pass filter (Wavetek 852 Dual filter, San Diego, CA).

### 3.3.5. Effect of carbidopa on evoked dopamine release in the striatum of anesthetized rats

A microcylinder electrode (400 μm in length) was placed in the striatum of the rat, positioned at 2.5 mm anterior with respect to bregma, 2.5 mm lateral with respect to the midline and 4.5 mm below dura. The MFB was stimulated with a constant current, biphasic square wave with a frequency of 60 Hz, a pulse width of 2 ms, a pulse height of 280 μA, and a train length of 10 s. Experiments commenced only after stimulated dopamine release produced a response of at least 50 nA in amplitude at the voltammetric electrode. Stimuli were delivered at 20 min intervals. Carbidopa (150 mg/kg i.p.) or vehicle (PBS) was administered immediately after the third stable stimulus response. Electrical stimulation commenced 20 min later and continued at 20 min intervals.

### 3.3.6. Effect of carbidopa on evoked dopamine release 220-250 µm from microdialysis probes

In this set of experiments, evoked dopamine was monitored 220-250 µm from an implanted microdialysis probe. A microelectrode was aligned at an angle to a microdialysis probe and lowered into the striatum. The ipsilateral MFB was stimulated with constant current, biphasic square wave with a frequency of 60 Hz, a pulse width of 2 ms, a pulse height of 280 µA, and a train length of 10 s. After a series of stable evoked dopamine responses at least 50 nA in amplitude, the microdialysis probe was slowly lowered over 30 min to a final position of 2.5 mm anterior to bregma, 2.5 mm lateral from midline and 7.0 mm below dura. Electrical stimulation commenced 2 hours after probe placement. Immediately after the first stimulation after probe implantation, carbidopa (150 mg/kg i.p.) or vehicle (PBS) was administered. Electrical stimulation continued at 20 min intervals following drug administration.

### 3.3.7. Chemicals and solutions

Chloral hydrate, carbidopa and dopamine were used as received from Sigma (St. Louis, MO, USA). Chloral hydrate was dissolved in phosphate buffered saline (PBS: 155 mM NaCl, 100 mM phosphate, pH 7.4). Carbidopa was administered as a suspension in PBS. All solutions were prepared with ultrapure water (NANOPure; Barnstead, Dubuque, IA, USA).

## 3.4. RESULTS

### 3.4.1. Analysis of rat brain microdialysate for carbidopa and dopamine

The rat brain microdialysis samples were analyzed at the optimal separation conditions to determine the carbidopa and dopamine concentrations. Calibration fits were constructed using standard solutions containing 0 – 100 nM carbidopa and dopamine before analyzing each set of rat brain dialysates. Typical regression equations for peak heights versus concentrations (mV/nM) were: $y = 1.58 x + 1.63$ ($r^2 = 0.9993$) for dopamine and $y = 2.84 x + 1.99$ ($r^2 = 0.9997$) for carbidopa. The concentration detection limits were calculated from the calibration fit using signal to noise ratio of 3. Typical concentration detection limits were 570 pM for dopamine and 320 pM for carbidopa. Corresponding mass detection limits based on 500 nL injection were 290 amol for dopamine and 160 amol for carbidopa.

Concentration changes of dopamine and carbidopa with time are shown in Figure 3.1. The concentration of carbidopa increased just after the injection of carbidopa, with no observable change upon injection of PBS. The apparent presence of carbidopa in the brain dialysates of rats treated with PBS and in the dialysate samples taken prior to treatment in the carbidopa-treated rats is due to an unidentified transient peak overlapping the carbidopa peak. The unidentified peaks were not found in all dialysates, and dialysates from the same set showed different responses, as well. Regardless, the height of the unidentified peak was always negligible compared to that of carbidopa peak. Thus it is unlikely that the large increase in the peak height after the injection was due to the unidentified peak. Moreover, an increase in the peak height was never observed when the rat was given PBS.

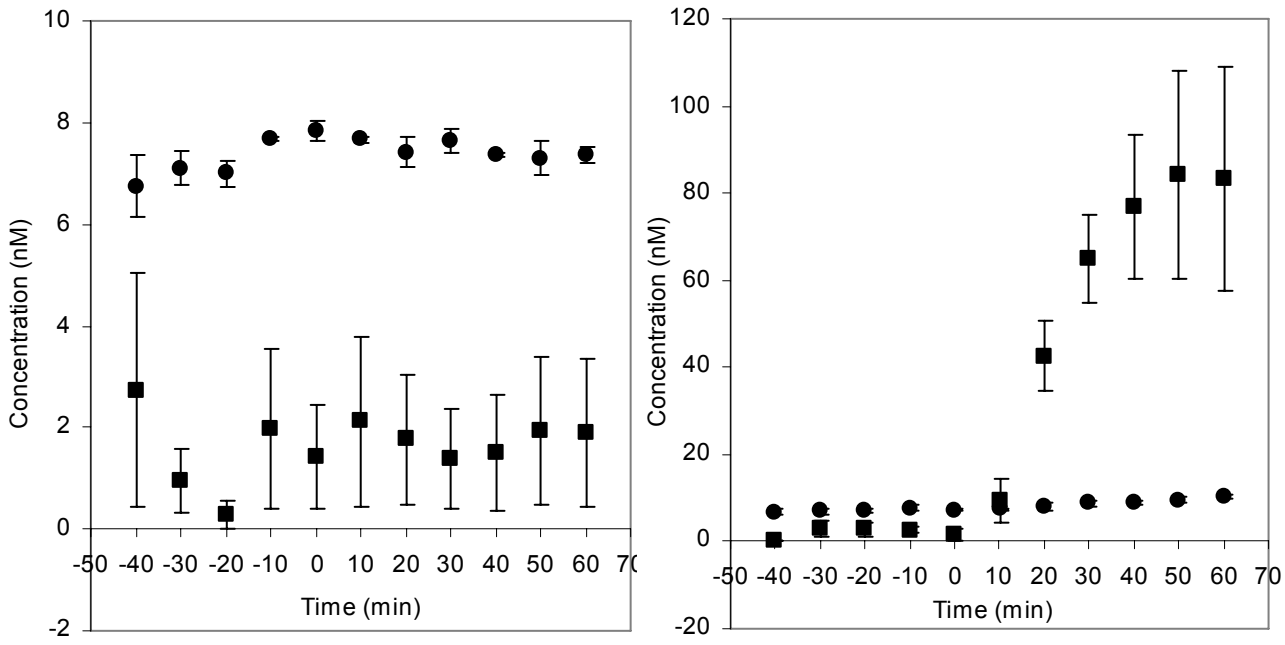


**Figure 3.1. (Top) Concentrations of dopamine and carbidopa in microdialysate of rats treated with PBS (vehicle). (Bottom) Concentrations of dopamine and carbidopa in microdialysate of rats treated with carbidopa (150 mg/kg i.p.). In both set of experiments, the injection took place at t = 0 minutes. The symbols indicate the mean ± standard error (n=3).**

### 3.4.2. Voltammetric response of stimulated dopamine to systemic carbidopa after probe implantation

As previously reported, stimulated dopamine release decreased significantly after microdialysis probe implantation. The stimulated dopamine response decreased 91 ± 8 % (mean ± s.d., n=3) from the pre-implantation response after probe implantation. Systemic administration of carbidopa (150 mg/kg i.p.) did not alter the stimulated dopamine response after probe implantation (Figure 3.2). The response following probe implantation remained steady 2 hours after carbidopa administration. Systemic treatment with PBS (vehicle) after probe implantation also had no effect on the voltammetric response, with a steady decrease of 82 ± 14 % (mean ±

s.d., n=3) from the pre-probe levels. Neither systemic carbidopa nor PBS (vehicle) administered after probe implantation caused a change in the stimulated dopamine response after probe implantation.

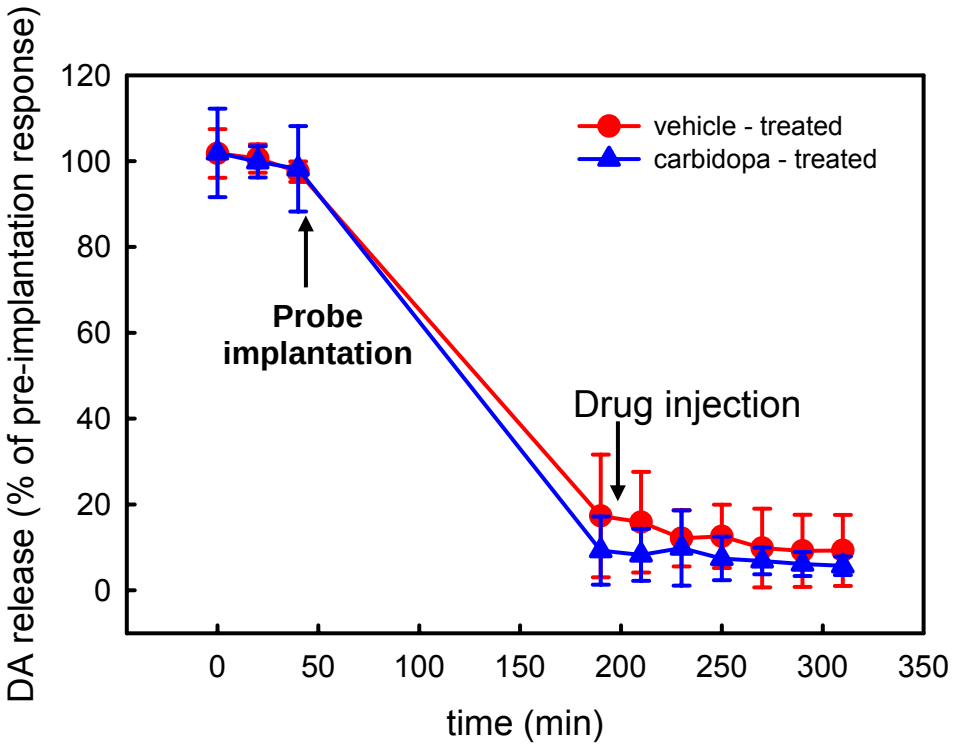


**Figure 3.2. Stimulated dopamine release after probe implantation and carbidopa administration. Probe implantation caused a significant decrease in stimulated dopamine release from pre-probe levels in both the carbidopa (91 ± 8%, n=3) and the PBS (vehicle) (82 ± 14%, n=3) pretreated animals; however no additional changes in stimulated dopamine release were observed following systemic drug administration.**

### 3.4.3. Voltammetric response of stimulated dopamine to systemic carbidopa

Systemic administration of carbidopa (150 mg/kg i.p.) decreased stimulated dopamine release in the striatum of the anesthetized rat (Figure 3.3). The decrease reached a maximum nearly 2 hours after carbidopa administration, decreasing 36 ± 13 % (mean ± s.d., n=3) from the pre-drug

level. However, stimulated dopamine release also decreased significantly in rats treated with PBS (vehicle). This decrease also reached a maximum after 2 hours for a 30 ± 5 % (mean ± s.d., n=3) decrease from the pre-treatment response. Two-way ANOVA analysis helps to explain that there is no significant difference between the treatments (carbidopa vs. PBS (vehicle)), verifying that the response after systemic carbidopa administration has no effect on the stimulated dopamine response. The steady decrease in the stimulated responses probably arises from a slow and steady depletion of the vesicular pool of dopamine, from which the stimulated response is generated. Due to the magnitude of the stimulation (60 Hz, 10 sec, 280 μA), it is no surprise that the stimulated dopamine response would decrease slowly after three hours of continuous stimulation.

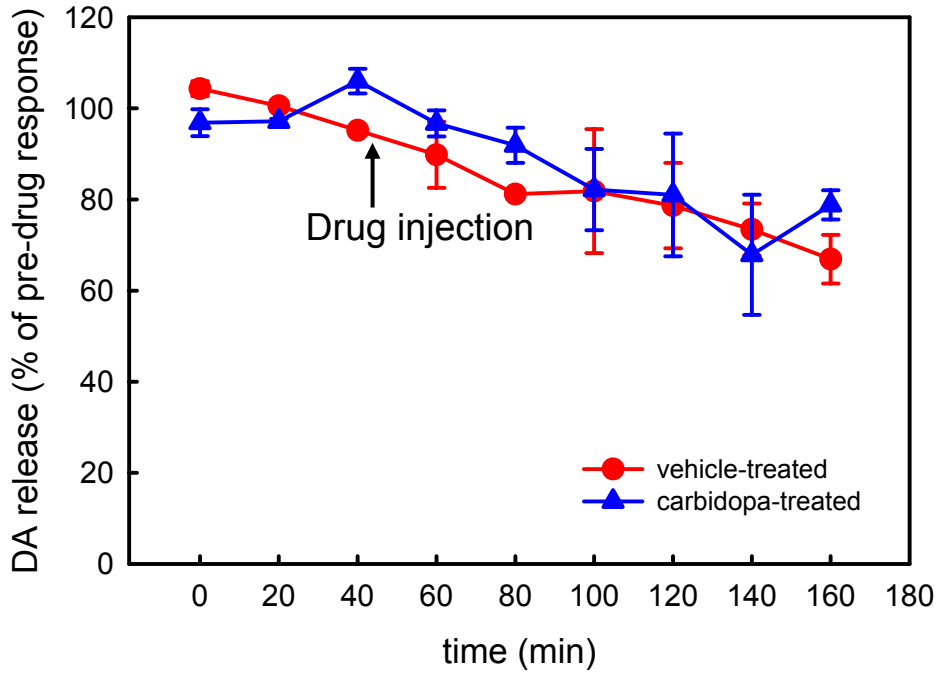


**Figure 3.3. Stimulated dopamine release after drug administration. Two-way ANOVA shows that there is no significant difference between the treatments (PBS (vehicle) vs. carbidopa; F=1.17, df=1,53). The symbols indicate the mean ± standard deviation of the signal (n=3).**

## 3.5. DISCUSSION

Analysis of dialysate from rats treated systemically with the BBB-restricted aromatic amino acid decarboxylase (AADC) inhibitor, carbidopa, confirmed that BBB permeability increased in the presence of a microdialysis probe. Carbidopa was detected in dialysate samples 10 minutes after systemic administration (carbidopa: 150mg/kg, i.p.) This observation is supported by an earlier report of carbidopa detection in microdialysate by HPLC (Kaakkola et al., 1992), confirming that carbidopa crosses the BBB during microdialysis. Dialysate samples from animals treated with much lower concentrations of carbidopa (i.e. 25 mg/kg i.p.) also exhibited increased carbidopa levels, suggesting that the ability of carbidopa to cross the BBB is not entirely concentration dependent (Kaakkola et al., 1992). Evidence of significantly elevated levels of carbidopa in the tissue homogenate from the probe-impaled striatum, compared to the contralateral striatum, further suggests a breakdown of the BBB (Kaakkola et al., 1992). Interestingly, both studies observed no significant change in the extracellular levels of dopamine after the systemic administration of carbidopa. These results are in contrast to earlier research on the BBB which show an intact BBB immediately after microdialysis probe implantation. (Benveniste et al., 1984; Tossman and Ungerstedt, 1986). Later reports of focal disturbances of blood flow and glucose metabolism around implanted microdialysis probes (Benveniste et al., 1987) suggest that the BBB may not be as intact as previously concluded.

As stated previously, HPLC results indicate that carbidopa did cross the blood brain barrier and thus was detectable in the dialysate. The concentration of carbidopa increased just after the injection of carbidopa, with no observable change upon injection of PBS. The apparent presence of carbidopa in the brain dialysates of rats treated with PBS and in the dialysate samples taken prior to treatment in the carbidopa-treated rats is due to an unidentified transient

peak overlapping the carbidopa peak. The unidentified peaks were not found in all dialysates, and dialysates from the same set showed different responses, as well. Regardless, the height of the unidentified peak was always negligible compared to that of carbidopa peak. Thus it is unlikely that the large increase in the peak height after the injection was due to the unidentified peak. Moreover, an increase in the peak height was never observed when the rat was given PBS.

Carbidopa had no effect on stimulated dopamine release in the absence of the microdialysis probe implantation, which was expected since carbidopa does not readily cross BBB, even at high (>100 mg/kg) doses. In agreement with previous microdialysis data, carbidopa did not affect stimulated dopamine release after probe implantation, when the BBB was compromised and the permeability of carbidopa into the striatum increased. The inability of carbidopa to decrease extracellular dopamine levels might be due to other underlying deficits in dopamine function in the terminals surrounding implanted microdialysis probes. If, perhaps, the synthesis mechanism is destroyed by probe insertion, subsequent inhibition of dopamine synthesis by carbidopa would be ineffective or superfluous. The remaining response from stimulated dopamine release observed after probe implantation may be remnants of old vesicular stores, which are recycled after stimulation, eliminating the need for additional synthesis. Naturally, there is need for additional investigations into the functionality of the tissue surrounding microdialysis probes, including synthesis, receptor activity, and transport activity, in order to complete the picture of dopamine function in this damaged region.

## 3.6. CONCLUSION

Implantation of microdialysis probes creates tissue damage that alters blood flow, dopamine activity, and the functionality of the blood-brain barrier. The tissue surrounding the site of probe implantation exhibits a 90% decrease in stimulated dopamine release, in addition to a compromised BBB. Dialysate collected from animals treated with the BBB-impermeable drug, carbidopa, showed traces of the drug, but with no effects on dopamine levels in the area. Lack of a dopaminergic response to carbidopa suggests another level of compromised tissue functionality that requires additional study.

# 4. VOLTAMMETRIC STUDY OF THE CONTROL OF STRIATAL DOPAMINE RELEASE BY GLUTAMATE

## 4.1. ABSTRACT

The central dopamine systems are involved in several aspects of normal brain function and are implicated in a number of human disorders. Hence, it is important to understand the mechanisms that control dopamine release in the brain. The striatum of the rat receives both dopaminergic and glutamatergic projections that synaptically target striatal neurons but not each other. Nevertheless, these afferents do form frequent appositional contacts, which has engendered interest in the question of whether they communicate with each other despite the absence of a direct synaptic connection. In this study, we used voltammetry in conjunction with carbon fiber microelectrodes in anesthetized rats to further examine the effect of the ionotropic glutamate antagonist, kynurenate, on extracellular dopamine levels in the striatum. Intrastriatal infusions of kynurenate decreased extracellular dopamine levels, suggesting that glutamate acts locally within the striatum *via* ionotropic receptors to regulate the basal extracellular dopamine concentration. Infusion of tetrodotoxin into the medial forebrain bundle or the striatum did not alter the voltammetric response to the intrastriatal kynurenate infusions, suggesting that glutamate receptors control a nonvesicular release process that contributes to the basal extracellular dopamine level. However, systemic administration of the dopamine uptake inhibitor, nomifensine (20 mg/kg i.p.), markedly decreased the amplitude of the response to kynurenate infusions, suggesting that the dopamine transporter mediates nonvesicular dopamine release.

Collectively, these findings are consistent with the idea that endogenous glutamate acts locally within the striatum via ionotropic receptors to control a tonic, impulse-independent, transporter-mediated mode of dopamine release. Although numerous prior in vitro studies had suggested that such a process might exist, it has not previously been clearly demonstrated in an in vivo experiment.

## 4.2. INTRODUCTION

The nigrostriatal and mesolimbic dopamine pathways of the brain play significant roles in motor control, cognitive function, and the regulation of mood and affect (Cousins and Salamone, 1996; Schultz et al., 1997; Diehl and Gershon, 1992). These pathways are also implicated in the pathophysiology of human diseases, including schizophrenia, Parkinson's disease, attention deficit/hyperactivity disorder, and substance abuse (Carlsson et al., 1999; Carlsson and Carlsson, 1990; Koob and Bloom, 1988). Hence, it is important to understand the mechanisms that regulate dopamine release the brain.

Early studies involving *in vitro* preparations, such as tissue slices and synaptosomes, suggested that both impulse-dependent and impulse-independent mechanisms might contribute to dopamine release in the striatum (Giorguieff et al., 1977; Raiteri et al., 1979; Desce, et al., 1992). These mechanisms have also been called phasic release and tonic release, respectively (Grace, 1991). Phasic release involves the fusion of synaptic vesicles to terminal membranes, while some evidence suggests that reversal of the dopamine transporter (DAT) might mediate tonic release (Raiteri et al., 1979; Lonart and Zigmond, 1991; Leviel, 2001). It has been hypothesized that phasic and tonic release contribute synergistically to central dopaminergic

transmission (Grace, 1991), with tonic release modulating the responsiveness of dopamine receptors to phasic release.

In contrast, *in vivo* studies, mainly based on microdialysis, have suggested that striatal dopamine release occurs primarily in an impulse-dependent fashion (Westerink et al., 1987; Westerink and deVries, 1988). Although certain drugs, such as amphetamine, may stimulate impulse-independent dopamine release (Leviel, 2001; Westerink et al., 1987), dopamine as measured by microdialysis is generally highly sensitive to tetrodotoxin (Westerink et al., 1987). In light of this point, some authors have begun to attribute tonic release to the non-burst firing activity of midbrain dopamine neurons (Floresco et al., 2001; Floresco et al., 2003) rather than reverse transport.

*In vitro* studies had also suggested that impulse-independent dopamine release in the striatum is stimulated by glutamate possibly derived from terminals of the corticostriatal projection (Morari et al., 1998; Roberts and Sharif, 1978; Roberts and Anderson, 1979; Clow and Jhamandas, 1989; Krebs et al., 1991; Iravani and Kruk, 1996). This putative action of glutamate on striatal dopamine terminals attracted much attention due to its potential significance in the mechanisms underlying schizophrenia (Grace, 1991; Moghaddam and Adams, 1998; Adams and Moghaddam, 1998; Carlsson et al., 1999). However, *in vivo* microdialysis studies have suggested instead that cortico-midbrain projections control subcortical dopamine release by affecting the impulse activity of dopaminergic neurons (Youngren et al., 1993; Karreman and Moghaddam, 1996; Taber et al., 1996; Takahata and Moghaddam, 2000). Microdialysis results do not support the idea that the corticostriatal projection acts locally on striatal dopamine terminals (Moghaddam et al., 1990; Moghaddam and Gruen, 1991; Keefe et al., 1992).

On other the hand, we have recently studied striatal dopamine release in the anesthetized rat using *in vivo* voltammetry in conjunction with carbon fiber microelectrodes (Kulagina et al., 2001). In our hands, the intrastriatal infusion of kynurenate, a broad-spectrum antagonist of the ionotropic glutamate receptors (Stone, 1993), significantly decreased the extracellular dopamine concentration (Kulagina et al., 2001). This observation is consistent with the idea that endogenous glutamate, by acting at ionotropic receptors located within the striatum, controls basal dopamine release. In the present study, we further show that the effect of kynurenate on extracellular dopamine levels is independent of nigrostriatal impulse activity but is dependent on DAT activity.

## 4.3. MATERIALS AND METHODS

### 4.3.1. Voltammetric microelectrodes and techniques

Voltammetric microelectrodes were of conventional design. A single carbon fiber (3.5-μm radius T300 fiber, Union Carbide, Inc) was sealed with epoxy into a pulled borosilicate glass capillary. The exposed fiber, which served as the active sensing region of the electrode, was trimmed with a scalpel to a length of 400 μm. The electrodes were pretreated with 100 cycles of 0-2 V vs. Ag/AgCl triangular waveform delivered at 200 V/s. Dopamine was detected by fast-scan cyclic voltammetry (EI-400; Ensman Instruments, Bloomington, IN, U.S.A.). The applied potential was held at 0 V vs. Ag/AgCl between voltammetric scans. During each voltammetric scan the potential was swept linearly to 1.0 V, then to –0.5 V, and back to the starting potential of 0 V. The scan rate was 300 V/s and scans were repeated at 400-ms intervals.

Conversion of signals recorded during *in vivo* experiments to units of dopamine concentration was based on electrode sensitivity values obtained during post-calibration after the microelectrodes were removed from the rat brain. For calibration purposes, the microelectrodes were mounted in the center of a small flow-through chamber. A flow of artificial cerebrospinal fluid (aCSF: 145 mM $Na^+$, 1.2 mM $Ca^{2+}$, 2.7 mM $K^+$, 1.0 mM $Mg^{2+}$, 152 mM $Cl^-$ and 2.0 mM phosphate adjusted to pH 7.4) (Moghaddam and Bunney, 1989) was maintained by gravity feed from an elevated reservoir. Standard solutions of dopamine at concentrations ranging from 100 nM to 10 μM dissolved in aCSF were introduced to the flowing stream by means of a sample-loop valve.

The *in vivo* experiments performed during this work involved inspection of voltammetric signals over time periods lasting up to 40 min. Over time periods of this duration, drift in the voltammetric background signal is possible and may confound observation of the voltammetric dopamine signal. Throughout this work, the following procedure was used to correct for baseline drift. The time course of the voltammetric response was recorded in two windows of the applied potential, one corresponding to a background response (200-300 mV vs Ag/AgCl) and one corresponding the dopamine oxidation response superimposed on the background response (500-700 mV vs Ag/AgCl). Correction for background drift was accomplished by subtracting the response recorded in the 200-300 mV potential window from that recorded in the 500-700 mV potential window. This procedure was applied to both the data collected during *in vivo* experiments and during *in vitro* calibration procedures. Further details of this procedure are provided in the Results section.

Difference voltammograms were used to aid in the identification of the substance responsible for changes in the voltammetric signal observed during *in vivo* experiments. All the

voltammograms recorded over selected 200-s time windows (500 voltammograms in each time window) were averaged. Difference voltammograms were calculated by subtracting the averaged voltammograms obtained in different time windows (details in the Results section). The features of the resulting difference voltammogram were compared to those of difference voltammograms obtained during postcalibration of the microelectrode in dopamine standard solutions. The presence of features corresponding to the oxidation of dopamine and the reduction of dopamine's oxidation product, dopamine-o-quinone, served to identify whether dopamine was the substance responsible for changes in the voltammetric signal observed *in vivo*.

### 4.3.2. Animals and surgical procedures

Experiments involving animals were in accordance with NIH guidelines and were conducted with the approval of the Animal Care and Use Committee of the University of Pittsburgh. Male Sprague-Dawley rats weighing 250-300 g were anesthetized with chloral hydrate (300 mg/kg i.p.) and wrapped in a homeothermic blanket to maintain a body temperature of 37$^{o}$C. The rats were placed in a stereotaxic frame (David Kopf Instruments, Tujunga, CA, U.S.A.) with the upper incisor bar raised 5 mm above the interaural line (Pellegrino et al., 1979). Holes were drilled through the skull to permit placement of voltammetric microelectrodes and microinfusion pipets in the striatum or parietal cortex, as well as stimulating electrodes in the medial forebrain bundle. A single voltammetric microelectrode was lowered into the striatum (4.5 mm below dura, 2.5 mm lateral from midline, and 2.5 mm anterior to bregma) or the cortex (1.5 mm below dura, 2.3 mm lateral from midline, and 3.0 mm anterior to bregma).

Microinfusion pipets were fashioned from short lengths of fused silica capillary tubing with a nominal inner diameter of 25 μm. Several millimeters of the outlet end of the capillary were etched in HF until the wall thickness at the outlet was ~2 μm. For intrastriatal infusions, the inlet end of the capillary was epoxy-sealed to a gas-tight 50-uL syringe mounted on a stepper-motor driver (NA-1, Sutter Instruments) and preloaded with a 1-mM solution of kynurenate dissolved in aCSF or aCSF vehicle alone. The pipets were lowed into the striatum such that the outlet of the pipet was positioned 150 μm laterally from the mid-point of the active sensing portion of the carbon fiber microelectrode. For microinfusion into the MFB, a pipet of the same style was attached with epoxy to a bipolar stimulating electrode such that the outlet of the pipet was aligned vertically with the tip of the electrode. The combination device was lowered to a point just above the MFB (7.5 mm below dura, 1.6 mm lateral from midline, 2.2 mm posterior to bregma). The final vertical coordinate of the stimulation electrode was determined by slowly lowering it until the stimulation evoked dopamine release in the ipsilateral striatum. Electrical stimulation of the MFB was performed with a train of biphasic constant current square pulse with the following parameters: duration 10 s, frequency 60 Hz, pulse width 2 ms, intensity 280 μA peak-to-peak. Once in place, microinfusions of TTX (100 μM in 200 nL) or aCSF vehicle (200 nL) into the MFB were performed. This concentration and volume of TTX was found to cause a long lasting, complete abolition of evoked dopamine release, indicating effective blockade of nigrostriatal impulse traffic.

### 4.3.3. Chemicals and drugs

Nomifensine maleate, kynurenic acid and chloral hydrate were used as received from Sigma (St. Louis, Mo, U.S.A.). Tetrodotoxin with citrate was used as received from Alomone Labs (Jerusalem, Israel). Kynurenic acid and tetrodotoxin were dissolved in aCSF. Chloral hydrate and nomifensine were dissolved in phosphate buffered saline (PBS; 155 mM NaCl, 100 mM phosphate, pH 7.4). All solutions were prepared with ultrapure water (NANOPure; Barnstead, Dubuque, IA, U.S.A.).

## 4.4. RESULTS

### 4.4.1. Intrastriatal delivery of kynurenate inhibits dopamine release

Intrastriatal microinfusion of kynurenate caused a decrease in the dopamine signal at a nearby carbon fiber voltammetric microelectrode (Fig. 4.1). Microelectrodes and microinfusion pipets were implanted ~150 μm apart in the dorsal striatum of anesthetized rats. Recording by fast-scan cyclic voltammetry was initiated immediately after implantation and continued for the duration of the experiment. Microinfusion of kynurenate (1 mM in 200 nL) was initiated after an equilibration period of at least 2 hr. The temporal features of the voltammetric response to the microinfusions were examined in two separate windows of the applied potential (Fig 4.1, inset), one corresponding to the dopamine oxidation signal (500-700 mV v. Ag/AgCl) and the other corresponding to the nondopamine background signal (200-300 mV v. Ag/AgCl). The difference between the temporal profiles recorded in each potential window (Fig 4.1, main panel)

usually exhibited a biphasic response to the microinfusion. The first phase of the response was a rapid rise and fall of the signal that began with the microinfusion itself and usually lasted about 5 min. This was followed by a prolonged second phase of the response, during which the signal remained well below the preinfusion baseline.

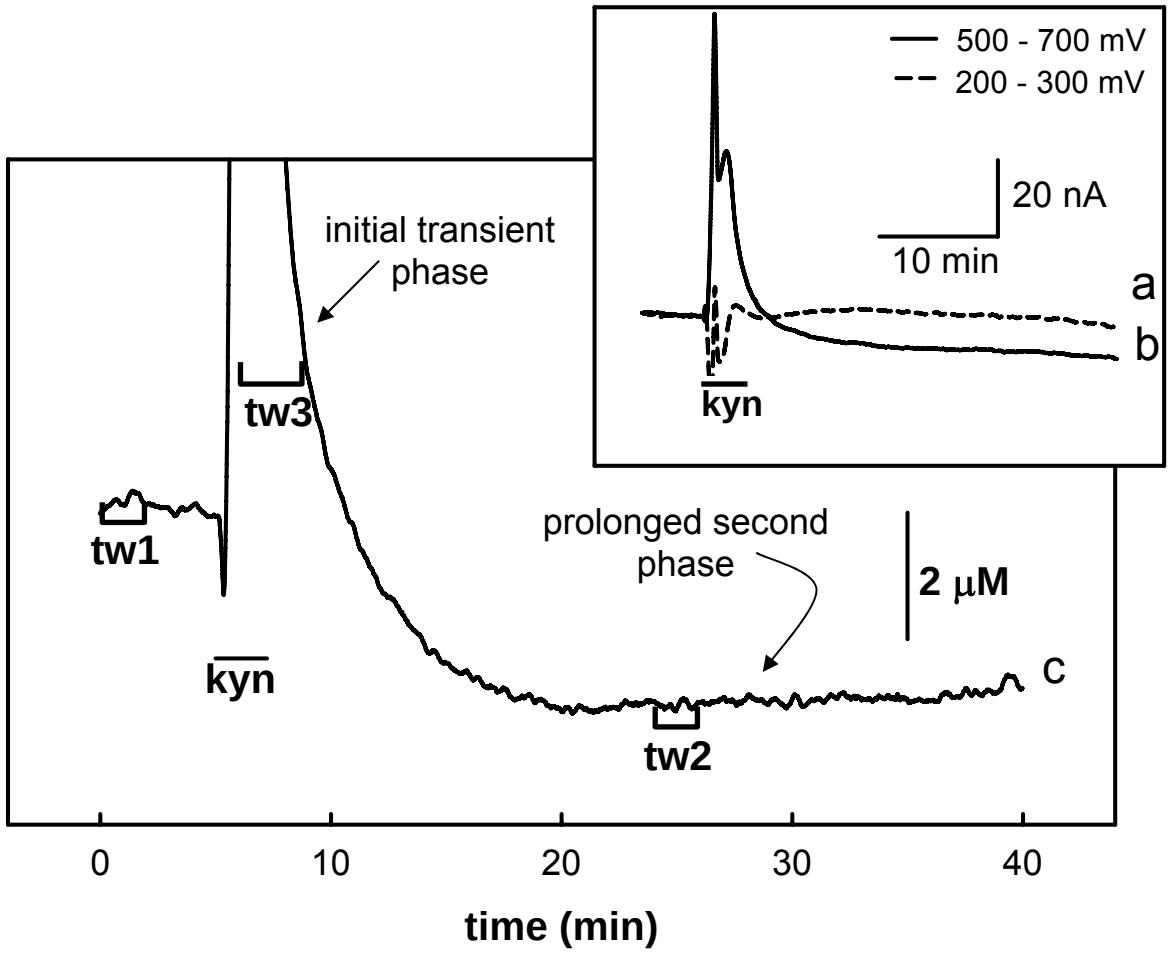


**Figure 4.1. Fast scan cyclic voltammetry shows that intrastriatal infusion of kynurenate decreases extracellular dopamine levels. Inset panel: Traces of the raw signals recorded in two separate windows of the applied voltammetric waveform (trace a, 200 300 mV; trace b, 500 700 mV). Main panel: Trace c is the difference signal obtained by subtracting trace a (inset panel) from trace b (inset panel). The difference signal (trace c) responds in a biphasic manner to the kynurenate infusion, which took place during the time interval indicated by the horizontal bars labeled kyn. An initial transient phase lasting approximately 5 min is followed by a prolonged second phase during which the signal stabilizes at a level well below the preinfusion baseline. The vertical concentration scale bar in the main panel was determined by post-calibration of the microelectrode immediately after it was removed from the rat brain. (The time windows labeled tw1, tw2, and tw3 are discussed in the legend of Fig. 4. 2.)**

Cyclic voltammograms (i.e. plots of the current v. potential response recorded during each voltammetric scans of the applied potential) obtained before and after the kynurenate microinfusion were used to identify whether the responses were related to changes in the extracellular concentration of dopamine (Fig 4.2). For this purpose, the voltammograms recorded in 200-s time windows (labeled tw1, tw2, and tw3 in Fig. 4.1) prior to the infusion (tw1), during the initial transient phase of the response (tw3), and during the prolonged second phase of the response (tw2) were averaged. The left panel of Fig. 4.2 compares the averaged voltammograms obtained in tw1 and tw2. The voltammograms are indistinguishable until they are plotted on an expanded scale (left panel, inset). Subtraction is used to accentuate the small difference between these voltammograms (Fig 4.2, right panel, voltammogram a). The resultant difference voltammogram exhibits a distinct oxidation peak in the vicinity of 500 to 700 mV and a distinct reduction peak in the vicinity of 0 to –200 mV. These oxidation and reduction peaks compare well with those obtained during postcalibration of the microelectrode in a 5-μM DA standard (Fig. 4.2, right panel, voltammogram b). The correspondence between the oxidation and reduction features of the difference voltammogram obtained upon infusion of kynurenate into the striatum with those features obtained during postcalibration provide a voltammetric basis for concluding that the prolonged decrease in the signal observed *in vivo* is due to a prolonged decrease in the extracellular concentration of dopamine. The difference voltammogram associated with the initial transient phase of the response was not consistent with dopamine (Fig. 4.2, right panel, voltammogram c), which shows that the initial transient is not related to dopamine and is therefore presumed to be an infusion artifact. The transient signal was inconsistent in amplitude, and on numerous occasions was absent altogether. The transient response is more pronounced in the present study compared to our earlier report (Kulagina et al.,

2001) because the pipet used for kynurenate infusion in the present study was placed about 100 μm closer to the voltammetric microelectrode, which increased the amplitude and reproducibility of the second phase of the response.

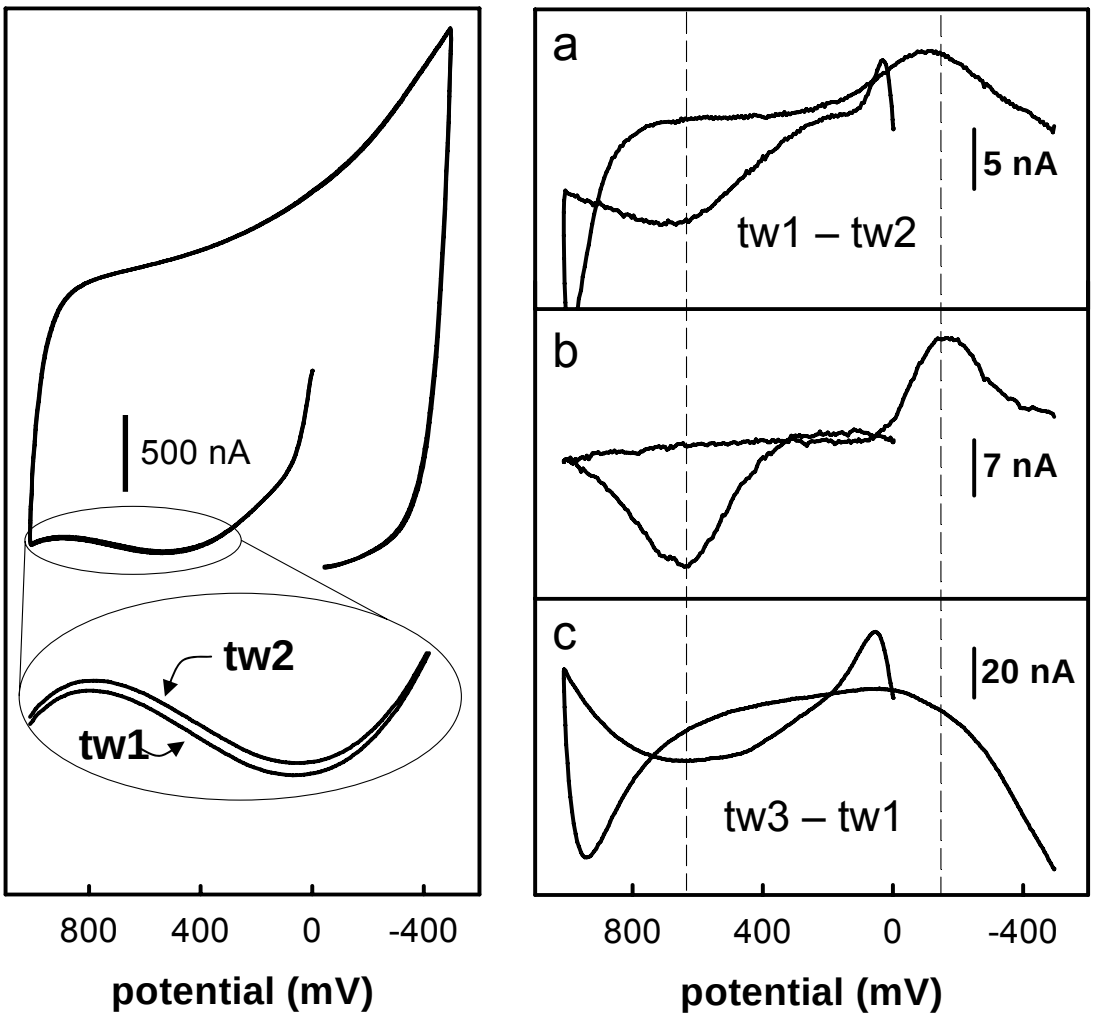


**Figure 4.2. Left panel: Non-subtracted voltammograms recorded during time windows before (tw1, Fig. 4.1) and after (tw 2, Fig 4.1) kynurenate infusion. Differences between the voltammograms are subtle but become evident when they are plotted on an expanded scale (inset). Right panel. Difference voltammograms obtained by background subtraction. Difference voltammogram a was obtained by subtracting the voltammogram obtained after kynurenate infusion (tw2, Fig. 4.1) from that obtained before the infusion (tw1, Fig 4.1). Difference voltammogram b was obtained during postcalibration of the microelectrode in dopamine (5 μM). Difference voltammogram c was obtained by subtracting the preinfusion voltammogram (tw1, Fig. 4.1) from that recorded during the initial transient phase of the infusion response (tw3, Fig. 4.1).**

The second prolonged phase of the voltammetric response to the intrastriatal infusion of kynurenate was consistently observed in multiple animals (Fig. 4.3). Furthermore, when both the microelectrodes and the micropipets were implanted in the parietal cortex instead of the striatum, microinfusion of kynurenate had no prolonged effect on the signal (Fig. 4.3), which demonstrates that the effect of kynurenate on the voltammetric response is anatomically specific. This anatomical specificity contributes to demonstrating that the prolonged phase of the voltammetric response to the infusion observed in the striatum is not an artifact.

Figures 4.1-4.3 extend the previous report of Kulagina et al. (2001), which also showed that the prolonged decrease in the voltammetric signal was sensitive to the inhibition of dopamine synthesis with α-methyl-p-tyrosine, resistant to the blockade of dopamine metabolism with pargyline, diminished in the presence of exogenous glutamate, and absent if the experiment was performed in the thalamus rather than the striatum. Thus, the prolonged decrease in the signal following intrastriatal infusion of kynurenate meets voltammetric, pharmacological, and anatomical criteria for being identified as a decrease in the extracellular dopamine concentration pursuant to the blockade of ionotropic glutamate receptors located within the striatum.

The voltammetric signals recorded *in vivo* were converted to values of dopamine concentration by calibration of the electrodes after they were removed from the brain. According to this procedure, the maximum decrease in the voltammetric signal following the kynurenate infusion corresponds to a decrease in the extracellular dopamine concentration of 2.6 ± 0.7 μM (mean ± standard deviation, n = 26 infusions performed in 19 rats). The decrease in dopamine concentration observed during the present study was larger than we reported before (Kulagina et al., 2001), which we attribute to the closer placement of the infusion pipet to the microelectrode causing a larger effective dose of kynurenate in the present study.

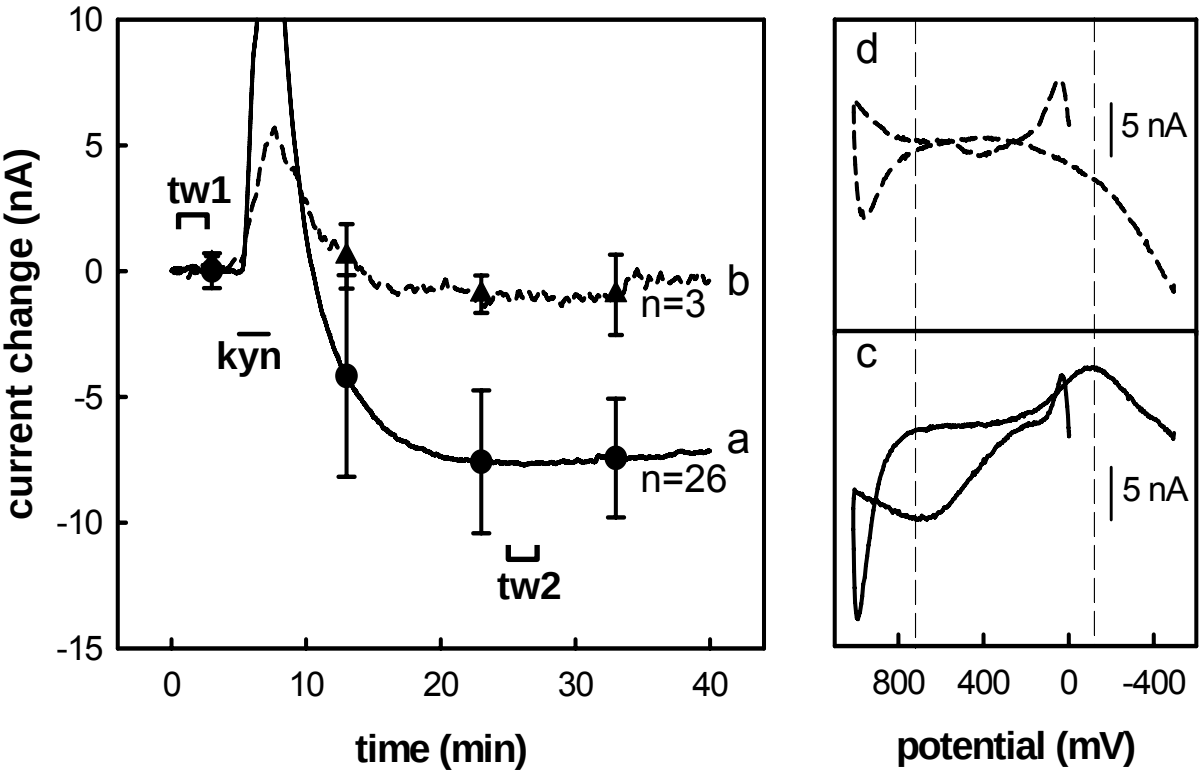


**Figure 4.3. Left panel: Intrastriatal microinfusion of kynurenate significantly decreases extracellular dopamine as measured by voltammetry in the striatum (a, solid line). Microinfusion of kynurenate into the parietal cortex had no prolonged effect on the voltammetric signal recorded at a nearby carbon fiber microelectrode (b, dashed line). The horizontal bar labeled kyn indicates when the infusion took place. The lines were obtained by averaging the traces recorded in each of a group of animals (a, n= 26 in 19 animals: b, n=3 in 3 animals). The symbols indicate the mean and the standard deviations upon which statistical analyses were based. The infusion had a significant effect in the striatum (one-way ANOVA: f = 43.97, df = 3,103, $p<0.001$) but not in the parietal cortex. Right panel: Difference voltammograms obtained in the striatum (c, solid line) and cortex (d, dashed line). These difference voltammograms were obtained by subtracting the voltammograms recorded after the infusions (tw2, left panel) from those recorded before the infusion (tw1, left panel). The difference voltammogram obtained in the striatum exhibits dopamine oxidation and reduction features whereas that obtained in the cortex does not.**

### 4.4.2. Kynurenate inhibits tonic, impulse-independent dopamine release

Delivery of tetrodotoxin to the medial forebrain bundle (MFB) by means of a micropipet mounted on a stimulating electrode (stimulus-guided infusion) was highly effective at terminating nigrostriatal impulse traffic (Fig. 4.4). A micropipet was glued to a bipolar stainless

steel stimulating electrode. The stimulating electrode was lowered slowly towards the MFB until electrical stimulation evoked dopamine release in the ipsilateral striatum as measured by the voltammetric microelectrode (Kuhr et al., 1984). Subsequent infusion of tetrodotoxin (100 µM in 200 nL) into the MFB completely abolished any further response to electrical stimulation, indicating that TTX was accurately and effectively delivered so as to terminate impulse traffic in the nigrostriatal dopamine fibers.

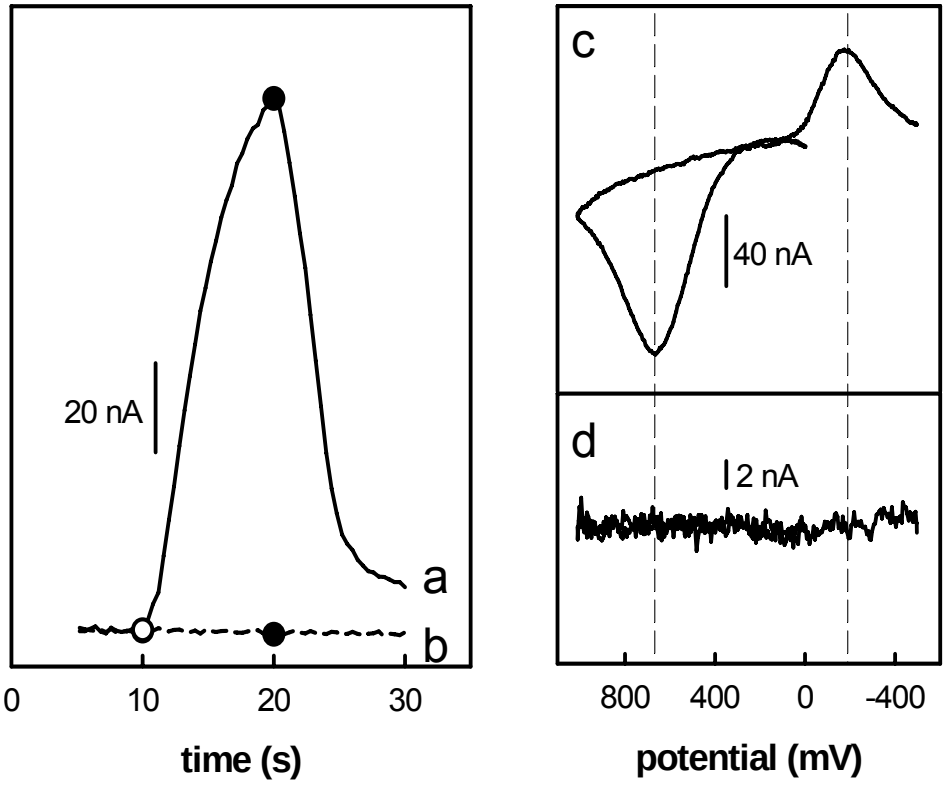


**Figure 4.4. Left panel: Electrical stimulation of the MFB evokes dopamine release in the striatum before (a, solid line) but not after (b, dashed line) the microinfusion of TTX into the MFB. The open circle indicates when the stimulus began and the closed circles indicate when it stopped. Right panel: Background-subtracted cyclic voltammograms obtained during electrical stimulation of the MFB before (c) and after (d) the TTX infusion.**

Stimulus-guided infusions of vehicle (aCSF) or TTX into the MFB had no impact on the prolonged decrease in extracellular dopamine following intrastriatal microinfusion of kynurenate (Fig. 4.5). The voltammetric response to an initial infusion of kynurenate was recorded as described above. A stimulus-guided infusion of aCSF or TTX into the MFB was performed 70 min after the first intrastriatal infusion of kynurenate. Then, 20 min after the infusion into the MFB, a second intrastriatal kynurenate infusion was performed. There were no statistically significant differences between the voltammetric response to the first and second kynurenate infusion (Fig. 4.5). Hence, kynurenate appears to act within the striatum to inhibit a dopamine release process that occurs independently of nigrostriatal impulse traffic.

The intrastriatal infusion of TTX also abolished evoked dopamine release during electrical stimulation of the MFB without affecting the voltammetric response to kynurenate infusions (not shown). A voltammetric microelectrode was placed in the striatum along with two microinfusion pipets, one on either side of the microelectrode. One pipet was used for the intrastriatal infusion of vehicle or TTX between two consecutive infusions of kynurenate via the other pipet. Infusion of vehicle or TTX directly into the striatum had no impact on the prolonged decrease in extracellular dopamine evoked by intrastriatal infusion of kynurenate. Thus, kynurenate also acts on dopamine release in the absence of local impulse activity within the striatum.

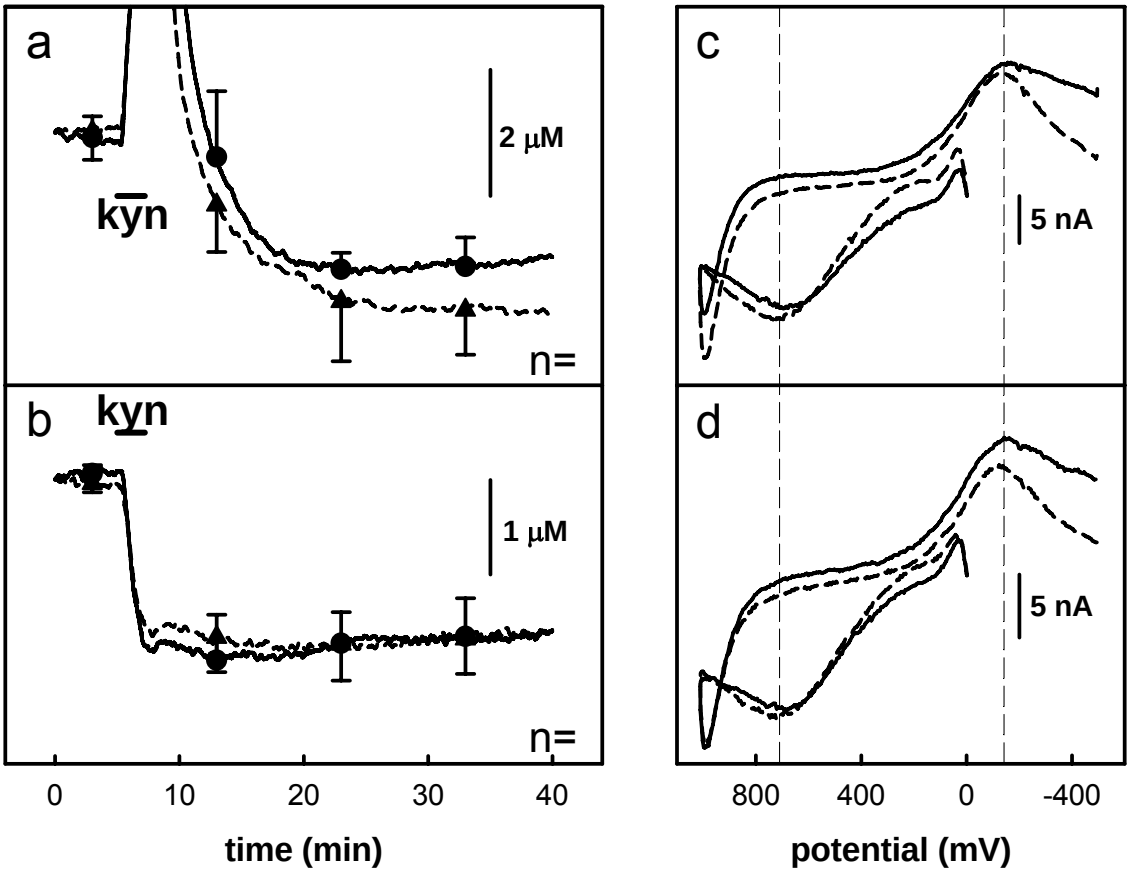


**Figure 4.5. Intrastriatal microinfusion of kynurenate affects an impulse-independent mode of dopamine release. Left panel: The responses to intrastriatal infusion of kynurenate before (solid line) and after (dashed line) infusion of either aCSF (**a**) or TTX (**b**) into the MFB. The symbols show the mean and standard deviation of the responses at 10 min intervals. According to 2-way ANOVA, neither the infusion of aCSF nor the infusion of TTX significantly changed the response to the infusion of kynurenate. The horizontal bars indicate when the infusion of kynurenate took place. Right panel: Difference voltammograms obtained by subtracting the voltammograms recorded after the kynurenate infusion from those recoded before the kynurenate infusion. The difference voltammograms obtained before (dashed) and after (solid) the infusion of either aCSF (c) or TTX (d) all exhibit the dopamine oxidation and quinone reduction features.**

### 4.4.3. The role of the dopamine transporter

Blockade of the dopamine transporter (DAT) by means of the systemic administration of nomifensine either decreased or abolished the prolonged decrease in the voltammetric signal after the intrastriatal microinfusion of kynurenate (Fig. 4.6). Two groups of rats received an

intraperitoneal injection of saline or nomifensine 70 min after an initial kynurenate infusion and 20 min prior to the second kynurenate infusion. At the dose used here, 20 mg/kg, nomifensine is well-known to block dopamine uptake in the striatum (Church et al., 1987; Yang et al., 1998). In half of the rats studied (4 of 8), nomifensine completely abolished the prolonged decrease in the voltammetric signal following the second kynurenate infusion: the time trace exhibited no prolonged decrease in the signal (Fig 4.6a) and the difference voltammogram exhibited no oxidation or reduction features to indicate that a change in dopamine concentration had occurred (Fig 4.6b). In the other 4 rats studied, nomifensine diminished the amplitude of the prolonged response to kynurenate (Fig. 4.6c) and the difference voltammograms before and after nomifensine exhibited the oxidation and reduction features consistent with dopamine (Fig. 4.6d). Intraperitoneal injection of saline had no effect on the response to kynurenate (Fig. 4.6e) and again the difference voltammograms obtained before and after saline exhibited oxidation and reduction features consistent with dopamine (Fig. 4.6f). These findings suggest that DAT is involved in the mechanism by which glutamate locally regulates basal extracellular dopamine concentrations via striatal ionotropic receptors. This is consistent with the idea that a DAT-mediated reverse-transport process contributes to the basal extracellular dopamine concentration in the striatum.

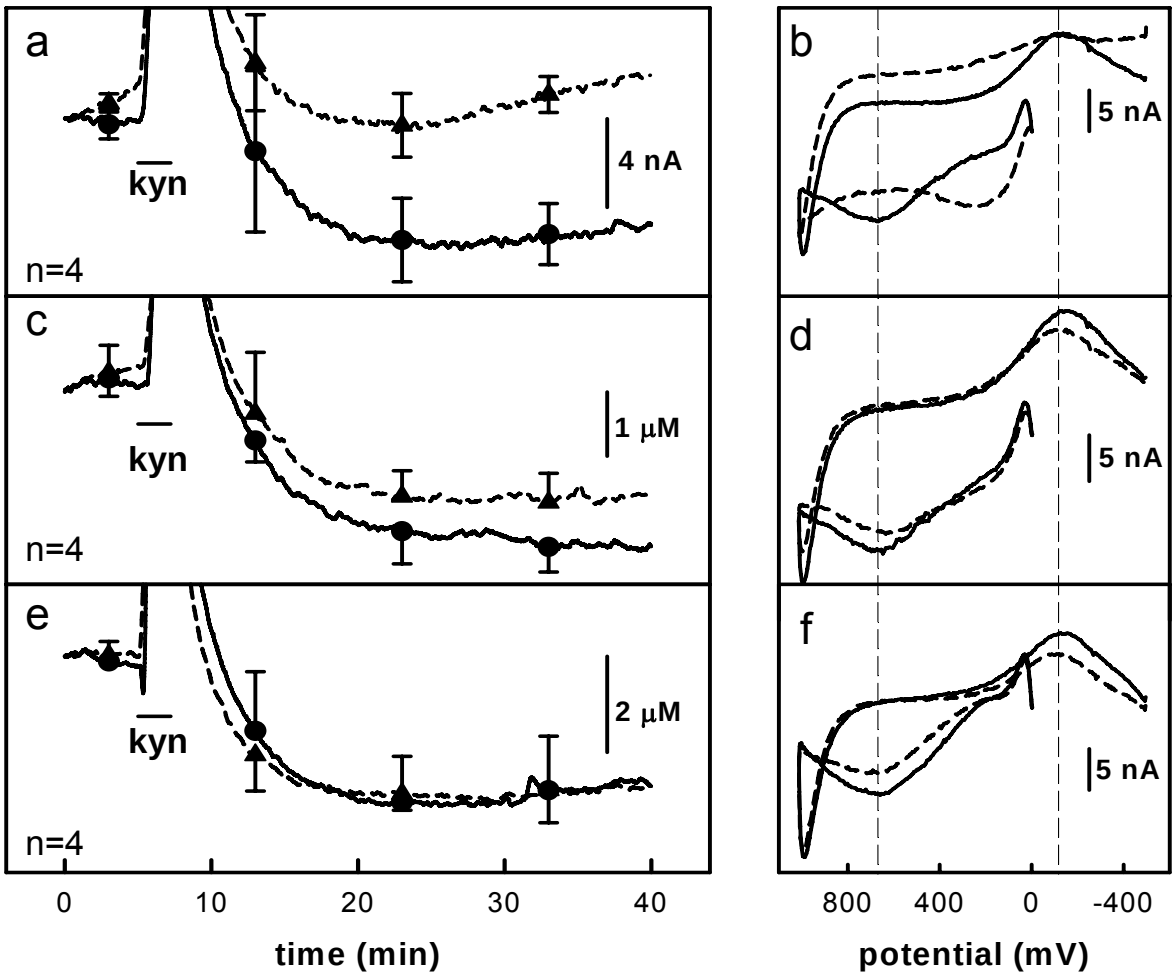


**Figure 4.6. Systemic administration of the nomifensine (20 mg/kg i.p.) either abolishes (a and b) or significantly diminishes (c and d) the effect of kynurenate on extracellular dopamine. (**a**) In 4 of 8 animals (dashed line) nomifensine eliminated the effect of kynurenate (two-way ANOVA; $p<0.001$). (**b**) In these animals, subtracted cyclic voltammograms obtained prior to nomifensine administration (solid line) were characteristic of dopamine. Voltammograms obtained after nomifensine administration were not characteristic of dopamine (dashed line). (**c**) In 4 other animals, systemic administration of nomifensine (dashed line) significantly diminished the response to kynurenate infusion (two-way ANOVA, $p<0.05$). (**d**) In these animals, subtracted voltammograms were characteristic of dopamine both before (solid line) and after (dashed line) nomifensine administration. (**e**) Systemic administration of saline had no affect on the response to kynurenate (two-way ANOVA). (**f**) Voltammograms obtained before (solid line) and after (dashed line) saline were characteristic of dopamine. The horizontal bars indicate when the infusions took place.**

## 4.5. DISCUSSION

This report contains the first collective body of evidence obtained under *in vivo* conditions to suggest that 1) tonic dopamine release occurring via an impulse-independent mechanism contributes to basal dopamine in the striatal extracellular space of the anesthetized rat, 2) glutamatergic tone on striatal ionotropic glutamate receptors is necessary for the maintenance of tonic dopamine release in the striatum, and 3) tonic dopamine release occurs via DAT-mediated reverse transport. In previous *in vivo* experiments, impulse-independent dopamine release has mainly been observed in animals treated with amphetamine-like substances (Westerink et al., 1987; Westerink and deVries, 1988). The findings of the present study, however, suggest that impulse-independent dopamine release contributes to the basal extracellular dopamine concentration in the striatum of the anesthetized rat even in the absence of amphetamine-like substances. Furthermore, these findings support the conclusion that impulse-independent dopamine release is a component of both normal brain physiology and, possibly, the pathophysiology of dopamine-related disorders.

### 4.5.1. Methodological considerations

The results of this study suggest that a DAT-mediated reverse transport process gives rise to an impulse-independent mode of dopamine release that, under the influence of glutamate acting at ionotropic receptors located within the striatum, contributes to the extracellular concentration of dopamine in the rat striatum. While studies conducted on *in vitro* preparations reached a similar conclusion (Giorguieff et al., 1977; Desce et al., 1992; Lonart and Zigmond, 1991; Morari et al., 1998; Roberts and Anderson, 1979; Iravani and Kruk, 1996), *in vivo* microdialysis studies

reached the different conclusion that basal dopamine release is strictly impulse-dependent (Westerink et al., 1987; Westerink and deVries, 1988). Hence, there is a notable difference between the present voltammetry-based findings and prior microdialysis-based finding.

Bungay et al. (2003) have considered the origins of differences between voltammetry and microdialysis results relevant to striatal dopamine (Bungay et al., 2003). Some of those origins may be attributed to the trauma associated with the implantation of microdialysis probes (Clapp-Lilly et al., 1999; Zhou et al., 2001). This trauma appears to slow the kinetics of dopamine release and uptake in the tissue surrounding microdialysis probes (Yang et al., 1998; Bungay et al., 2003). The same might occur in the case of glutamate. Using microsensors designed to detect glutamate (Kulagina et al., 1999), we found the extracellular glutamate concentration in striatum to be about 10-fold higher than that reported by quantitative microdialysis (Miele et al., 1996). So, we speculate that tonic dopamine release may not be clearly detected by *in vivo* microdialysis because there is insufficient tone on ionotropic glutamate receptors, a necessary condition for tonic dopamine release, in the tissue surrounding the probes. Some existing microdialysis data are consistent with this speculation. For example, adding glutamate agonists to the perfusion medium caused a TTX-insensitive increase in dopamine concentrations in striatal dialysate samples (Keefe et al., 1992; Verma and Moghaddam, 1998), which could signify that perfusing with a glutamate agonist reinstates a normally occurring tone on the ionotropic glutamate receptors near the probe, thereby reinstating a normally occurring tonic mode of dopamine release.

The magnitude of the decrease in the dopamine concentration upon intrastriatal infusion of kynurenate is considerably larger than previous estimates of the basal dopamine concentration obtained with both microdialysis (Smith and Justice, 1994) and voltammetric methods (Gonon

and Buda, 1985; Marcus et al., 2001). Bungay et al. (2003) have discussed the possibility that the trauma associated with microdialysis probes may lead to an underestimation of basal dopamine concentrations. However, since Gonon and coworkers (Gonon and Buda, 1985) obtained their estimate of the basal concentration using a carbon fiber microelectrode of similar dimensions to the ones we used, differences between the amount of trauma in our work and Gonon's seem unlikely. The different concentration estimates may be related to differences between the styles of voltammetry we used, fast-scan cyclic voltammetry, and that Gonon and coworkers used, differential normal pulse voltammetry. Also, Gonon and coworkers used a more extensive electrode pretreatment regimen that we do. The details as to why these two voltammetric procedures would lead to such different estimates of extracellular dopamine concentrations are not clear. However, numerous differences can be found between the outcome of experiments based on these different voltammetric procedures. For example, when fast-scan voltammetry is used to monitor evoked dopamine release during electrical stimulation of the MFB, many laboratories have found that dopamine concentrations increase immediately with the start of the electrical stimulation and return to baseline within a few seconds when the stimulation ends (Garris et al., 1994; Cragg et al., 1997; Gonon, 1997; Dickinson et al., 1999; Peters and Michael, 2000). However, according to differential normal pulse voltammetry, dopamine levels may not increase until after the stimulation and may take several minutes to return to baseline (Gonon and Buda, 1985). Because we do not have first-hand experience with the differential normal pulse technique, we are not in a position to offer a detailed explanation for the different results these procedures yield.

### 4.5.2. Physiological significance of tonic dopamine release

In our hands, intrastriatal microinfusions of kynurenate caused extracellular dopamine concentrations to drop by micromolar amounts. This suggests that tonic dopamine release, mediated by reversal of the dopamine transporter, produces an extracellular dopamine concentration sufficient to occupy both $D_1$ and $D_2$ receptors (Missale et al., 1998). Hence, similar to the conclusion reached in the case of transporter-mediated glutamate release (Baker et al., 2002a; Baker et al., 2002b), the present study suggests that transporter-mediated dopamine release might play a physiological role in dopaminergic transmission within the striatum.

The present study did not address the nature of the physiological role of tonically released dopamine but Grace (Grace, 1991) has previously hypothesized that tonically released dopamine modulates the responsiveness of dopamine receptors to phasic dopamine release. Grace also hypothesized that a decrease in tonic dopamine release caused by inadequate tone on striatal glutamate receptors might trigger a hyper-responsiveness of postsynaptic targets to phasically released dopamine, possibly eliciting the symptoms of schizophrenia. Hence, the results of the present study are significant in that they provide the most direct *in vivo* neurochemical evidence available to date that endogenous glutamate acts within the striatum to control tonic dopamine release.

### 4.5.3. Modes of dopamine transmission in the striatum

Together with other reports (Floresco et al., 2001; Floresco et al., 2003), the present study suggests that three distinct modes of dopamine release might contribute synergistically to dopaminergic transmission in the striatum: a tonic, DAT-mediated mode of release as revealed by the present study; a slow phasic mode of release associated with the non-burst firing of midbrain dopamine neurons; and an impulse-dependent mode of release associated with the burst firing of midbrain dopamine neurons. Several studies have demonstrated that midbrain afferents may differentially affect the non-burst firing and burst firing of dopamine neurons, suggesting the existence of two distinct modes of impulse-dependent dopamine transmission (Floresco et al., 2001; Floresco et al., 2003).

### 4.5.4. Dopamine-glutamate interactions

One argument against direct interactions between dopaminergic and glutamatergic striatal afferents originates in ultrastructural findings that they do not form direct synaptic connections with each other (Sesack and Pickel, 1992). They do, however, make frequent appositional contacts (Sesack and Pickel, 1992), which raises the possibility that volume transmission could be involved. Consistent with this ides, some studies have suggested that dopamine molecules readily escape the small synaptic clefts found in the striatum (Gonon, 1997; Zoli et al., 1998; Garris et al., 1994), possibly enabling volume transmission. Our finding that DAT-mediated transport contributes to dopamine release increases the likelihood that dopaminergic transmission occurs in the volume mode, because ultrastructural studies have located DAT protein on the

extrasynaptic surfaces of striatal terminals (Nirenberg et al., 1996), suggesting that reverse transport might deliver dopamine directly to the extrasynaptic space. In addition, ultrastructural studies have located dopamine receptors on the extrasynaptic surfaces of pre- and post-synaptic membranes (Pickel et al., 1996), suggesting that dopamine molecules exiting terminals via the transporter may directly affect such receptors.

Possible targets of dopaminergic volume transmission within the striatum include the glutamate-releasing terminals of the corticostriatal pathway, which have recently been shown to express $D_2$ dopamine receptors (Wang and Pickel, 2002), and which are a potential source of the glutamate responsible for maintaining tone at the ionotropic glutamate receptors that seems to drive dopamine reverse transport. Since glutamate release also involves a transporter (Baker et al., 2002a; Baker et al., 2002b) and because the response to the kynurenate infusion was not altered by the intrastriatal application of TTX, it may be possible that the local effect of glutamate on striatal dopamine terminals is also mediated by volume transmission. This point, however, can not be made with certainty because to date evidence for the presence of ionotropic glutamate receptors on dopamine terminals has not been obtained (Bernard et al., 1997; Chen et al., 1998). So, although the results of our study are consistent with a local action involving ionotropic glutamate receptors within the striatum, our results to not demonstrate that the action is direct. The recent studies of Avshamulov (2003), for example, raise the possibility that diffusible messengers might carry information between striatal terminals.

# 5. VOLTAMMETRIC STUDIES IN THE ANESTHETIZED RAT BRAIN FOR INVESTIGATING THE MECHANISMS OF DOPAMINE RELEASE AFTER UPTAKE INHIBITION

## 5.1. ABSTRACT

Drugs of abuse, such as cocaine and amphetamine, block dopamine uptake, causing changes in dopamine activity in the brain. Dopamine receptors and different mechanisms of dopamine release also regulate dopamine levels in the brain. Vesicular release, which is driven by dopamine nerve impulse firing, and dopamine transporter-assisted release, also known as reverse transport, are two mechanisms of dopamine release that may be involved in the changes in extracellular dopamine after uptake inhibition. In this study, we used fast-scan cyclic voltammetry in conjunction with carbon fiber microelectrodes to determine by what mechanism dopamine $D_2$ receptors control dopamine release after uptake inhibition.

Systemic administration of the uptake blocker, nomifensine, increased extracellular dopamine levels in the striatum of anesthetized rats pretreated with the $D_2$ receptor blocker, sulpiride. Local treatment with the sodium channel blocker, tetrodotoxin (TTX), in the medial forebrain bundle (MFB) or the striatum blocked the effect of systemic nomifensine administration in the striatum of sulpiride-pretreated rats. Blockade of dopamine nerve impulses by TTX, both locally in the striatum and along the MFB, prevented the nomifensine-induced increase in extracellular dopamine in the sulpiride pretreated rats. We conclude that $D_2$ receptors

mediate control of extracellular dopamine after uptake inhibition through a dopamine nerve impulse-dependent mechanism.

## 5.2. INTRODUCTION

The nigrostriatal dopamine pathway is a carefully regulated system, containing numerous processes that actively participate in maintaining dopamine homeostasis. Striatal ionotropic glutamate receptors regulate striatal dopamine levels through their control of the dopamine transporter (Kulagina et al., 2001, Borland and Michael, 2004). These same dopamine transporters act to remove excess dopamine from the extracellular space, in a process known as reuptake. Dopamine $D_2$ receptors control the rate of reuptake of the transporters, while simultaneously controlling dopamine synthesis, neuronal firing and vesicular release of dopamine into the synapse ((Mercuri et al., 1991; Mercuri et al., 1992; Mercuri et al., 1997; Mereu et al., 1983; Werkman et al., 2001; Meiergerd et al., 1993; Dickinson et al., 1999; Wu et al., 2002). These checks and balances within the striatum are essential for maintaining a healthy dopamine system.

Drugs of abuse, such as cocaine and amphetamine, have a profound affect on dopamine neurotransmission in the striatum. Numerous studies show that cocaine and similar drugs of abuse act by blocking dopamine transporters, thereby inhibiting reuptake and, by consequence, increasing extracellular dopamine levels (Church et al., 1987; DiChiara et al., 1996). Although cocaine directly decreases the rate of uptake, other processes involved in regulating dopamine levels are affected. Dopamine $D_2$ receptors, for example, are found to play a role in mediating drug-induced changes in dopamine levels. Studies involving $D_2$ receptor knock-out mice reveal

a link between $D_2$ receptors and an increased susceptibility to drug abuse (Schmitz et al., 2001; Benoit-Marand et al., 2001; Rougé-Pont et al., 2002). After systemic cocaine administration, dopamine levels increased significantly in mice lacking $D_2$ receptor function. Cocaine, however, did not significantly increase dopamine levels in mice with full $D_2$ receptor function (Rougé-Pont et al., 2002). In addition to mediating resting extracellular dopamine levels, $D_2$ receptors also participate in the regulation of drug-induced alterations in the striatal dopamine.

Overstimulation of dopamine receptors by a drug-induced increase in dopamine is the prevailing model used to explain the effects of drug abuse on the brain. This model relies on inactivated dopamine receptors to be activated by increases in dopamine, through changes in neuronal firing and release, or through a reduction in transporter reuptake, like that caused by cocaine. However, recent evidence suggests that glutamate regulates a resting extracellular pool of dopamine of ~2 μM (Borland and Michael, 2004). At this concentration, dopamine receptors would be activated, suggesting that $D_2$ receptors would prevent a large increase in extracellular dopamine after uptake inhibition, which is consistent with previous reports (Benoit-Marand et al., 2001; Rougé-Pont et al., 2002).

In this study, we used carbon fiber microelectrodes in conjunction with fast-scan cyclic voltammetry to test the hypothesis that $D_2$ receptors participate in a feedback mechanism that regulates extracellular dopamine levels after uptake inhibition. We monitored the change in dopamine after systemic administration of the uptake inhibition, nomifensine, in anesthetized rats pretreated with the $D_2$ receptor antagonist sulpiride. Tetrodotoxin was infused locally and at the medial forebrain bundle (MFB) to examine the impact of impulse inhibition on basal dopamine levels after uptake inhibition in $D_2$-antagonized rats.

## 5.3. MATERIALS AND METHODS

### 5.3.1. Voltammetric electrodes and techniques

Carbon fiber microcylinder electrodes were constructed as previously described (Yang et al., 1998). Briefly, 7 μm diameter carbon fibers (Thornell Carbon Fiber, T300, Amoco Performance Products, Inc., Greenville, SC, USA) were pulled and epoxy sealed into borosilicate glass capillaries (Sutter Instruments, Novato, CA, USA) and trimmed to 400 μm. Electrical contact was made using mercury and a nichrome wire. Prior to use, the microelectrodes were placed in a gravity-fed flow stream apparatus. The flow cell was filled with room temperature, $N_2$-purged artificial cerebral spinal fluid (aCSF, 145 mM $Na^+$, 1.2 mM $Ca^{2+}$, 2.7 mM $K^+$, 1.0 mM $Mg^{2+}$, 152 mM $Cl^-$ and 2.0 mM phosphate adjusted to pH 7.4) (Moghaddam and Bunney, 1989). The electrodes were electrically pretreated (Kovach et al., 1984; Feng et al., 1987) with a triangular potential waveform (0-2 V vs. Ag/AgCl reference at 200 V/s for 1s).

Fast scan cyclic voltammetry (Borland and Michael, 2004; Baur et al., 1988) was performed with a computer-controlled potentiostat (EI-400, Ensman Instruments, Bloomington, IN, USA) and software developed in-house. The potential was scanned in the positive direction to +1.0 V, then to -0.5 V and back to a resting potential of 0 V vs. Ag/AgCl at a rate of 300 V/s. The applied potential was held at 0 V vs. Ag/AgCl between voltammetric scans. Scans were repeated at 400 ms intervals for all experiments.

Dopamine oxidation signals were monitored by integrating the current between 500 mV-700 mV vs. Ag/AgCl on the initial sweep of each scan. Conversion of the dopamine oxidation current to dopamine concentration was based on post-calibration of the electrode after immediate removal from the rat brain. Identification of dopamine was accomplished by comparing the

background-subtracted voltammograms in vivo to those obtained during post-calibration of the electrode. The response of the microelectrode to other analytes, as well as its sensitivity and response time towards dopamine, was also tested as during post-calibration.

### 5.3.2. Microinfusion pipets

Microinfusion pipets were constructed using fused silica capillary tubing (350 μm O.D., 25 μm I.D., Polymicro Technologies, Phoenix, AZ, USA). The outlet tip of the capillary was etched to 40 μm O.D. with concentrated hydrofluoric acid. The inlet end of the capillary was attached to a 50 μL syringe (Hamilton, Reno, NV, USA) driven by a microprocessor-controlled driver (Sutter Instruments, Novato, CA, USA) and pre-filled with the appropriate drug solution. The rate of delivery of the infusion solution was 90 μL/min.

### 5.3.3. Animals and surgical procedures

All procedures involving animals were carried out with the approval of the Institutional Animal Care and Use Committee of the University of Pittsburgh. Male Sprague-Dawley rats (Hilltop, Scottsdale, PA, USA) (250-375g) were anesthetized with chloral hydrate (400 mg/kg i.p.) and wrapped in a homoeothermic blanket (EKEG Electronics, Vancouver, BC, Canada) to maintain a body temperature of 37$^{o}$C. The rats were placed in a stereotaxic frame (David Kopf Instruments, Tujunga, CA, USA) with the incisor bar 5 mm above the interaural line (Pellegrino et al., 1979). Holes were drilled through the skull in the appropriate positions to expose the underlying dura and brain tissue. A reference electrode made contact with the brain tissue via a modified salt

bridge. The dura was removed with a scalpel to allow for placement of the microelectrode into the brain tissue with minimal disruption to the surrounding blood vessels.

In all experiments, a microcylinder electrode (400 μm in length) was placed in the striatum of the rat, positioned at 2.5 mm anterior with respect to bregma, 2.5 mm lateral with respect to the midline and 4.5 mm below dura. The voltammetric signal was recorded every 400 ms beginning two hours after electrode implantation. Nomifensine was delivered i.p. 60 min after vehicle or sulpiride.

### 5.3.4. Pharmacological agents and procedures

Approximately two hours after microelectrode implantation, each rat was pretreated with sulpiride (100 mg/kg i.p.) or vehicle (i.p.). Nomifensine (20 mg/kg i.p.) was administered one hour after either sulpiride or vehicle. Where designated, tetrodotoxin (100 μM, 200 nL) was delivered via a micropipette to either the striatum or MFB 10 or 15 min prior to nomifensine administration.

### 5.3.5. Materials and solutions

Chloral hydrate, nomifensine maleate salt, (-)-sulpiride and dopamine were used as received from Sigma (St. Louis, MO, USA). Tetrodotoxin (with citrate) was used as received from Alomone Labs (Jerusalem, Israel). Chloral hydrate and nomifensine were dissolved in phosphate buffered saline (PBS: 155 mM NaCl, 100 mM phosphate, pH 7.4). Sulpiride was dissolved in

1% (wt/vol) tartaric acid/0.9% saline (155 mM NaCl). Vehicle was a solution of 1% (wt/vol) tartaric acid/0.9% saline. TTX was dissolved in aCSF. All solutions were prepared with ultrapure water (NANOPure, Barnstead, Dubuque, IA, USA).

### 5.3.6. Local delivery of tetrodotoxin to the striatum

In a series of experiments, a microinfusion pipet containing tetrodotoxin (TTX) was placed in the striatum 200 μm from the microelectrode. The voltammetric current was recorded as above. TTX was delivered locally to the striatum 50 min after systemic sulpiride administration. Nomifensine was administered 10 min later. Figure 5.1A shows the arrangement of the micropipette and the microelectrode in the striatum of the rat brain.

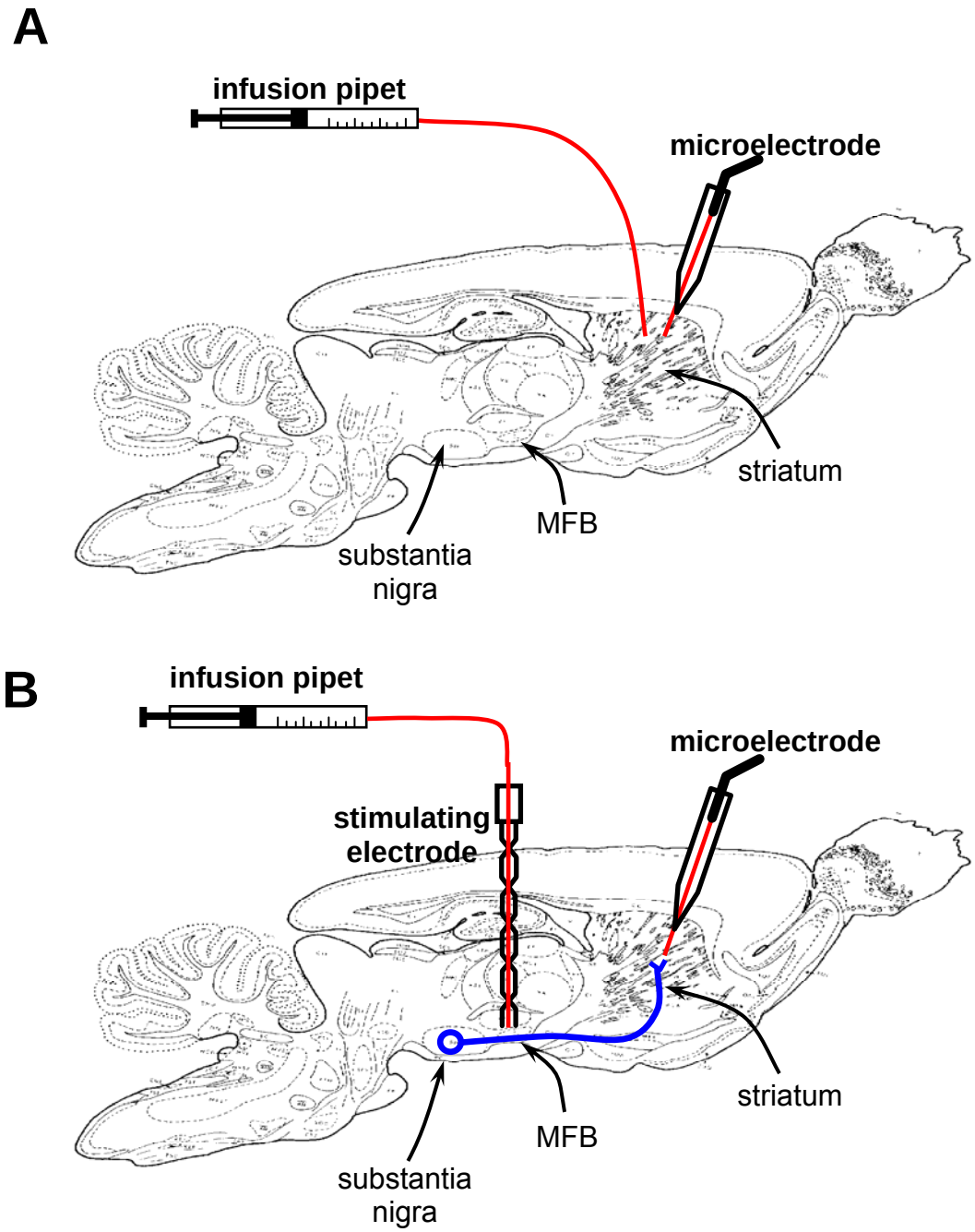


**Figure 5.1. Schematic diagrams showing the position of devices in the rat brain. (A) Voltammetric microelectrodes placed 200 µm from infusion pipet in the striatum. (B) Voltammetric microelectrode in the striatum with stimulation electrode-infusion pipet located at the medial forebrain bundle (MFB).**

### 5.3.7. Local delivery of tetrodotoxin to the medial forebrain bundle

In another series of experiments, a TTX-filled microinfusion pipet glued to a stimulation electrode was placed in the ipsilateral medial forebrain bundle (MFB, 2.2 mm posterior to bregma, 1.6 mm from midline, and initially 7.5 mm below dura). Figure 5.1B shows the placement of the stimulation electrode-infusion pipet in relation to the carbon fiber microelectrode in the dopamine nigrostriatal pathway of the rat brain. The MFB was stimulated with an optically isolated, constant current, biphasic square wave with a pulse duration of 2 ms, a pulse height of 280 μA, a frequency of 60 Hz, and a train length of 10 s. The position of the stimulating electrode was adjusted until evoked dopamine release produced a response of at least 50 nA. TTX was delivered locally to the MFB 45 min after systemic sulpiride administration. An additional MFB stimulation was delivered 5 min after TTX infusion to confirm delivery of the drug to the MFB. Nomifensine was administered systemically 10 min after local infusion of TTX to the MFB. A time line of events is featured in Figure 5.2, displaying the time and voltammetric response following the initial MFB stimulation, sulpiride injection, TTX infusion to the MFB, "confirmation" stimulation, nomifensine injection and subsequent voltammetric response.

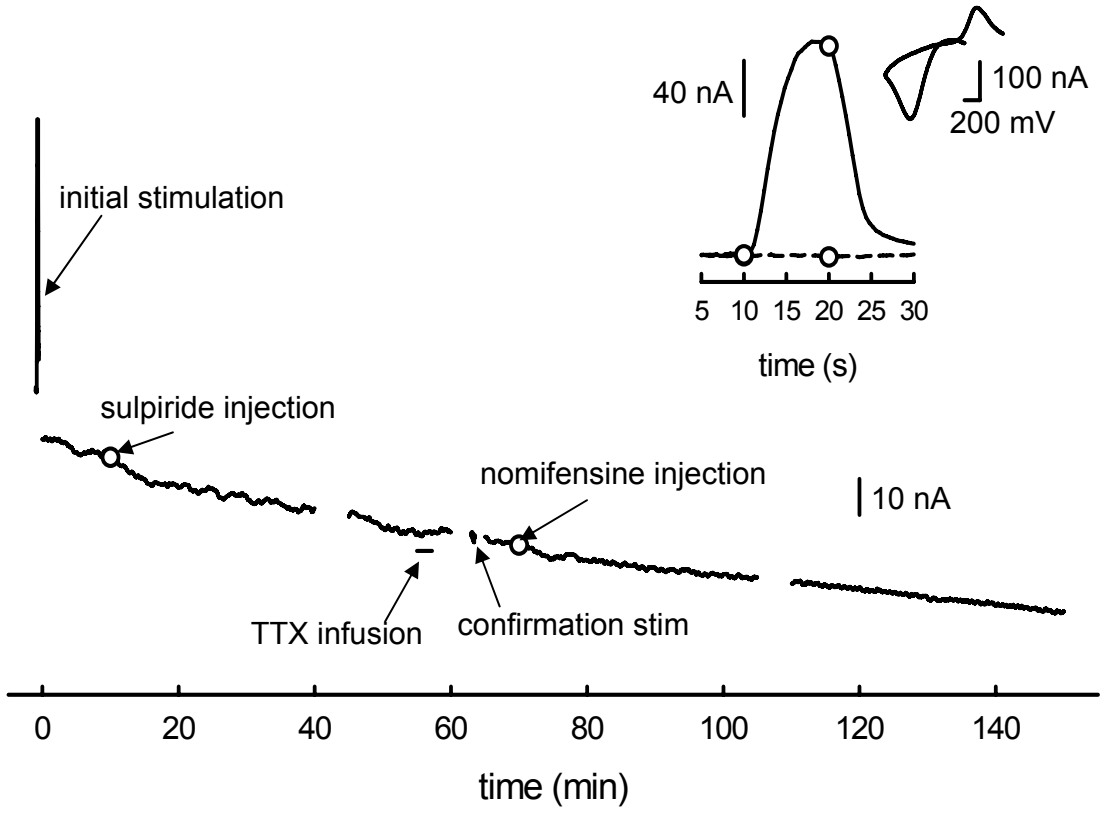


**Figure 5.2. Timeline of events for experiments containing local delivery of tetrodotoxin (TTX) to the medial forebrain bundle (MFB). After implantation of the stimulation electrode-micropipet device, the MFB was stimulated, producing an initial stimulation response (far left) corresponding to an increase in dopamine (inset). Ten minutes later, i.p. sulpiride was administered. Fifty minutes later, TTX was delivered to the MFB via the stim electrode-micropipet device. The effectiveness of the TTX in shutting off stimulated dopamine release was confirmed by a second, confirmation stim. Nomifensine was administered systemically five minutes after the confirmation stimulation.**

## 5.4. RESULTS

### 5.4.1. Data analysis

The current response of each experiment was recorded before, during and after drug administration. The current signal was continuously monitored at potentials corresponding to the maximum of the dopamine oxidation peak (50-700 mV vs. Ag/AgCl). Difference voltammograms (Borland and Michael, 2004) were used to determine if the substance causing the change in the voltammetric response was dopamine. Briefly, cyclic voltammograms recorded over a 200 s interval prior to drug administration are averaged and subtracted from voltammograms averaged over a 200 s interval near the peak of the response. A difference voltammogram exhibiting a distinct oxidation peak in the vicinity of 500-700 mV and a distinct reduction peak in the vicinity of 0-200 mV signals the detection of a change in dopamine. In the event that the difference voltammogram resembled dopamine, the current response is converted to units of dopamine by means of the sensitivity values obtained during in vitro post-calibration of the microelectrodes. Pooled data at specific time points were analyzed by one-way ANOVA followed by Duncan's multiple range test.

Difference voltammograms recorded *in vivo* after A) stimulated dopamine release in the striatum, B) after systemic administration of the uptake inhibitor, nomifensine, and C) after nomifensine administration in a sulpiride-pretreated rat are compared to D) the difference voltammogram recorded during microelectrode post-calibration *in vitro* in a 5 μM dopamine standard (Figure 5.3). The voltammogram recorded after nomifensine in the sulpiride-pretreated rat (Figure 5.3C) very closely resembles both the *in vitro* post-calibration voltammogram (Figure 5.3D) and the voltammogram of stimulated dopamine release (Figure 5.3A). The shape and

location of the oxidation and reduction peaks of the sulpiride-pretreated rat voltammogram correspond precisely with that of the *in vitro* and stimulated voltammograms, confirming that the change in signal after nomifensine after sulpiride-pretreatment is caused by dopamine. The difference voltammogram from the rat treated with nomifensine alone did not exhibit these characteristic peaks. The peak in the potential range for dopamine oxidation to dopamine-o-quinone (500-700 mV) is too broad and the peak corresponding to the reduction of the dopamine-o-quinone back to dopamine (-100 – -300 mV) is nonexistent. Comparison of the difference voltammograms confirms that administration of nomifensine alone does not cause an increase in dopamine.

### 5.4.2. Voltammetric response to dopamine after uptake inhibition and blockade of $D_2$ receptors

Administration of the uptake inhibitor, nomifensine, caused an increase in the voltammetric response in both vehicle and sulpiride-pretreated rats (Figure 5.4). In the vehicle-pretreated rats, nomifensine caused an average signal increase of 6.66 ± 0.623 nA (mean ± standard error, n=4). The average signal is plotted along with error bars showing the standard error at several time points (Figure 5.4A). According to one-way ANOVA, the increase in the signal caused by nomifensine was significant ($f=11.69$, $df=3,15$, $p<0.001$). Duncan's multiple range test confirms that the current recorded at 15, 25, and 35 min was significantly different ($p<0.01$) from the current recorded 5 min, immediately before nomifensine.

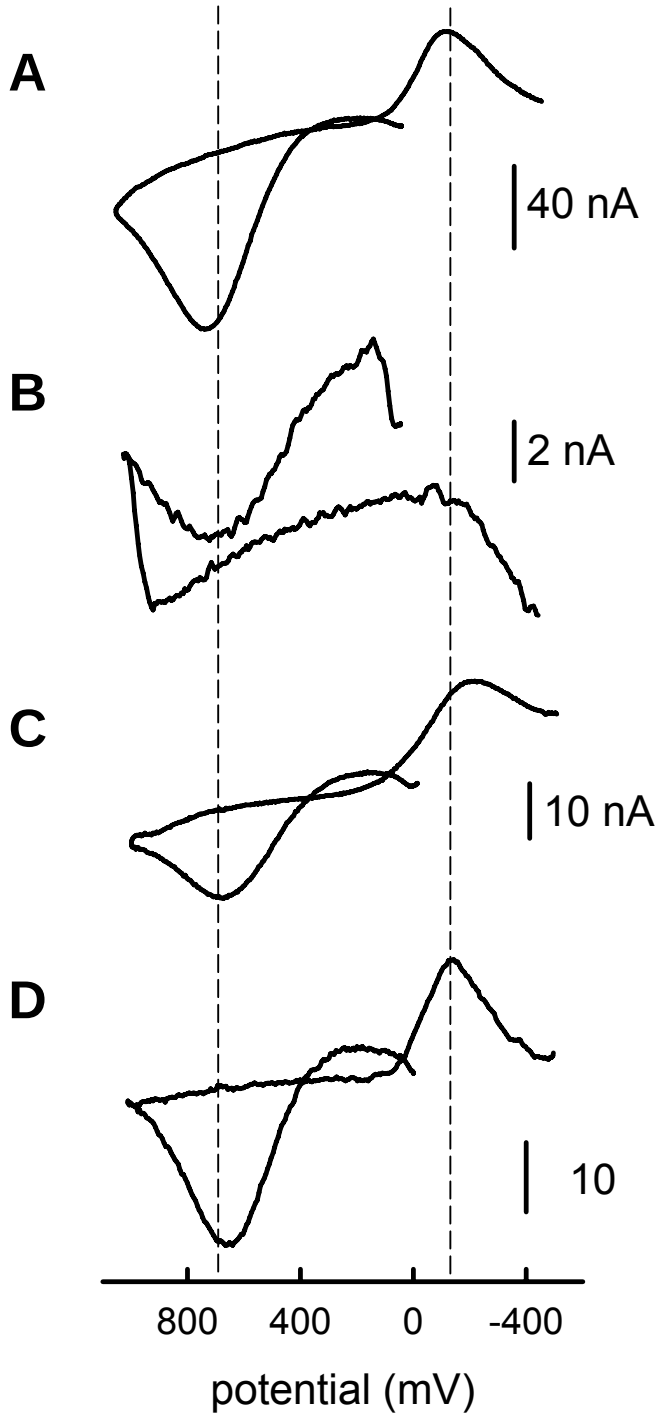


**Figure 5.3. Background-subtracted fast scan cyclic voltammograms recorded: A) after stimulated dopamine release in the striatum, B) after systemic administration of nomifensine, C) after nomifensine in a sulpiride-pretreated rat, D) during in vitro post-calibration with 5 µM dopamine.**

Nomifensine, alone, did not induce a change in dopamine in 75% of the animals tested, as detected by fast-scan cyclic voltammetry. In 3 out of the 4 vehicle-pretreated rats, the background-subtracted voltammograms exhibited none of the features attributed to dopamine. Changes in brain pH have been observed by microelectrodes after uptake inhibition, identifying a likely cause of the observed increase in current in these animals, even in the absence of any changes in dopamine.

Blockade of the dopamine $D_2$ receptors caused a much larger increase in the effect of nomifensine on the voltammetric signal, as seen in Figure 5.4B. Unlike the vehicle-pretreated rats, each sulpiride-pretreated rat exhibited background-subtracted voltammograms resembling dopamine. The current responses were, therefore, converted to units of dopamine concentration using the sensitivity values obtained during *in vitro* post-calibration of each microelectrode. The maximum signal increase after nomifensine, converted to dopamine concentration, was 3.58 ± 0.38 μM (mean ± standard error, n=4). For comparison, the average signal response of the sulpiride-pretreated rats is shown as a current response in Figure 5.4B. The maximum signal increase after nomifensine administration was 18.58 ± 3.49 nA (mean ± standard error, n=4). One-way ANOVA showed a significant increase in signal after nomifensine ($f=6.07$, $df=3,15$, $p<0.01$). Duncan's multiple range test revealed significant differences ($p<0.01$) between the current recorded at 5 min, immediately before nomifensine administration, and the current at 15, 25 and 35 min. Two-way ANOVA of the sulpiride-pretreated and vehicle-pretreated current responses confirms that sulpiride-pretreatment has a significant effect on the increase in signal after nomifensine administration ($f=31.67$, $df=1,31$ ,$p<0.001$)

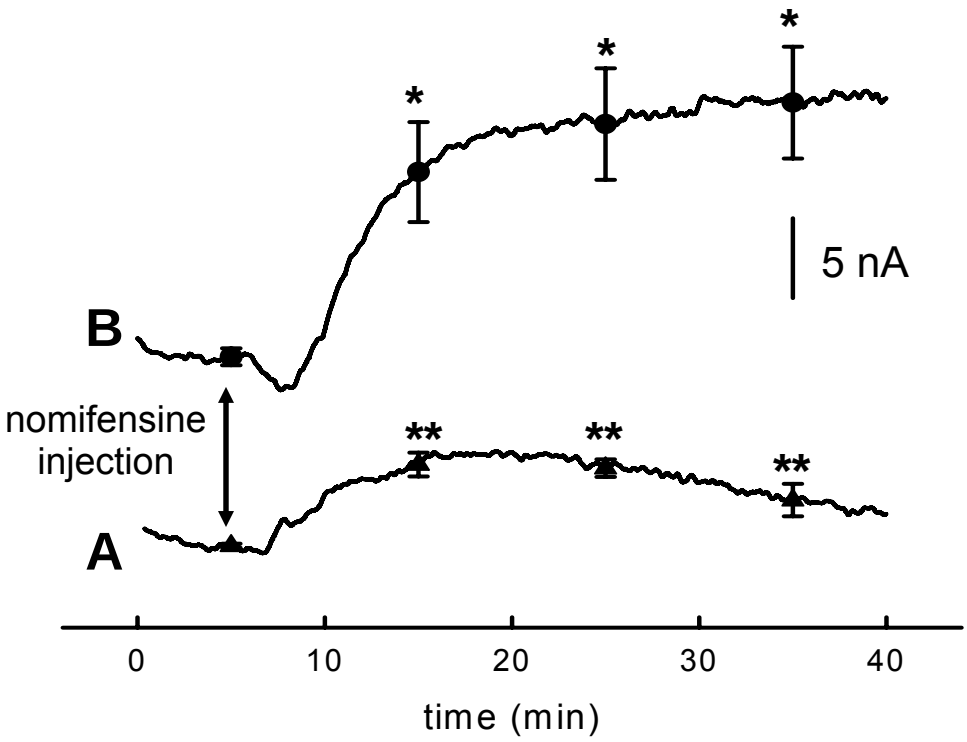


**Figure 5.4. Summary of nomifensine-induced voltammetric response observed in vehicle-pretreated rats (A) and sulpiride-pretreated rats (B). The error bars represent the standard error of the signal at the time point indicated. The asterisks indicate significance compared to t = 5 min, determined by one-way ANOVA followed by Duncan's multiple range test (*p<0.01, **p<0.001).**

### 5.4.3. Inhibition of local impulse traffic blocks the dopaminergic response after uptake inhibition and $D_2$ receptor antagonism

The average current responses following systemic nomifensine administration immediately following the local administration of aCSF or tetrodotoxin to the striatum in sulpiride-pretreated rats is compared in Figure 5.5. Microinfusion of aCSF or TTX caused a small, transient increase in the voltammetric responses. The microinfusion, itself, did not cause any changes in dopamine, as confirmed by examination of the background-subtracted voltammograms. After

nomifensine, a steady and prolonged increase in the voltammetric signal was observed in the rats treated locally with aCSF (Figure 5.5B). The average signal is plotted along with error bars showing the standard error at several time points. The maximum signal increase was 10.66 ± 4.82 nA (mean ± standard error, n=3). Background-subtracted voltammograms obtained after nomifensine administration resembled dopamine and the current signal was converted to dopamine concentration, yielding an increase of 2.15 ± 1.77 μM (mean ± standard error, n=3) (Figure 5.5B). The increase in signal was significant, according to one-way ANOVA ($f=4.33$, $df=3,11$, $p<0.05$). In the 3 rats treated locally with TTX, the nomifensine-induced increase in dopamine was abolished completely (Figure 5.5A). For comparison, the average current response of the TTX-treated rats was plotted with representative time points and standard error bars.

### 5.4.4. Inhibition of nigrostriatal impulse traffic blocks the dopaminergic response after uptake inhibition and $D_2$ receptor antagonism

Figure 5.6 compares the voltammetric response obtained following systemic nomifensine administration after TTX or aCSF delivery to the medial forebrain bundle (MFB) in sulpiride-pretreated rats. An increase in the voltammetric signal was observed after nomifensine in the aCSF-treated rats. Background-subtracted voltammograms confirmed the change in current to be from dopamine. The average current response is plotted with time points and standard error bars in Figure 5.6B. The maximum increase in current was 14.08 ± 2.84 nA (mean ± standard error, n=5), while conversion of the current signal to dopamine concentration shows an increase in dopamine of 2.94 ± 0.75 μM (mean ± standard error, n=5). One-way ANOVA showed that

the increase in signal did reach significance (f=4.59, df=3,19, p<0.05). As shown in Figure 5.2, delivery of TTX to the MFB effectively eliminated the stimulated dopamine response in the striatum. Tetrodotoxin-induced blockade of impulse traffic from the MFB eliminated the increase in signal after systemic nomifensine. The average current response is plotted as Figure 5.6A, for comparison.

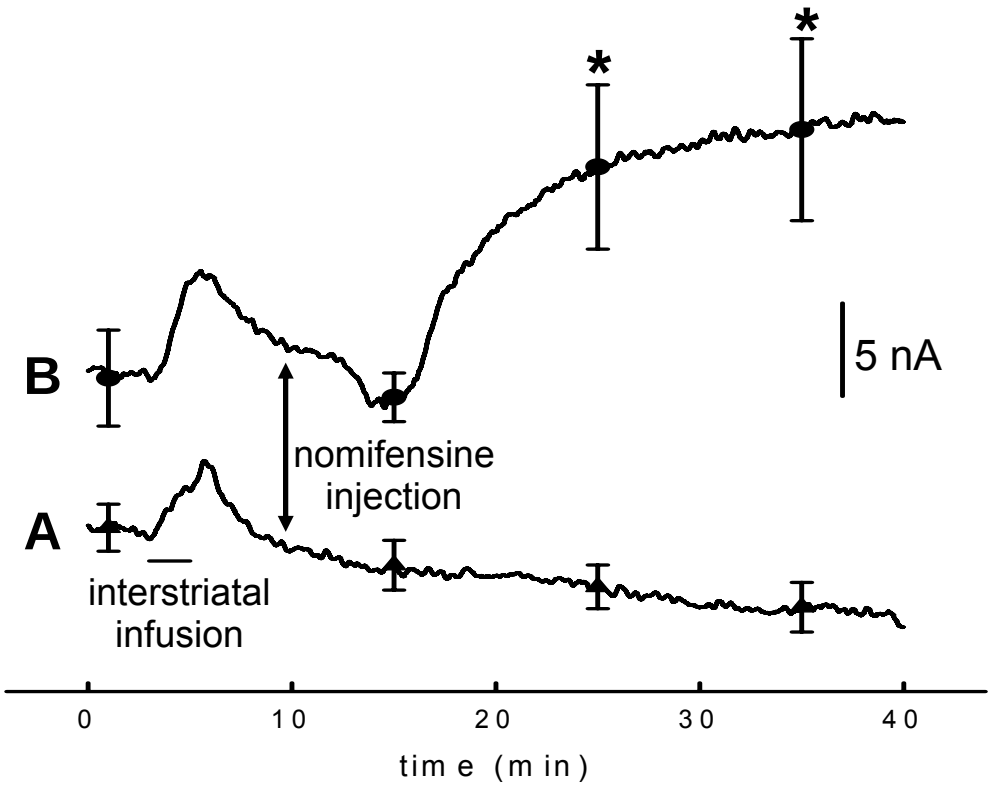


**Figure 5.5. Summary of nomifensine-induced voltammetric response observed in sulpiride-pretreated rats interstriatally infused with TTX (A) or aCSF (B). The error bars represent the standard error of the signal at the time point indicated. The asterisks indicate significance compared to t = 1 min, determined by one-way ANOVA followed by Duncan's multiple range test (*p<0.05).**

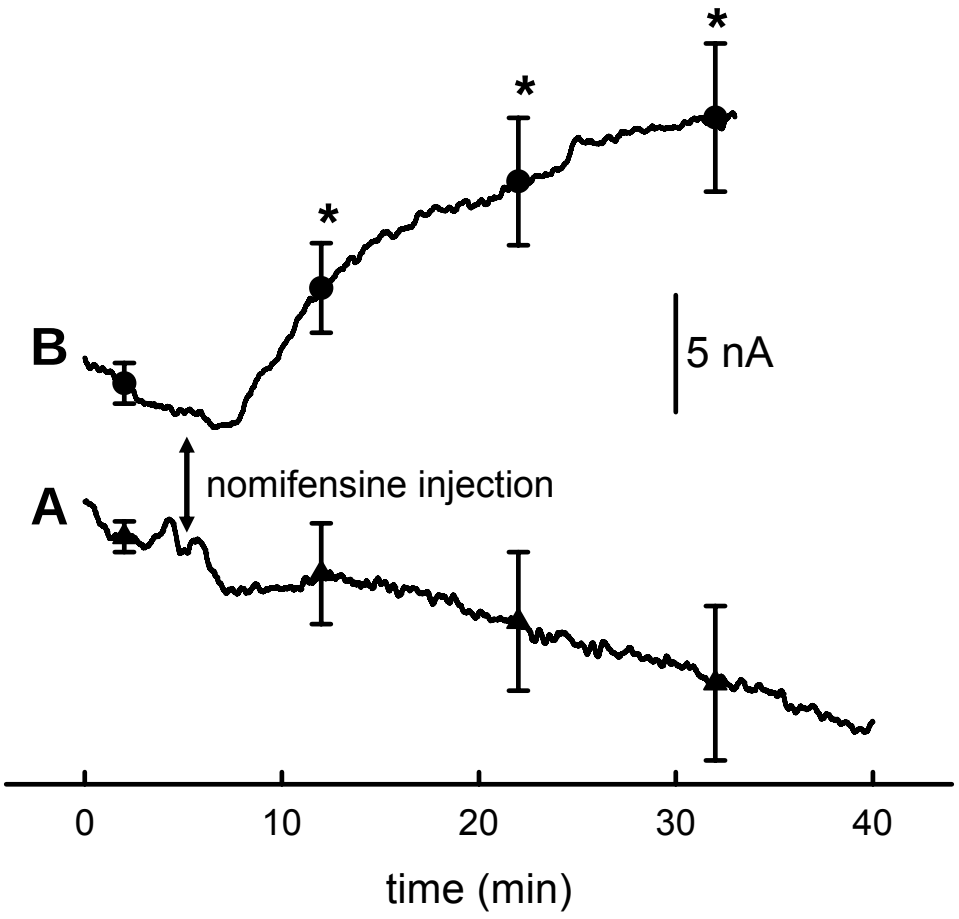


**Figure 5.6. Summary of nomifensine-induced voltammetric response observed in sulpiride-pretreated rats infused with TTX (A) or aCSF (B) at the MFB. The error bars represent the standard error of the signal at the time point indicated. The asterisks indicate significance compared to t = 2 min, determined by one-way ANOVA followed by Duncan's multiple range test (*p<0.05).**

## 5.5. DISCUSSION

In this voltammetric study, we showed that dopamine levels are homeostatically controlled by tonically activated $D_2$ receptors via an impulse-dependent mechanism. Uptake inhibition, alone, failed to cause an increase in dopamine levels, as measured by fast scan cyclic voltammetry with

carbon fiber microelectrodes. Dopamine levels only increased after uptake inhibition in animals pretreated with the $D_2$ receptor antagonist, sulpiride. Tetrodotoxin effectively blocked impulse activity locally in the striatum and along the medial forebrain bundle, preventing the dopamine increase after uptake inhibition in sulpiride-pretreated rats. These data suggest that dopamine $D_2$ receptors participate in a mechanism that regulates dopamine levels in the striatum under normal, resting conditions, as well as after uptake inhibition.

### 5.5.1. Methodological considerations

Previous work in dopamine $D_2$ receptor knock-out mice support the idea that $D_2$ receptors regulate extracellular dopamine levels after uptake inhibition. An increase was clearly noticeable after uptake inhibition, although significantly attenuated, in the mice with full $D_2$ receptor function (Rougé-Pont et al., 2002). In the present study, however, 75% of the animals exhibited no increase in dopamine after uptake inhibition. We attribute this response to the difference in the techniques used to monitor extracellular dopamine in the brain.

Carbon fiber microcylinder electrodes are 10,000 times smaller in area than microdialysis probes and ultramicrostructural analysis shows that the implantation damage from these devices does not extend beyond 6.5 μm. Implantation of microdialysis probes, on the other hand, causes considerable trauma to the surrounding tissue (Clapp-Lilly et al., 1999; Zhou et al., 2001), with the damaged area extending at least 250 μm away from the probe (Borland et al., 2005). Significant alterations in dopamine uptake and release exist in the damaged area, with a gradient of dopamine activity extending into the traumatized tissue zone (Borland et al., 2005). Presumably, other neuronal processes that would normally regulate dopamine levels in the brain

could be adversely affected. Glutamate afferents, in particular, could be badly damaged upon microdialysis probe implantation, destroying another key regulatory component of dopamine in the striatum.

### 5.5.2. An impulse-dependent mechanism regulates DA release after $D_2$ receptor inhibition

The experiments performed utilizing tetrodotoxin in the striatum and MFB exclude dopamine transporters from contributing to the modulation of dopamine release after nomifensine administration. Tetrodotoxin inhibits propagation of the action potential by blocking $Na^+$ permeability through voltage-gated ion channels. Inhibition of the action potential suppresses neuronal firing and subsequent exocytosis, which would normally result in neurotransmitter release. The reverse transport of dopamine, which accompanies the drug action of uptake inhibitors in the family of amphetamines, causes a release of dopamine from the transporter that is tetrodotoxin-insensitive (impulse-independent) (Westerink et al., 1987; Lonart and Zigmond, 1991; Leviel, 2001). Since no change in the current signal was observed after locally applied tetrodotoxin to either the striatum or the MFB, reverse transport as a mechanism for dopamine release after nomifensine administration in rats pretreated with a $D_2$ antagonist is ruled out.

A probable mechanism for $D_2$ receptor control of release is modulation of the vesicles (Reimer et al., 1998; Pothos et al., 1998; Pothos et al., 2000; Colliver et al., 2000; Sulzer and Edwards, 2000). Various studies into the quantal size and volume of dopamine-containing vesicles provide evidence that the rate of vesicular fusion and release is maintained, while the amount of neurotransmitter released is severely reduced. Pothos et al. (1998) found that activation of $D_2$

receptors decreased the quantal size by inhibiting tyrosine hydroxylase activity, which reduced cytosolic dopamine available for vesicle accumulation. Pothos et al. (1998) also suspect that $D_2$ agonists do not decrease the rate of vesicular exocytosis, rather, that the quanta are simply releasing levels of neurotransmitter below the detection limit. The discovery of terminal-level $D_2$ receptor modulation of extracellular levels of dopamine (Mitala and Michael, unpublished results) agrees with the idea of $D_2$ receptor control of quantal size rather than firing rates. Furthermore, the tetrodotoxin data presented in this report supports vesicular modulation, since no change in dopamine was observed following inhibition of the action potential at either site. Such observations support $D_2$ receptor control of vesicular modulation as a possible feedback mechanism after uptake inhibition.

## 5.6. CONCLUSION

Evidence of dopamine $D_2$ receptor modulation of extracellular dopamine after uptake inhibition is abundant in our lab. In this study, we discovered that $D_2$ receptor control of dopamine release after uptake inhibition was impulse-dependent. The use of tetrodotoxin to inhibit the propagation of the action potential at both the medial forebrain bundle and in the striatum revealed that $D_2$ receptor mediation of dopamine release is dependent upon neuronal firing, an idea supported by electrophysiological studies utilizing $D_2$ agonists and antagonists (Mercuri et al., 1991; Mercuri et al., 1992; Mercuri et al., 1997; Einhorn et al., 1988). Our study also rules out the involvement of reverse transport by the dopamine transporter as a mechanism of increased release after $D_2$ receptor blockade followed by uptake inhibition.

## BIBLIOGRAPHY


Avshalumov, M.V. and Rice, M.E. (2003) Activation of ATP-sensitive $K^+$ ($K_{ATP}$) channels by $H_2O_2$ underlies glutamate-dependent inhibition of striatal dopamine release. *PNAS* **100**, 11729-11734.

Avshalumov, M.V., Chen, B.T., Marshall, S.P., Peña, D.M. and Rice, M.E. (2003) Glutamate-dependent inhibition of dopamine release in striatum is mediated by a new diffusible messenger, $H_2O_2$. *J. Neurosci.* **23**, 2744-2750.

Adams, B. and Moghaddam, B. (1998) Corticolimbic dopamine neurotransmission is temporarily dissociated from the cognitive and locomotor effects of phencyclidine. *J. Neurosci.* **18**, 5545-5554.

Adams, R.N. (1976) Probing brain chemistry with electroanalytical techniques. *Anal. Chem.* **48**, 1128A-1138A.

Baker, D.A., Shen, H. and Kalivas, P.W. (2002a) Cystine/glutamate exchange serves as the source for extracellular glutamate: Modifications by repeated cocaine administration. *Amino Acids* **23** 161-162.

Baker, D.A., Xi, Z., Shen, H. Swanson, C.J. and Kalivas, P.W. (2002b) The origin and neuronal function of *in vivo* nonsynaptic glutamate. *J. Neurosci.* **22**, 9134-9141.

Barlett, P.N. and Cooper, J.M. (1993) A review of the immobilization of enzymes in electropolymerized films. *J. Electroanal. Chem.* **362**, 1-12.

Baur, J., Kristensen, E.W., May, L.J., Weidemann, D.J. and Wightman, R.M. (1988) Fast scan voltammetry of biogenic amines. *Anal. Chem.* **60**, 1268-1272.

Beisler, A.T., Sahlin, E., Schaefer, K.E., and Weber, S.G. (2004) Analysis of the performance of a flow reactor for use with microcolumn HPLC. *Anal. Chem.* **76**, 639-645.

Benard, V., Somogyi, P., and Bolam, J.P. (1997) Cellular, subcellular, and subsynaptic distribution of AMPA-type glutamate receptor subunits in the neostriatum of the rat. *J. Neurosci.* **17**, 819-833.

Benoit-Marand, M., Borrelli, E., and Gonon, F. (2001) Inhibition of dopamine release via presynaptic D2 receptors: time course and functional characteristics *in vivo*. *J. Neurosci.* **21**, 9134-9141.

Benveniste, H., Drejer, J., Schousboe, A., and Diemer, N.H. (1984) Elevation of the extracellular concentrations of glutamate and aspartate in rat hippocampus during transient cerebral ischemia monitored by intracerebral microdialysis. *J. Neurochem.* **43**, 1369-1374.

Benveniste, H., Drejer, J., Schousboe, A., and Diemer, N.H. (1987) Regional cerebral glucose phosphorylation and blood flow after insertion of a microdialysis fiber through the dorsal hippocampus in the rat. *J. Neurochem.* **49**, 729-734.

Borland, L.M. and Michael, A.C. (2004) Voltammetric study of the control of striatal dopamine release by glutamate. *J. Neurochem.* **91**, 220-229.

Borland, L.M., Shi, G., Yang, H., and Michael, A.C. (2005) Voltammetric study of extracellular dopamine near microdialysis probes acutely implanted in the striatum of the anesthetized rat. *J. Neurosci. Meth.* **146**, 149-158.

Boudko, D.Y., Moroz, L.L., Linser, P.J., Trimarchi, J.R., Smith, P.J.S., and Harvey, W.R. (2001)

In situ analysis of pH gradients in mosquito larvae using noninvasive, self-referencing, pH-sensitive microelectrodes. *J. Exp. Bio.* **204**, 691-699.

Bradberry, C.W. (2002) Dynamics of extracellular dopamine in the acute and chronic actions of cocaine. *Neuroscientist* **8**, 315-322.

Bungay, P.M., Morrison, P.F. and Dedrick, R.L. (1990) Steady-state theory for quantitative microdialysis of solutes and water *in vivo* and *in vitro*. *Life Sci.* **46**, 105-119.

Bungay, P.M., Newton-Vinson, P., Isele, W., Garris, P.A. and Justice, J.B. Jr (2003) Microdialysis of dopamine interpreted with quantitative model incorporating probe implantation trauma. *J. Neurochem.* **86**, 932-946.

Camp, D.M., DeJonghe, D.K. and Robinson, TE. (1997) Time-dependent effects of repeated amphetamine treatment on norepinephrine in the hypothalamus and hippocampus assessed with in vivo microdialysis. *Neuropsychopharmacology* **17**, 130-140.

Carlsson, M and Carlsson, A. (1990) Interactions between glutamatergic and monoamergic systems within the basal ganglia – implications for schizophrenia and Parkinson's disease. *TINS* **13**, 272-276.

Carlsson, A., Waters, N. and Carlsson, M.L. (1999) Neurotransmitter interactions in schizophrenia – therapeutic implications. *Biol. Psychiatry* **46**, 1388-1395.

Cass, W.A. and Gerhardt, G.A. (1994) Direct *in vivo* evidence that $D_2$ dopamine receptors can modulate dopamine uptake. *Neurosci. Lett.* **176**, 259-263.

Cheer, J.F., Wassum, K.M., Heien, M.L.A.V., Phillips, P.E.M. and Wightman, R.M. (2004) Cannabinoids enhance subsecond dopamine release in the nucleus accumbens of awake rats. *J. Neurosci.* **24**, 4393-4400.

Chen, K.C. (2005a) Preferentially impaired neurotransmitter release sites not their discreteness compromise the validity of microdialysis zero-net-flux method. *J. Neurochem.* **92**, 29-45.

Chen, K.C. (2005b) Evidence on extracellular dopamine level in rat striatum: implication for the validity of quantitative microdialysis. *J. Neurochem.* **92**, 46-58.

Chen, Q., Veenman, L., Knopp, K., Yan, Z., Medina, L., Song, W.-J., Surmeier, D.J., and Reiner, A. (1998) Evidence for the preferential localization of glutamate receptor-1 subunits of AMPA receptors to the dendritic spines of medium spiny neurons in rat striatum. *Neurosci.* **83**, 749-761.

Christensen, J.C., Wang, Z. and Rebec, G.V. (2000) γ-aminobutyric acid infusion in substantia nigra pars reticulata in rats inhibits ascorbate release in ipsilateral striatum. *Neurosci. Lett.* **280**, 191-194.

Church, W.H., Justice, J.B. and Byrd, L.D. (1987) Extracellular dopamine in rat striatum following uptake inhibition by cocaine, nomifensine and benztropine. *Eur. J. Pharmacol.* **139**, 345-348.

Clapp-Lilly, K.L., Roberts, R.C., Duffy, L.K., Irons, K.P., Hu, Y. and Drew, K.L. (1999) An ultrastructural analysis of tissue surrounding a microdialysis probe. *J. Neurosci. Meth.* **90**, 129-142.

Clow, D.W. and Jhamandas, K. (1989) Characterization of l-glutamate action on the release of endogenous dopamine from the rat caudate-putamen. *J. Pharm Exp. Theur.* **248**, 722-728.

Colliver, T.L., Pyott, S.J., Achalabun, M., and Ewing, A.G. (2000) VMAT-mediated changes in quantal size and vesicular volume. *J. Neurosci.* **20**, 5276-5282.

Cousins M.S. and Salamone, J.D. (1996) Involvement of ventrolateral striatal dopamine in movement initiation and execution: A microdialysis and behavioral investigation. *Neuroscience* **70**, 849-859.

Cragg S. J., Rice M. E., and Greenfield S. A. (1997) Heterogeneity of electrically evoked dopamine release and reuptake in substantia nigra, ventral tegmental area and striatum. *J. Neurophysiol.* **77**, 661-671.

Cui, J., Kulagina, N.V., and Michael, A.C. (2001) Pharmacological evidence for the selectivity of in vivo signals obtained with enzyme-based electrochemical sensors. *J. Neurosci. Meth.* **104**, 183-189.

Daws, L.C., Toney, G.M., Gerhardt, G.A., and Frazer, A. (1998) In vivo chronoamperometric measures of extracellular serotonin clearance in rat dorsal hippocampus: contribution of serotonin and norepinephrine transporters. *J. Pharmacol. Exp. Ther.* **286**, 967-976.

DeBoer, P. and Abercrombie, E.D. (1996) Physiological release of striatal acetylcholine *in vivo*: modulation by $D_1$ and $D_2$ dopamine receptor subtypes. *J. Pharm. Exp. Ther.* **277**, 775-783.

Desce, J.M., Godeheu, G., Galli, T., Artaud, F., Cheramy, A. and Glowinski, J. (1992) L-glutamate-evoked release of dopamine from synaptosomes of the rat striatum: involvement of AMPA and N-methyl-D-aspartate receptors. *Neuroscience* **47**, 333-339.

DiChiara, G., Tanda, G. and Carboni, E. (1996) Estimation of in-vivo neurotransmitter release by brain microdialysis: the issue of validity. *Behav. Pharmacol.* **7**, 640-657.

Dickinson S. D., Sabeti J., Larson G. A., Giardina K., Rubinstein M., Kelly M. A., Grandy D. K., Low M. J., Gerhardt G. A., and Zahniser N. R. (1999) Dopamine $D_2$ receptor-deficient

mice exhibit decrease dopamine transporter function but no changes in dopamine release in dorsal striatum. *J. Neurochem.* **72**:148-156.

Diehl, D.J. and Gershon, S. (1992) The role of dopamine in mood disorders. *Compr. Psychiatry* **33**, 115-120.

Einhorn, L.C., Johansen, P.A., and White, F.J. (1988) Electrophysiological effects of cocaine in the mesoaccumbens dopamine system: Studies in the ventral tegmental area. *J. Neurosci.* **8**, 100-112.

Feng, J.X., Brazell, M., Renner, K., Kasser, R., and Adams, R.N. (1987) Electrochemical pretreatment of carbon fibers for in vivo electrochemistry: Effects on sensitivity and response time. *Anal. Chem.* **59**, 1863-1867.

Floresco, S.B., Todd, C.L. and Grace, A.A. (2001) Glutamatergic afferents from the hippocampus to the nucleus accumbens regulate activity of ventral tegmental area dopamine neurons. *J. Neurosci.* **21**, 4915-4922.

Floresco, S.B., West, A.R., Ash, B., Moore, H. and Grace A.A. (2003) Afferent modulation of dopamine neuron firing differentially regulates tonic and phasic dopamine transmission. *Nature Neurosci.* **6**, 968-973.

Garris, P. A., Budygin, E. A., Phillips, P. E. M., Venton, B. J., Robinson, D. L., Bergstrom, B. P., Rebec, G. V., and Wightman, R. M. (2003) A role for presynaptic mechanisms in the actions of nomifensine and haloperidol. *Neurosci.* **118**, 819-829.

Garris, P.A., Ciolkowski, E.L., Pastore, P. and Wightman, R.M. (1994) Efflux of dopamine from the synaptic cleft in the nucleus accumbens of the rat brain. *J. Neurosci*. **14**, 6084-6093.

Gaudiello, J.G., Bradley, P.G., Norton, K.A., Woodruff, W.H., and Bard, A.J. (1984)

Electrochemistry in liquid sulfur dioxide. 5. Oxidation of bipyridine and phenanthroline complexes of osmium, ruthenium, and iron. *Inorg. Chem.* **23**, 3-10.

Giorguieff, M.F., Kemel, M.L. and Glowinski, J. (1977) Presynaptic effect of l-glutamic acid on the release of dopamine in rat striatal slices. *Neurosci. Lett.* **6**, 73-77.

Gerhardt, G.A., Oke, A.F., Moghaddam, B., and Adams, R.N. (1984) Nafion-coated electrodes with high selectivity for CNS electrochemistry. *Brain Res.* **290**, 390-395.

Gonon, F. (1997) Prolonged and extrasynaptic excitatory action of dopamine mediated by $D_1$ receptors in the rat striatum in vivo. *J. Neurosci*. **17**, 5972-5978.

Gonon, F. and Buda, M.J. (1985) Regulation of dopamine release by impulse flow and by autoreceptors as studied by *in vivo* voltammetry in the rat striatum. *Neuroscience* **14**, 765-774.

Gonon, F., Buda, M., Cespuglio, R., Jouvet, and Pujol, J.F. (1980) In vivo electrochemical detection of catechols in the neostriatum of anaesthetized rats: dopamine or DOPAC? *Nature* **286**, 902-904.

Gonon, F.G., Fombarlet, C.M., Buda, M.J., and Pujol, J.F. (1981) Electrochemical treatment of pyrolytic carbon fiber electrodes. *Anal. Chem.* **53**, 1386-1389.

Gonon, F.G., Navarre, F. and Buda, M.J. (1984) In vivo monitoring of dopamine release in the rat brain with differential pulse voltammetry. *Anal. Chem.* **56**, 573-575.

Grace, A.A. (1991) Phasic versus tonic dopamine release and the modulation of dopamine system responsivity: a hypothesis for the etiology of schizophrenia. *Neuroscience* **41**, 1-24.

Greco, P.G. and Garris, P.A. (2003) In vivo interaction of cocaine with the dopamine transporter as measured by voltammetry. *Eur. J. Pharmacol.* **479**, 117-125.

Gregg, B.A. and Heller, A. (1990) Crosslinked redox gels containing glucose oxidase for amperometric biosensor applications. *Anal. Chem.* **62**, 258-263.

Groothuis, D.R., Ward, S., Schlageter, K.E., Itskovich, A.C., Schwerin, S.C., Allen, C.V., Dills, C., and Levy, R.M. (1998) Changes in blood-brain barrier permeability associated with insertion of brain cannulas and microdialysis probes. *Brain Res.* **803**, 218-230.

Gulley, J.M. and Zahnizer N.R. (2003) Rapid regulation of dopamine transporter function by substrates, blockers and presynaptic ligands. *Eur. J. Pharmacol.* **479**:139-152.

Heller, A. (1992) Electrical connection of enzyme redox centers to electrodes. *J. Phys. Chem.* **96**, 3579-3587.

Hoffman, A.F., Zahniser, N.R., Lupica, C.R., and Gerhardt, G.A. (1999) Voltage-dependency of the dopamine transporter in the rat substantia nigra. *Neurosci. Letts.* **260**, 105-108.

Iravani, M.M. and Kruk, Z.L. (1996) Real-time effects of N-methyl-D-aspartic acid on dopamine release in slices of rat caudate putamen: a study using fast cyclic voltammetry. *J. Neurochem.* **66**, 1076-1085.

Jones, S.R., Garris, P.A. and Wightman, R.M. (1995) Different effects of coacaine and nomifensine on dopamine uptake in the caudate-putamen and nucleus accumbens. *J. Pharm. Exp. Ther.* **274**, 396-403.

Jung, M.C., Shi, G., Borland, L., Michael, A.C., and Weber, S.G. Simultaneous determination of biogenic monoamines in rat brain dialysates using capillary high-performance liquid chromatography with photoluminescence-following electron-transfer. *Anal. Chem.* submitted 2005.

Jung M.C. and Weber S.G. (2005) Influence of Chemical Kinetics on Postcolumn Reaction in a

Capillary Taylor Reactor with Catechol Analytes and Photoluminescence Following Electron Transfer. *Anal. Chem.* **77**, 974-982.

Kaakkola, A., Tuomainen, P., Wurtman, R.J., and Männistö, P.T. (1992) Effects of systemic carbidopa synthesis in rat hypothalamus and striatum. *J. Neural Transm.* **4**, 143-154.

Karreman, M. and Moghaddam, B. (1996) The prefrontal cortex regulates the basal release of dopamine in the limbic striatum: an effect mediated by ventral tegmental area. *J. Neurochem.* **66**, 589-598.

Keefe, K.A., Zigmond, M.J. and Abercrombie, E.D. (1992) Extracellular dopamine in striatum: influence of nerve impulse activity in medial forebrain bundles and local glutamatergic input. *Neuroscience* **47**, 325-332.

Kennedy, R.T., Jones, S.R., and Wightman, R.M. (1992) Simultaneous measurement of oxygen and dopamine – coupling of oxygen consumption and neurotransmission. *Neurosci.* **51**, 55-64.

Khan, A.S. and Michael, A.C. (2003) Voltammetric monitoring of dopamine in the awake rat: actions of cocaine. In: Monitoring Molecules in Neuroscience: Proceedings of the 10th International Conference on In Vivo Methods (Kehr., J., Fuxe, K., Ungerstedt, U., Svensson T.H., eds) pp177-179. Karolinska University Press, Stockholm.

Kissinger, P., T., Hart, J.B., and Adams, R.N. (1973) Voltammetry in brain tissue – a new neurophysiological measurement. *Brain Res.* **55**, 209-213.

Koob, G.F. and Bloom, F.E. (1988) Cellular and molecular mechanisms of drug dependence. *Science* **242**, 715-723.

Kovach, P.M., Ewing, A.G., Wilson, R.L. and Wightman, R.M. (1984) In vitro comparison of the selectivity of electrodes for in vivo electrochemistry. *J. Neurosci. Meth.* **10**, 215-227.

Kozminski, K.D., Gutman, D.A., Davila, V., Sulzer, D. and Ewing, A.G. (1998) Voltammetric and pharmacological characterization of dopamine release from single exocytotic events at rat pheochromocytoma (PC12) cells. *Anal. Chem.* **70**, 3123-3130.

Krebs, M.O., Desce, J.M., Kemel, M.L., Gauchy, C., Godeheu, G, Cheramy, A. and Glowinski, J. (1991) Glutamatergic control of dopamine release in the rat striatum: evidence for presynaptic N-methyl-D-aspartate receptors on dopaminergic nerve terminals. *J. Neurochem.* **56**, 81-85.

Kuhr, W.G., Ewing, A.G., Caudill, W.L. and Wightman, R.M. (1984) Monitoring the stimulated release of dopamine with in vivo voltammetry. I: characterization of the response observed in the caudate nucleus of the rat. *J. Neurochem*. **43**, 560-569.

Kulagina, N.V. and Michael, A.C. (2003) Monitoring hydrogen peroxide in the extracellular space of the brain with amperometric microsensors. *Anal. Chem.* **75**, 4875-4881.

Kulagina, N.V., Shankar, L. and Michael, A.C. (1999) Monitoring glutamate and ascorbate in the extracellular space of brain tissue with electrochemical microsensors. *Anal. Chem.* **71**, 5093-5100.

Kulagina, N.V., Zigmond, M.J. and Michael, A.C. (2001) Glutamate regulates the spontaneous and evoked release of dopamine in the rat striatum. *Neuroscience* **102**, 121-128.

Kumar, S.M., Porterfield, D.M., Muller, K.J., Smith, P.J.S., and Sahley, C.L. (2001) Nerve injury induces a rapid efflux of nitric oxide (NO) detected with a novel NO microsensor. *J. Neurosci.* **21**, 215-220.

Leszczyszyn, D.J., ankowski, J.A., Viveros, O.H., Diliberto, E.J., Near, J.A., and Wightman, R.M. (1991) Secretion of catecholamines from individual adrenal medullary chromaffin cells. *J. Neurochem.* **56**, 1855-1863.

Leviel, V. (2001) The reverse transport of DA, what physiological significance? *Neurochem. Int.* **38**, 83-106.

Lonart, G. and Zigmond, M.J. (1991) High glutamate concentrations evoke Ca++-independent dopamine release from striatal slices: a possible role of reverse transport. *J. Pharm Exp. Theur.* **256**, 1132-1138.

Lonnroth, M.T., Jansson, P.A. and Smith, U. (1987) A microdialysis method allowing characterization of intercellular water space in humans. *Am. J. Physio.* **253**, E228-231.

Lowry, J.P., Boutelle, M.G., and Fillenz, M. (1997) Measurement of brain tissue oxygen at a carbon paste electrode can serve as an index of increases in regional cerebral blood flow. *J. Neurosci. Meth.* **71**, 177-182.

Lu, Y., Peters, J.L. and Michael, A.C. (1998) Direct comparison of the response of voltammetry and microdialysis to electrically evoked release of striatal dopamine. *J. Neurochem.* **70**, 584-593.

Marcus, M.M., Mathé, J.M., Nomikos, G.G., and Svensson, T.H. (2001) Effects of competitive and non-competative NMDA receptor antagonists on dopamine output in the shell and core subdivisions of the nucleus accumbens. *Neuropharm.* **40**, 482-490.

Meiergerd, S.M., Patterson, T.A., and Schenk, J.O. (1993) $D_2$ receptors may modulate the function of the striatal transporter for dopamine: kinetic evidence from studies *in vitro* and in vivo. *J. Neurochem.* **61**, 764-767.

Mercuri, N.B., Stratta, F., Calabresi, P., and Bernardi, G. (1991) Nomifensine but not amantadine increases dopamine-induced responses on rat substantia nigra zona compacta neurons. *Neurosci. Lett.* **131**, 145-148.

Mercuri, N.B., Scarponi, M., Bonci, A., Siniscalchi, A., and Bernardi, G. (1997) Monoamine

oxidase inhibition causes a long-term prolongation of the dopamine-induced responses in rat midbrain dopaminergic cells. *J. Neurosci.* **17**, 2267-2272.

Mercuri, N.B., Calabresi, P., and Bernardi, G. (1992) The electrophysiological actions of dopamine and dopaminergic drugs on the neurons of the substantia nigra pars compacta and ventral tegmental area. *Life Sci.* **51**, 711-718.

Mereu, G., Casu, M., and Gessa, G.L. (1983) (-)-Sulpiride activates the firing rate and tyrosine hydroxylase activity of dopaminergic neurons in unanesthetized rats. *Brain Res.* **264**, 105-110.

Michael, A.C., Borland, L.M., Mitala, J.J.Jr., Willoughby, B.M. and Motzko, C.M. (2005) Theory for the impact of basal turnover on dopamine clearance kinetics in the rat striatum after medial forebrain bundle stimulation and pressure ejection. *J. Neurochem.* **94**, 1202-1211.

Miele, M., Boutelle, M.G. and Fillenz, M. (1996) The source of physiologically stimulated glutamate efflux from the striatum of conscious rats. *J. Physiol*. **497**, 745-751.

Missale, C., Nash, S.R., Robinson, S.W., Jaber, M. and Caron, M.G. (1998) Dopamine receptors: from structure to function. *Physiol. Rev*. **78**, 189-225.

Mitala, J.J., Jr., and Michael A.C. (2003) Role of nigrostriatal D2-like receptors in the regulation of striatal extracellular DA levels following uptake inhibition. In: Monitoring Molecules in Neuroscience: Proceedings of the 10th International Conference on In Vivo Methods (Kehr., J., Fuxe, K., Ungerstedt, U., Svensson T.H., eds) pp177-179. Karolinska University Press, Stockholm.

Moghaddam, B. and Bunney, B.S. (1989) Ionic composition of microdialysis perfusing solution alters the pharmacological responsiveness and basal outflow of striatal dopamine. *J. Neurochem.* **53**, 652-654.

Moghaddam, B., Gruen, R.J., Roth, R.H., Bunney, B.S. and Adams, R.N. (1990) Effect of l-glutamate on the release of striatal dopamine: in vivo dialysis and electrochemical studies. *Brain Research* **518**, 55-60.

Moghaddam, B. and Gruen, R.J. (1991) Do endogenous excitatory amino acids influence striatal dopamine release? *Brain Research* **544**, 329-330.

Moghaddam, B. and Adams, B.W. (1998) Reversal of phencyclidine effects by a group II metabotropic glutamate receptor agonist in rats. *Science* **281**, 1349-1352.

Morari, M., Marti, M., Sbrenna, S. Fuxe, K., Bianchi, C. and Beani, L. (1998) Reciprocal dopamine-glutamate modulationof release in the basal ganglia. *Neurochem. Int.* 33, 383-397.

Morgan, M.E., Singhal, D., and Anderson, B.D. (1996) Quantitative assessment of blood brain barrier damage during microdialysis. *Pharmacology* **277**, 1167-1176.

Morrison, P.F., Bungay, P.M., Hsiao, J.K., Mefford, I.N., Dykstra, K.H. and Dedrik, R.L. (1991) Quantitative microdialysis. In *Micodialysis in the Neurosciences*, Robinson, T.E. and Justice J.B.Jr. (eds.) Elsevier, Amsterdam.

Mosharov, E.V., Gong, L.W., Khanna, B., Sulzer, D. and Lindau, M. (2003) Intracellular patch electrochemistry: regulation of cytosolic catecholamines in chromaffin cells. *J. Neurosci.* **23**, 5835-5845.

Nirenberg, M.J., Vaughan, R.A., Uhl, G.R., Kuhar, M.J. and Pickel, V.M. (1996) The dopamine transporter is localized to dendridic and axonal plasma membranes of nigrostriatal dopaminergic neurons. *J. Neurosci.* **16**, 436-447.

Parsons, L.H. and Justice J.B. Jr. (1992) Extracellular concentration and in vivo recovery of dopamine in the nucleus accumbens using microdialysis. *J. Neurochem.* **58**, 212-218.

Pellegrino, L.J., Pellegrino, A.S. and Cushman, A.J. (1979) *A stereotaxic atlas of the rat brain, 2nd edit*., Plenum Press, New York.

Peters, J.L. and Michael, A.C. (1998) Modeling voltammetry and microdialysis of striatal extracellular dopamine: the impact of dopamine uptake on extraction and recovery ratios. *J. Neurochem.* **70**, 594-603.

Peters J. L. and Michael A. C. (2000) Changes in the kinetics of dopamine release and uptake have differential effects on the spatial distribution of extracellular dopamine concentration in rat striatum. *J. Neurochem.* **74**, 1563-1573.

Peters, J.L., Miner, L.H., Michael, A.C. and Sesack, S.R. (2004) Ultrastructure at carbon fiber microelectrode implantation sites after acute voltammetric measurements in the striatum of anesthetized rats. *J. Neurosci. Meth.* **137**, 9-23.

Phillips, P.E.M. and Wightman, R.M. (2003) Critical guidelines for validation of the selectivity of in vivo chemical microsensors. *TrACs* **22**, 509-514.

Pickel, V.M., Nirenberg, M.J. and Milner, T.A. (1996) Ultrastructural view of central catecholaminergic transmission: immunocytochemical localization of synthesizing enzymes, transporters and receptors. *J. Neurocytol*. **25**, 843-856.

Ponchon, J.L., Cespuglio, R., Gonon, F., Jouvet, M., and Pujol, J.F. (1979) Normal pulse

polarography with carbon fiber electrodes for in vitro and in vivo determination of catecholamines. *Anal. Chem.* **51**, 1483-1486.

Pothos, E.N., Przedborski, S., Davila, V., Schmitz, Y., and Sulzer, D. (1998) $D_2$-like dopamine autoreceptor activation reduces quantal size in PC12 cells. *J. Neurosci.* **18**, 5575-5585.

Pothos, E.N., Larsen, K.E., Krantz, D.E., Liu, Y., Haycock, J.W., Setlik, W., Gershon, M.D., Edwards, R.H., and Sulzer, D. (2000) Synaptic vesicle transporter expression regulates vesicle phenotype and quantal size. *J. Neurosci.* **20**, 7297-7306.

Raiteri, M., Cerrito, F., Cervoni, A.M. and Levi, G. (1979) Dopamine can be released by two mechanisms differentially affected by the dopamine transporter inhibitor nomifensine. *J. Pharm Exp. Theur.* **208**, 195-202.

Rebec, G.V. and Wang, Z. (2001) Behavioral activation in rats requires endogenous ascorbate release in striatum. *J. Neurosci.* **21**, 668-675.

Reimer, R.J., Fon, E.A., and Edwards, R.H. (1998) Vesicular neurotransmitter transport and presynaptic regulation of quantal size. *Curr.Op. Neurobio.* **8**,405-412.

Retterer, S.T., Smith, K.L., Bjornsson, C.S., Neeves, K.B., Spence, A.J.H., Turner, J.N., Shain, W., and Isaacson, M.S. (2004) Model neural prostheses with integrates microfluidics: a potential intervention strategy for controlling reactive cell and tissue responses. *IEEE Transaction on Biomedical Engineering*, **51**, 2063-2073.

Roberts, P.J. and Sharif, N.A. (1978) Effects of l-glutamate and related amino acids upon the release of [3H]dopamine from rat striatal slices. *Brain Res.* **157**, 391-395.

Roberts, P.J. and Anderson, S.D. (1979) Stimulatory effect of l-glutamate and related amino acids on [3H]dopamine release from rat striatum: an *in vitro* model for glutamate actions. J. *Neurochem.* **32**, 1539-1545.

Robinson, D.L. and Wightman, R.M. (2004) Nomifensine amplifies subsecond dopamine signals in the ventral striatum of freely-moving rats. *J. Neurochem.* **90**, 894-903.

Robinson, D.L., Heien, M.L.A.V. and Wightman, R.M. (2002) Frequency of dopamine concentration transients increases in dorsal and ventral striatum of male rats during introduction of conspecifics. *J. Neurosci.* **22**, 10477-10486.

Robinson, D.L., Venton, B.J., Heien, L.A.V., and Wightman RM. (2003) Detecting subsecond dopamine release with fast-scan cyclic voltammetry in vivo. *Clinical Chem.* **49**, 1763-1773.

Roitman, M.F., Stuber, G.D., Phillips, P.E.M., Wightman, R.M., and Carelli, R.M. (2004) Dopamine operates as a subsecond modulator of food seeking. *J. Neurosci.* **24**, 1265-1271.

Rougé-Pont, F., Usiello, A., Benoit-Marand, M., Gonon, F., Piazza, P.V., and Borrelli, E. (2002) Changes in extracellular dopamine induced by morphine and cocaine: crucial control of D2 receptors. *J. Neurosci*. **22**, 3293-3301.

Sabeti, J., Gerhardt, G.A., and Zahniser, N.R. (2003) Chloral hydrate and ethanol, but not urethane, alter the clearance of exogenous dopamine recorded by chronoamperometry in striatum of unrestrained rats. *Neurosci. Letts.* **343**, 9-12.

Sahlin, E., Beisler, A.T., Woltman, S.J., and Weber, S.G. (2002) Fabrication of microchannel structures in fluorinated ethylene propylene. *Anal. Chem.* **74**, 4566-4569.

Saunders, C., Ferrer, J.V., Shi, L., Chen, J., Merrill, G., Lamb, M.E., Leeb-Lundberg, L.M., Carvelli, L., Javitch, J.A., and Galli, A. (2000) Amphetamine-induced loss of human dopamine transporter activity: and internalization-dependent and cocaine-sensitive mechanism. *Proc. Natl. Acad. Sci. USA* **97**, 6850-6855.

Schenk, J.O., Miller, E., Rice, M.E., and Adams, R.N. (1983) Chronoamperometry in brain slices: quantitative evaluations of in vivo electrochemistry. *Brain Res.* **277**, 1-8.

Schmitz, Y., Lee, C.J., Schmauss, C., Gonon, F., and Sulzer, D. (2001) Amphetamine distorts stimulation-dependent dopamine overflow: effects on D2 autoreceptors, transporters, and synaptic vesicle stores. *J. Neurosci.* **21**, 5916-5924.

Schultz, W., Dayan, P, and Montague, P.R. (1997) A neural substrate of prediction and reward. *Science* **275**, 1593-1599.

Sesack, S.R. and Pickel, V.M. (1992) Prefrontal cortical efferents in the rat synape on unlabeled neuronal targets of catecholamine terminals in the nucleus-accumbens-septi and on dopamineneurons in the ventral tegmental area. *J. Comp. Neuro*. **320**, 145-160.

Smith, A.D. and Justice, J.B. Jr. (1994) The effect of inhibition of synthesis, release, metabolism and uptake on the microdialysis extraction fraction of dopamine. *J. Neurosci. Meth.* **54**, 75-82.

Smith, P.J.S. and Trimarchi, J.R. (2001) Noninvasive measurement of hydrogen and potassium ion influx from cells and epithelial structures. *Am J. Physiol. Cell Physiol.* **280**, 1-11.

Song, Y. and Lunte, C.E. (1999) Comparison of calibration by delivery versus no net flux for quantitative in vivo microdialysis sampling. *Anal. Chim. Acta* **379**, 251-262.

Stone, T.W. (1993) Neuropharmacology of quinolinic and kynurenic acids. *Pharmacol. Rev.* **45**, 309-379.

Stuber, G.D., Wightman, R.M. and Carelli, R.M. (2005) Extinction of cocaine self-administration reveals functionally and temporally distinct dopaminergic signals in the nucleus accumbens. *Neuron* **46**, 661-669.

Sulzer, D. and Edwards, R. (2000) Vesicles: Equal in neurotransmitter concentration, but not in

volume. *Neuron* **28**, 5-7.

Szarowski, D.H., Anderson, M.D., Retterer S., Spence, A.J., Isaacson, M., Craighead, H.G., Turner, J.N., and Shain, W. (2003) Brain responses to micro-machined silicon devices. *Brain Res.* **983**:23-35.

Taber, M.T., Baker, G.B. and Fibiger, H.C. (1996) Glutamate receptor agonists decrease extracellular dopamine in the rat nucleus accumbens in vivo. *Synapse* **24**, 165-172.

Takahata, R. and Moghaddam, B. (2000) Target-specific glutamatergic regulation of dopamine neurons in the ventral tegmental area. *J. Neurochem.* **75**, 1775-1778.

Tang, A., Bungay, P.M. and Gonzales, R.A. (2003) Characterization of probe and tissue factors that influence interpretation of quantitative microdialysis experiments for dopamine. *J. Neurosci. Meth.* **126**, 1-11.

Timmerman, W. and Westerink, B.H.C. (1997) Brain microdialysis of GABA and glutamate: what does it signify? *Synapse* **27**, 242-261.

Tossman, U. and Ungerstedt, U. (1986) Microdialysis in the study of extracellular levels of amino acids in the rat brain. *Acta Physiol. Scand.* **128**: 9-14.

Venton, B.J., Zhang, H., Garris, P.A., Phillips, P.E.M., Sulzer, D. and Wightman, R.M. (2003) Real-time decoding of dopamine concentration changes in the caudate-putamen during tonic and phasic firing. *J. Neurochem.* **87**, 1284-1295.

Verma, A. and Moghaddam, B. (1998) Regulation of striatal dopamine release by metabotropic glutamate receptors. *Synapse* **28**, 220-226.

Wang, H. and Pickel, V.Cm (2002) Dopamine $D_2$ receptors are present in prefrontal cortical afferents and their targets in patches of the rat caudate-putamen nucleus. *J. Comp. Neurol.* **442**, 392-404.

Werkman, T.R., Kruse, C.G., Nievelstein, Long, S.K., and Wadman, W.J. (2001) In vitro modulation of the firing rate of dopamine neurons in the rat substancia nigra pars compacta and the ventral tegmental area by antipsychotic drugs. *Neuropharm.* **40**, 927-936.

West, A.R. and Grace, A.A. (2002) Opposite influences of endogenous dopamine D-1 and D-2 receptor activation on activity states and electrophysiological properties of striatal neurons: Studies combining in vivo intracellular recordings and reverse microdialysis. *J. Neurosci.* **22**, 294-304.

Westerink, B.H.C., Tuntler, J., Damsma, G., Rollema, H. and deVries J.B. (1987) The use of tetrodotoxin for the characterization of drug-enhanced dopamine release in conscious rats studied by brain dialysis. *Naunyn-Schmiedeberg's Arch. Pharmacol.* **336**, 502-507.

Westerink, B.H.C. and deVries, J.B. (1988) Characterization of in vivo dopamine release as determined by brain microdialysis after acute and subchronic implantations: methodological aspects. *J. Neurochem*. **51**, 683-687.

Wightman, R.M. (1981) Microvoltammetric electrodes. *Anal. Chem.* **53**, 1125A-1130A.

Wightman, R.M., Strope, E., Plotsky, P.M. and Adams, R.N. (1976) Monitoring of transmitter metabolites by voltammetry in cerebrospinal fluid following neural pathway stimulation. *Nature* **262**, 145-146.

Wightman, R.M. and Zimmerman, J.B. (1990) Control of dopamine extracellular concentration in rat striatum by impulse flow and uptake. *Brain Res. Rev.* **15**, 135-144.

Wu, Q., Reith, M.E.A., Walker, Q.D., Kuhn, C.M., Carroll, F.I., and Garris, P.A. (2002) Concurrent autoreceptor-mediated control of dopamine release and uptake during neurotransmission: An in vivo voltammetric study. *J. Neurosci.* **22**, 6272-6281.

Wu, Q., Reith, M.E.A., Kuhar, M.J., Carroll, F.I. and Garris, P.A. (2001) Preferential increases in nucleus accumbens dopamine after systemic cocaine administration are caused by unique characteristics of dopamine neurotransmission. *J. Neurosci.* **21**, 6338-6347.

Yang, H., Peters, J.L. and Michael, A.C. (1998) Coupled effects of mass transfer and uptake kinetics on in vivo microdialysis of dopamine. *J. Neurochem.* **71**, 684-692.

Yang, H., Peters, J.L., Allen, C., Chern, S., Coalson, R.D. and Michael, A.C. (2000) A theoretical description of microdialysis with mass transport coupled to chemical events. *Anal. Chem.* **72**, 2042-2049.

Youngren, K.D., Daly, D.A. and Moghaddam, B. (1993) Distinct actions of endogenous excitatory amino acids on the outflow of dopamine in the nucleus accumbens. *J. Pharm. Exp. Thera.* **264**, 289-293.

Zhang, X., Cardosa, L., Broderick, M., Fein, H. and Lin, J. (2000) An intergrated nitric oxides sensor based on carbon fiber coated with selective membranes. *Electroanalysis* **12**, 1113-1117.

Zhang, X., Kislyak, Y., Lin, J., Dickson, A., Cardosa, L., Broderick, M. and Fein, H. (2002) Nanaometer size electrodes for nitric oxide and S-nitrosothiols measurement. *Electrochem. Comm.* **4**, 11-16.

Zhou, F., Zhu, X, Castellani, R.J., Stimmelmayr, R., Perry, G., Smith, M.A. and Drew, K.L. (2001) Hibernation, a model of neuroprotection. *Am. J. Pathol.* **158**, 2145-2151.

Zhao, Y.P, Liang, X.Z. and Lunte, C.E. (1995) Comparison of recovery and delivery in-vitro for calibration of microdialysis probes. *Anal. Chim. Acta* **316**, 403-410.

Zoli, M., Torri, C., Ferrari, R., Jansson, A., Zini, I., Fuxe, K. and Agnati, L.F. (1998) The emergence of the volume transmission concept. *Brain Res. Rev*. **26**, 136-147.